Spring 2021

Loss of ATRX Confers DNA Repair Defects and PARP Inhibitor Sensitivity in Glioma

Jennifer Mary Garbarino
Yale University Graduate School of Arts and Sciences, jennifer.garbarino@yale.edu

Abstract

Loss of ATRX Confers DNA Repair Defects and PARP Inhibitor Sensitivity in Glioma

Jennifer Mary Garbarino

2021

Alpha Thalassemia/Mental Retardation Syndrome X-Linked (ATRX) is mutated frequently in gliomas and represents a potential target for cancer therapeutics development. ATRX is known to function as a histone chaperone that incorporates the histone variant, H3.3, into the genome. Studies have implicated ATRX in key DNA damage response (DDR) pathways, including non-homologous end joining (NHEJ), homologous recombination (HR), and replication stress response, but a distinct role for this protein in DNA repair has yet to be fully elucidated. To further investigate ATRX function in glioma, I created CRISPR knockout clones in multiple glioma cell lines. These cell lines were found to have DNA repair defects that indicated increased replication stress. I then determined that the immortalized astrocyte ATRX KO cell line is sensitive to PARP inhibitors. This sensitivity is due to an increase in replication stress identified through increased ATR activation. The DNA repair defect in these cells overlaps with a frequently co-occurring mutation in gliomas, IDH1 R132H, and so leads to equal sensitivity compared to either mutation alone. I also performed a CRISPR screen which highlighted the importance of the chromatin modifications made by ATRX and how knockout cells are more susceptible to chromatin instability. Taken together, these data reveal that ATRX may be used as a molecular marker for DDR defects and PARP inhibitor sensitivity, which is independent of IDH1/2 mutations. These data highlight the important role of common glioma-associated mutations in the regulation of DDR, and they highlight novel avenues for molecularly guided therapeutic intervention.

Loss of ATRX Confers DNA Repair Defects and PARP Inhibitor Sensitivity in Glioma

A Dissertation

Presented to the Faculty of the Graduate School

Of

Yale University

In Candidacy for the Degree of

Doctor of Philosophy

By

Jennifer Mary Garbarino

Dissertation Directors: Ranjit Bindra and Ryan Jensen

June 2021

Table of Contents

Acknowledgements

I am very grateful for the support I have received over the course of my dissertation. Thank you to my advisors, Ranjit Bindra and Ryan Jensen for their support and guidance over the years. I would also like to thank my committee members, Sandy Chang and Yong Xiong for their valuable feedback and suggestions. Thank you also to Robert Mutter for being my outside reader and taking the time to evaluate my work. I also thank the members of the Bindra and Jensen labs for their support and friendship. Without them I would not have had nearly as much fun coming to lab every day and so many fewer stories to share. Thank you specifically to Amrita Sule and Gregory Breuer for their help with the CRISPR screen work. I also especially thank Ranjini Sundaram for her advice and assistance whenever I needed it. I am extremely grateful to my friends who have supported me in and outside of lab and made my time in New Haven so enjoyable. I also thank my family for their love and support throughout my life and through grad school. They are always willing to ask about how my cells are doing and listen to me go on about experiments. I especially thank my loving husband, Sam Friedman who has always been a sounding board and support for me throughout the journey of graduate school. He is always willing to spend time helping me, from writing programs to automate my data analysis to proofreading the entirety of this document.

List of Figures

List of Tables

1. Introduction

Alpha Thalassemia Retardation syndrome X-linked (ATRX) is chromatin modifier that is mutated frequently in gliomas. Its main function is to incorporate histone 3.3 into specific regions of the genome, such as telomeres, heterochromatin, rRNA and pericentric heterochromatin regions (Figure 1.1) (Dyer et al., 2017). It has been widely studied for its role in chromatin maintenance and DNA repair, but more work needs to be done to further characterize this protein.

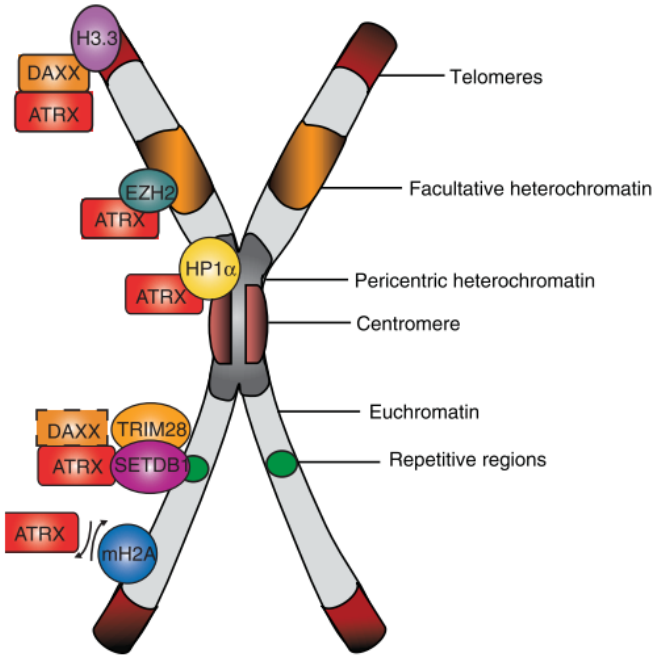

Figure 1.1: Regions of ATRX chromosomal localization

ATRX localizes at distinct regions of the genome such as telomers, facultative heterochromatin, pericentric heterochromatin and repetitive regions. While DAXX is important for the incorporation of H3.3 in these regions, there are other factors specific to each of these areas that can interact with ATRX. Image from (Dyer et al., 2017)

1.1. Discovery

ATRX was first identified through mutational analysis of patients with ATRX syndrome, a developmental disorder that leads to various symptoms such as alpha globin deficiencies (alpha thalassemia), facial deformities, psychomotor retardation and other abnormalities (Gibbons et al., 1995; Higgs et al., 2000). As ATRX is found on the X-chromosome, these symptoms are primarily seen in men, with heterozygous women having only mild affects (Gibbons et al., 1995).

ATRX mutation was found to cause alpha globin deficiencies (alpha thalassemia) through decrease in mRNA expression. This gene is very close to a telomere and GC-rich, both locations where ATRX normally is targeted (Law et al., 2010). Further work has also found that ATRX's role in alpha globin expression could be due to its lesser known role as a regulator of histone macroH2A.1 (Ratnakumar et al., 2012). Since its discovery, ATRX has been studied for its function not only in this genetic disorder, but also when it is mutated in glioma.

1.2. Mutations in Glioma

ATRX is mutated frequently in glioma, the most common form of brain cancer (He et al., 2018). Up to forty percent of low grade gliomas have ATRX mutation, as well as 7% of glioblastoma multiforme, 9% of diffuse pontine gliomas, and 15% of high risk neuroblastoma (Haase et al., 2018). These mutations tend to occur throughout the length of the protein, and mostly lead to truncation of the protein (Cerami et al., 2012). This leads to a lack of expression, which can be tested for in the clinic (Reifenberger et al., 2016).

Due to this frequent mutation, ATRX status is used diagnostically in the clinic to characterize these tumors (Reifenberger et al., 2016). As seen in Figure 1.3, ATRX expression status is used

as one of four clinical markers utilized to identify specific differences between astrocytoma and oligodendroglioma.

Also seen in Figure 1.3, ATRX in these classifications is always associated with IDH1 mutation. These mutations co-occur very frequently and so their characterization together is very important. In fact, ATRX mutation often co-occurs with many other common glioma and glioblastoma mutations. ATRX mutation occurs in three different glioblastoma molecular subgroups (Figure 1.2). However, IDH1 R132H mutation is the most common, as IDH1 mutation cooccurs in up to 90% of ATRX mutant cases (Cerami et al., 2012).

ATRX is an important diagnostic marker in glioma and glioblastoma. These mutations are mostly truncating and so while there are few common mutations between tumors, the lack of ATRX expression is common to these cancers (Cerami et al., 2012). Utilizing initial work done on ATRX to further understand ATRX syndrome, many studies have been done to identify potential mechanism of action of ATRX loss in cancer.

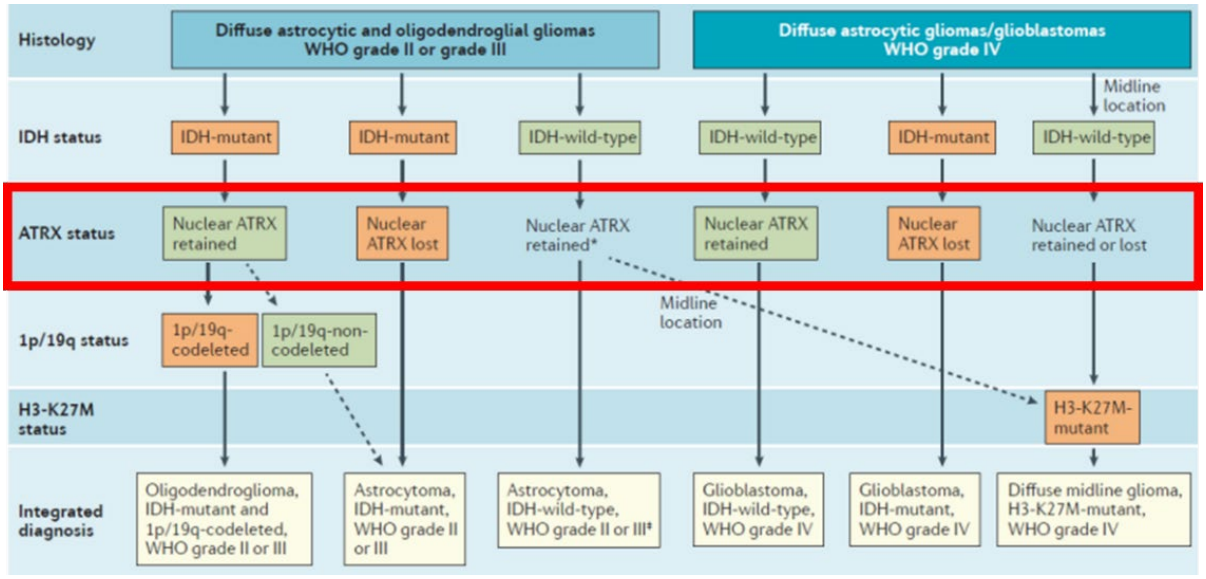

Figure 1.3 ATRX expression status is used diagnostically in the clinic

ATRX expression is an important marker clinically for determining a specific diagnosis for glioma and glioblastoma. Image from (Reifenberger et al., 2016)

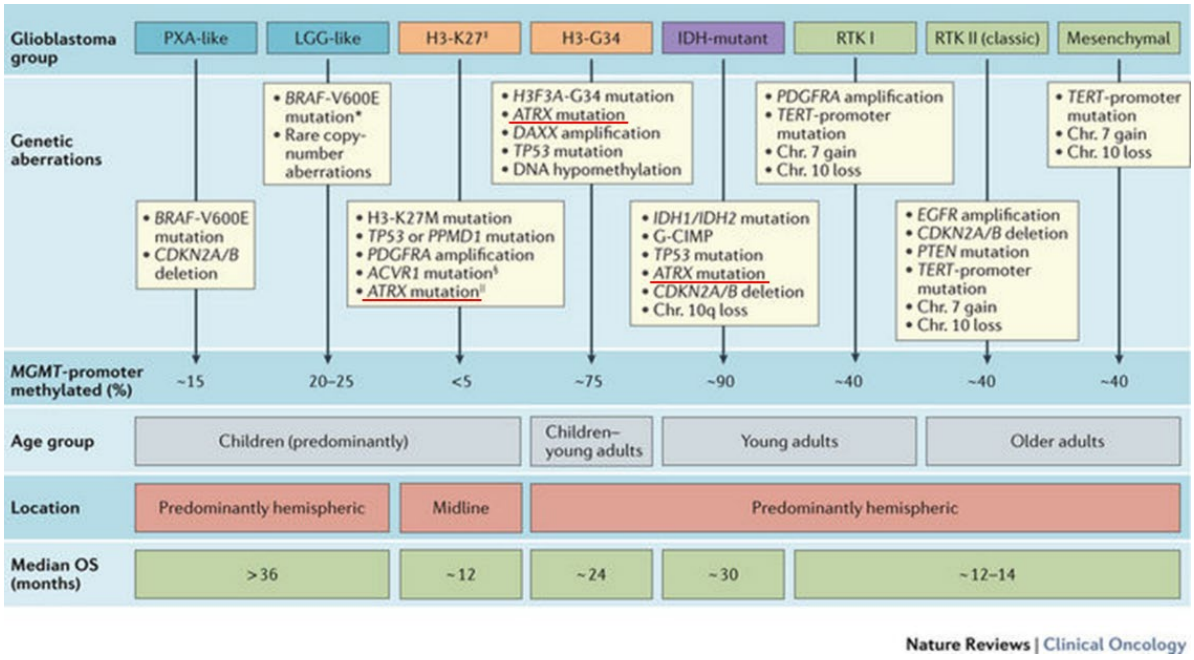

Figure 1.2: ATRX mutation co-occurs with other common glioma mutations.

ATRX mutation is found in multiple molecular subgroups of glioblastoma (underlined in red). Specifically, ATRX mutation can occur with IDH1 mutation, histone 3 mutations and MGMT promoter methylation. Image from (Reifenberger et al., 2016)

1.3. Role in chromatin modification

ATRX is a 300 kda protein with 2 domains: the n-terminal ATRX-DNMT3-DNMT2L (ADD) domain and the C-terminal ATP SNF2 type remodeling domain (Iwase et al., 2011). It is known to incorporate histone 3.3 into repetitive, often silenced parts of the genome. Histone 3.3 differs from H3.1 and H3.2 by only 5 amino acids. This allows H3.3 to have an additional phosphorylation site at S31. H3.3 is incorporated throughout the cell cycle into transcriptional areas by HIRA and to more repetitive regions, such as telomeres and heterochromatin by ATRX and DAXX (Szenker et al., 2011). DAXX and ATRX work together to incorporate H3.3 in these regions and often exist bound together (Lewis et al., 2010). DAXX binds the histone 3.3 being incorporated, and then ATRX recruits this complex to regions such as the telomere for histone incorporation. ATRX has been found to localize to these regions both during and independent from replication (Lewis et al., 2010; Wong et al., 2010).

ATRX's role in histone incorporation can lead to overall epigenetic changes in cells deficient in ATRX. Loss of ATRX can lead to an increase in H3.3 throughout the genome as it is not being specifically incorporated into telomeres and other repeat regions (Danussi et al., 2018). Histone 3.3 is incorporated into other euchromatin regions of the genome by the protein HIRA, which would now have a greater supply of the histone (Voon et al., 2015). There is also evidence of an increase in DNA methylation in regions such as telomeres with ATRX deficiency (Cai et al., 2015). These epigenetic changes lead to large differences in gene expression with ATRX KO that can lead to increased migration and changes in differentiation, which could help drive ATRX mutant cancers (Cai et al., 2015; Danussi et al., 2018; Oppel et al., 2019).

ATRX is targeted to the telomeres and heterochromatin by binding to H3K9 trimethylation (Iwase et al., 2011). This methylation, performed by SETDB1 and SUV39h1/2, is known for its

role as a mark in heterochromatin, an important modification of H3.3 at telomeres. ATRX localization to this methylation occurs through its ADD domain. The ADD domain binds this trimethylation and so can be used to help properly locate ATRX to heterochromatin. Additional binding factors such as Mcep2 and Hp1α have been seen in mouse cells to play an important role in ATRX localization as well. Both of these proteins bind to ATRX and have some evidence of being necessary for ATRX recruitment (Iwase et al., 2011; Udugama et al., 2018).

It has been shown that loss of H3.3 causes a loss of chromatin repression and ATRX levels at telomeres and rDNA (Udugama et al., 2015, 2018). Interestingly, loss of H3.3 and ATRX have similar effects, indicating the importance of ATRX's incorporation of H3.3 at these regions (Udugama et al., 2015). This marker is also seen at other repeat regions such as ribosomal DNA (Udugama et al., 2018) and pericentric heterochromatin (Iwase et al., 2011; Voon et al., 2015; Wong et al., 2010).

In addition to its role in incorporation of H3.3, ATRX is also a regulator of macroH2A1. A variant of H2A, macroH2A1 is nearly three times larger than typical histones with a large non-histone C-terminal region causing the size increase to 42 kda (Pehrson and Fried, 1992). This histone variant has two isoforms, macroH2A1.1 and macroH2A1.2 (Kim et al., 2019). ATRX can bind both of these isoforms which are found at telomeres and involved in the alternative lengthening of telomeres pathway.

1.4. Alternative Lengthening of Telomeres

ATRX loss is a key feature of the Alternative Lengthening of Telomeres (ALT) pathway. ALT is a mechanism for cancer cells to extend their telomeres without utilizing telomerase. It is thought to use homology-directed recombination (HDR), using telomeres as templates for other

telomeres to lengthen. This process is associated with genome instability, micronuclei, and G2/M checkpoint issues as well as DNA repair deficiency (Lovejoy et al., 2012). While ATRX loss alone typically isn't enough for ALT to occur, most cell lines utilizing the ALT pathway have lost ATRX (Brosnan-Cashman et al., 2018). Much work is being done to understand why ATRX loss is so prevalent in cells undergoing ALT. A few suggested mechanisms investigate the requirement of macroH2A1 (Kim et al., 2019; Ramamoorthy and Smith, 2015), the requirement of TERRA (Chu et al., 2017; Flynn et al., 2015) and overall telomere cohesion (Clynes et al., 2015).

As discussed above, macroH2A1.1 and macroH2A1.2 can bind ATRX, both of which are incorporated at telomeres. When ATRX is lost, macroH2A1.1 is no longer binding ATRX, and so has availability for other proteins to bind. In this study, it was found that macroH2A1.1 binds tankeryase1, which helps keep sister chromatid telomeres together. If ATRX is reintroduced, telomeres are able to perform HDR with any other telomere and can lead to excessive recombination and telomeric instability (Ramamoorthy and Smith, 2015). This suggests that ATRX loss is needed for cell survival when ALT is occurring.

While Ramamoorthy and Smith identified that ATRX loss lead to increase telomere sister chromatid binding through tankerayse1, Lovejoy and others found that ATRX loss actually decreases telomere cohesion. In this study, it was found that ATRX is needed for telomere cohesion, and when lost this is decreased allowing for increased interactions between non sister chromatids (Lovejoy et al., 2020). Further work needs to be done to further understand telomere cohesion in ATRX deficient cells.

MacroH2A1.2 is thought to act in independently from macroH2A1.1 When ATRX is lost, macroH2A1.2 levels decrease at telomeres during replication stress (hydroxyurea

treatment). This is needed for double strand breaks to occur and allows for ALT. Interestingly, restoration of macroH2A1.2 after the transient depletion is also required for HDR to occur (Kim et al., 2019). This suggests that ATRX loss allows for the macroH2A1.2 cycling required for the ALT pathway to successfully be performed at telomeres.

Another hypothesis for the relationship between ATRX and ALT involves the long noncoding RNAs TERRA (Telomeric Repeat-containing RNAs). TERRA binds to telomeres and around the genome and seems to work antagonistically of ATRX, as increases in ATRX levels leads to decreases in TERRA levels (Chu et al., 2017; Flynn et al., 2015; Goldberg et al., 2010). When TERRA levels increase, TERRA binds and inhibits telomerase. This then requires ALT for cell proliferation, as telomerase is no longer functioning (Chu et al., 2017). Increases in TERRA also can lead to increases in RPA levels at telomeres which helps promote strand exchange and the ALT process (Flynn et al., 2015).

An additional mechanism by which ATRX loss can mediate ALT is through increased replication stress at telomeres. In this mechanism the lack of H3.3 incorporation at telomeres leads to an increase in secondary structures such as G-quadruplexes (see Chapter 1.7). These structures lead to an increase in replication fork stalling, which requires repair through homologous recombination. This repair uses the sister telomere as a template, initiating the ALT pathway (Clynes et al., 2015).

There are many different avenues of exploration in the study of Alternative Lengthening of Telomeres pathway. While ATRX deficiency is known to be a crucial component for ALT to occur, there are many hypotheses for why this is the case. Overall, ATRX loss leads to an altered chromatin state that allows for increased prevalence of ALT. This can be due in part to the

overlapping mechanisms of telomere cohesion, macroH2A1.1/2 deposition, TERRA upregulation and increases in DNA breaks at telomeres.

1.5. Role in DNA repair

As DNA repair is an integral process in the ALT pathway, ATRX has also been studied for its role in the DNA repair process. There has been evidence for ATRX's role in homologous recombination and nonhomologous end joining when studying genome-wide repair defects as well as specific telomere-based studies. More work needs to be done in this field to validate these reports as well as to further explore ATRX's direct role in these mechanisms.

There is some evidence of ATRX's role in nonhomologous end joining (NHEJ). NHEJ is a template-free joining of DNA double strand breaks. In this pathway, the proteins Ku70 and Ku80 bind around the broken ends of DNA and recruit the DNA-dependent protein kinase catalytic subunit (DNA-PKcs) (Jette and Lees-Miller, 2015). This leads to end processing and the ligation of the DNA ends by XRCC4 and Ligase IV (Shibata and Jeggo, 2014).

In one study, a GBM mouse model was created by knocking down ATRX as well as p53 and overexpression of NRAS. These tumors were found to have increased microsatellite instability, ALT characteristics, and decreased NHEJ through a luciferase reporter assay and pDNA-PKcs staining. Additionally, these cells were found to be sensitive to high doses (10-30Gy) of radiation and other DNA damaging agents that cause double strand breaks (Koschmann et al., 2016). While much of this data could also lead to other pathways of repair, it is interesting to suggest a role for ATRX in NHEJ. Further work is needed to validate these findings and characterize a mechanism for this role.

ATRX is also thought to have a role in homologous recombination (HR). Homologous recombination requires the recognition of a template strand with homology to the broken strand. In this pathway, DNA is resected to form single stranded regions of DNA, where Replication Protein A (RPA) can bind. RPA helps to prevent secondary structure formation in the single stranded DNA (ssDNA). Through different mediator proteins, such as BRCA2, the protein Rad51 is targeted to the ssDNA to form filaments. These filaments search for homology in another region of the DNA, and then lead to strand invasion. Through one of multiple sub-pathways, new DNA is synthesized based on the homologous template, and the DNA is repaired (Heyer et al., 2010)

ATRX has been thought to be involved in multiple steps of this pathway. In one study, ATRX is found to bind FANCD2 (a recruiter of HR proteins and important for Fanconi Anemia inter-strand cross link repair) through immunoprecipitation. It is hypothesized that ATRX, DAXX, FANCD2 and the MRN complex (see Chapter 1.6) all bind in a super complex that incorporates histones H3.3 and H3.1. This then leads to HR-mediated replication fork restart. Overall homologous recombination levels are seen to be decreased with ATRX knockout and siRNA to ATRX (Raghunandan et al., 2019). While how this super complex would function is unclear, it is an interesting hypothesis that could be further studied.

Another study looks further along the HR pathway to synthesis of DNA repair. This report found that ATRX acts later in the HR pathway as changes in RAD51 foci were not seen with ATRX loss. However overall synthesis after damage such as radiation (measured by BrdU foci) was reduced. ATRX was also found to interact with DNA repair synthesis machinery and enable long-patch DNA repair synthesis. It was hypothesized that the incorporation of H3.3 during repair synthesis is important for successful DNA repair synthesis (Juhász et al., 2018).

While there are multiple studies looking at ATRX's role in NHEJ and HR, more work is needed to fully elucidate this mechanism. Since many factors overlap between DNA repair and replication, especially with DNA repair synthesis, much of this evidence also supports a role in DNA replication.

1.6. Role in DNA replication

DNA replication is a crucial function for cell proliferation. Movement of the replication fork throughout the genome requires precise timing and recruitment of many different factors. When this process is slowed or stalled this is referred to as replication stress. This can be caused by multiple factors, such as depletion of the nucleotide pool and legions in the path of the replication fork caused by DNA damage or DNA secondary structures (such as G-quadruplex) (Kotsantis et al., 2018).

One important factor in resection of a stalled fork is the MRN complex. The MRN complex is made of three different proteins, MRE11, RAD50 and NBS1. MRE11 is a nuclease, NBS1 signals for additional repair factors and RAD50 unwinds DNA. Together MRN complex can degrade a stalled fork and allow for replication restart (Lamarche et al., 2010).

Multiple studies show that ATRX can bind the MRN complex (Clynes et al., 2015; Huh et al., 2016; Leung et al., 2013). Without ATRX there is an increase in degradation of the replication fork by MRE11 (Huh et al., 2016). Others have shown that ATRX loss leads to an increased in stalled forks and longer time in S phase (Leung et al., 2013). Some of these studies suggest that increased G-quadruplex legions (see Chapter 1.7) are leading to these stalled forks (Clynes et al., 2015; Huh et al., 2016).

Additionally, since replication stress can lead to double strand breaks and homologous recombination, many of the factors are also present at the replication fork (Kolinjivadi et al., 2017). DNA legions can become double strand breaks as they are attempted to be replicated, and so increases in these legions could be causing both DNA repair defects and replication stress. While more work needs to be done to elucidate these the mechanism, ATRX seems to have an important role in DNA replication and repair, which could be exploited therapeutically.

1.7. ATRX drug sensitivities

As ATRX is mutated frequently in cancers (see Chapter 1.2) and so there have been multiple studies to identify drug sensitives specific to ATRX deficiency. There is currently evidence for sensitivity to inhibitors to ATR (Flynn et al., 2015), Pol1(Udugama et al., 2018), Wee1 (Liang et al., 2019), PARP (Huh et al., 2016; Juhász et al., 2018), and G-quadruplexes (Clynes et al., 2015; Wang et al., 2019) as well as DNA damaging agents such as radiation and chemotherapies (Koschmann et al., 2016; Leung et al., 2013).

Many of these drug targets require further characterization to validate these different drugs as potential therapeutic options. For example, Wee1 was found as a potential hit in a CRISPR screen, and had small but consistent differences between WT and ATRX knockout cells (Liang et al., 2019). ATR inhibitor was shown to be a potential sensitizer for ALT cells, which have more than just ATRX loss, due to increases in TERRA levels leading to more ATR activation at telomeres (see Chapter 1.4) (Flynn et al., 2015). Decrease in rDNA copy numbers from ATRX loss can lead to sensitivity to inhibition of RNA polymerase, Pol1 (Udugama et al., 2018). Additionally, Koschmann found sensitivity to DNA double strand breaks created by Doxorubicin, Topotecan, Irinotecan and Radiation in their cell model, but similar sensitivity was not seen by Leung et al (Koschmann et al., 2016; Leung et al., 2013). All of these disparate

results of drug sensitivities show the importance of a robust comparison of these compounds in an ATRX KO model cell line.

An interesting drug target in ATRX KO cells is G-quadruplexes. G-quadruplex is a DNA secondary structure that occurs in GC rich regions. This structure, seen in Figure 1.4, uses hoogsteen interactions to allow stacking of sets of 4 guanines binding in a plane (Weldon et al., 2016). This structure can occur in multiple areas of the genome, including telomeres, and can cause replication stress (Clynes et al., 2015; Hänsel-Hertsch et al., 2016; Wang et al., 2019; Zimmer et al., 2016). ATRX has been found to bind to G-quadruplexes (Law et al., 2010), and is known to be located at these GC rich regions, such as telomeres (Clynes et al., 2015). Clynes hypothesizes that the deposition of H3.3 at telomeres helps prevent double strand breaks at telomeres. Stabilization of G-quadruplex will cause the greater number of G-quadruplexes in ATRX KO cells to overwhelm the cell, leading to cell death. While some breaks are potentially needed for ALT (see Chapter 1.4), too many can become dangerous for the cell (Clynes et al., 2015). Additionally, Wang et al also shows sensitivity to the G-quadruplex stabilizer CX-3543 in shATRX cells, which have increased G-quadruplex levels. They showed that this sensitivity promotes replication stress, as this structure is difficult for the replisome to move through. Additionally, the effect with this stabilizer can be enhanced in ATRX KO cells with a DNA damaging agent causing double strand breaks or replication stress (Wang et al., 2019). Overall, G-quadruplex stabilization seems to be a very interesting avenue for further research in ATRX KO cells.

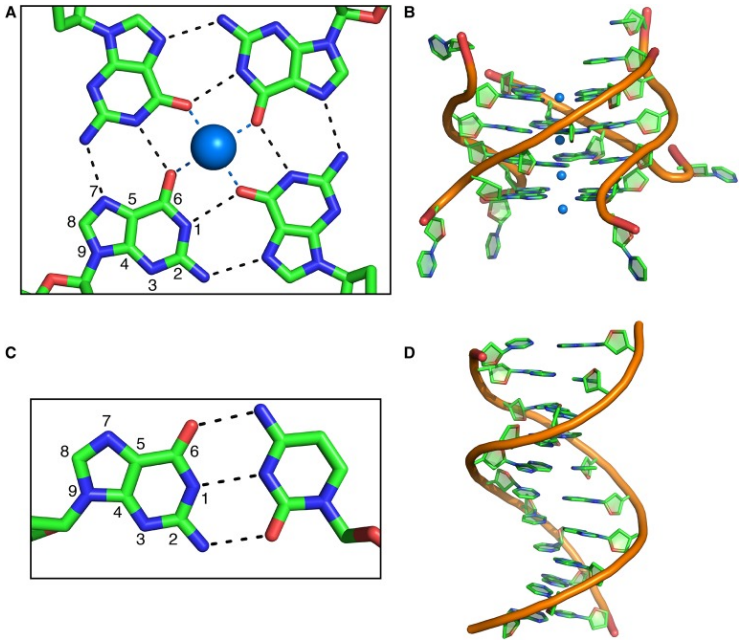

Figure 1.4: G-quadruplex structure comparison to normal helix.

A) Hoogsteen base pairing allowing for 4 guanine molecules to be bound and stabilized by magnesium. B) The stacking of multiple 4 guanine structures to form the G-quadruplex. C) Watson crick base pairing between guanine (left) and cytosine (right). D) Typical DNA helix without G-quadruplex. Image from (Weldon et al., 2016)

Some preliminary work has also been done to explore PARP inhibitor (PARPi) sensitivity in ATRX deficient cells. Poly (ADP-ribose) polymerase (PARP) have been widely studied in DNA repair, especially after it was discovered that their inhibition leads to decreased cell survival in BRCA mutant cells (Bryant et al., 2005). There are many questions in the field to understand the mechanism of this sensitivity, from PARP trapping to increased replication speeds (Maya-Mendoza et al., 2018; Murai et al., 2012; Panzarino et al., 2020; Zandarashvili et al., 2020). Many different cancer mutations have been suggested to lead to PARP inhibitor (PARPi) sensitivity and is a very popular target in the DNA repair field (González-Billalabeitia et al., 2014; Johnson et al., 2011; Stewart et al., 2014; Sulkowski et al., 2017; Turner et al., 2008).

ATRX deficiency has had minimal analysis in the field of PARP inhibition, despite ATRX loss's known potential for DNA repair defects. While this has been suggested in a few papers, it has not been robustly explored (Huh et al., 2016; Juhász et al., 2018). Huh and others identified PARPi sensitivity in their Hela cells with and without siATRX using a lesser known PARP inhibitor PJ-34. However it seems that the siATRX was fairly toxic without PARP inhibitor and so more work would be needed to explore this other model systems (Huh et al., 2016). Juhász and others focused on ATRX role in DNA repair synthesis (see Chapter 1.5). They showed sensitivty to PARP inhibitor in Hela cells to support a homolgous recombination deficiency, but did not investigate any mechansim of PARPi action in these cells (Juhász et al., 2018). Much more work could be done to further explore this interaction.

1.8. ATRX and IDH1

As discussed above in Chapter 1.2, ATRX loss and IDH1 R132H are frequently seen together in tumors. Despite this, little work has been done to understand why this occurs and how this can be exploited therapeutically. There are only a few papers that study both IDH1 mutation and ATRX mutation in the same cell line and more needs to be done to further explore this combination of mutations (Mukherjee et al., 2018; Núñez et al., 2019).

Isocitrate dehydrogenase (IDH1) is an enzyme in the citric acid cycle that converts isocitrate to α-ketoglutarate. When it was first identified as a common mutation in glioblastoma, with 12% of a cohort having the mutation, it was shown that these patients have increased overall survival compared to patients with wildtype IDH1. Additionally nearly every patient had a mutation at the same residue R132, a highly conserved residue in the IDH1 protein (Parsons et al., 2008). It was later shown that this mutation gives a new function to IDH1, converting its original product α-ketoglutarate to a new molecule, 2-hydroxyglutarate. This creates a nearly 100-fold increase in

the 2-hydroxyglutarate levels in the cell and surrounding media (Dang et al., 2009). These extremely high 2-hydroxyglutarate levels lead to inhibition of α-ketoglutarate dependent dioxygenases, which have a variety of functions throughout the cell (Xu et al., 2011). One inhibited dioxygenase is KDM4A, a histone demethylase that acts on H3K9 methylation. Not only is H3K9 methylation used to mark heterochromatin (see Chapter 1.3), it is also used for transient signaling of double strand breaks. With increased levels of H3K9 methylation, DNA repair factors are not able to properly target a DNA double strand break, leading to decreased homologous recombination (Sulkowski et al., 2020). This then leads to a "BRCAness" phenotype that causes cells with increased 2-hydroxyglutarate levels to be sensitive to PARP inhibitors. It is also thought that patients with IDH1 mutant tumors have greater overall survival due to this increased sensitivity to DNA damage (Sulkowski et al., 2017; Wang et al., 2020).

However, there is some work that contradicts this hypothesis. Núñez et al. finds that R132H mutation leads to an increase in the DNA damage response through epigenetic changes that upregulate HR genes. This leads to elevated HR levels and radiation resistance. Interestingly, this cell model also knocked down ATRX and overexpressed NRAS, and the authors argued that the combination with ATRX loss leads to this opposite result (Núñez et al., 2019). This shows the importance of further exploring the double mutation of IDH1 and ATRX, to validate this work and better understand these tumors.

Another study that looks at the combination of IDH1 R132H and ATRX instead investigates in role in Alternative Lengthening of Telomeres pathway (see Chapter 1.4) instead of overall DNA repair. Mukherjee et al. show that epigenetic changes in R132H mutant tumors lead to the downregulation of telomere capping protein RAP1 and the NHEJ factor XRCC1, increasing their ability for the homology directed repair used in ALT to occur. They found that both loss of

ATRX and overexpression of R132H mutant IDH1 was enough to cause the ALT phenotype, despite neither mutation alone allowing this to occur. This provides another mechanism that could explain the frequent co-occurrence of ATRX and IDH1 mutation.

1.9. Conclusions

ATRX is an important chromatin modifier that has been implicated in multiple DNA repair and regulation pathways. While much more work can be done to clarify its many activities within the cell, it is clearly important for telomeric and overall genomic stability. As is it mutated frequently in glioma and other cancers, further study of ATRX as a biomarker for potential therapeutics is critical for the successful treatment of patients with these mutations.

In this study, I developed three different cell lines with ATRX KO in cell lines relevant to glioma research. I then characterized the DNA repair capacity in these cells and found increases in replication stress and potential for decreased homologous recombination. Furthermore, I identified through CRISPR screen the importance of other chromatin modifiers in the survival of ATRX KO cells. I also determined that ATRX KO can lead to PARP inhibitor sensitivity, due to increased ATR activation in these cells. This further suggests the increased replication stress in ATRX mutant cells. I also showed that these cells have equal sensitivity to PARP inhibitor regardless of IDH1 status, suggesting overlapping mechanisms of DNA repair defect that can be explored further.

2. Materials and Methods

Antibodies and Reagents

Antibodies: ATRX: Millipore Sigma 39F MABE1798 and Santa Cruz sc-55584 were used 1:1000 overnight in 1X TBST after 5% milk block for western blot, pChk1: CST 2341 was used at 1:500 overnight at 5% BSA in 1X TBST . Drugs were purchased through Selleckchem.

Cell Culture

All cell lines were grown in DMEM with 10% FBS. For siRNA experiments, siRNAs were purchased from Dharmacon (siATRX (Dharmacon J-006524-05), XPC (L-016040-00), KDM2A (L-012458-02), CLK2 (L-004801-00), UHRF1(L-006977-00), XRCC3 (L-012067-00)) were transfected into cells using Life Technologies Lipofectamine RNAiMax (13778) and imaged 96 hours later or seeded for growth rate experiments 72 hours later. IDH1 R132H overexpression construct from Addgene (66803).

Clonogenic Survival Assay

Cells were seeded at a three-fold dilution between 9000 and 37 cells per well of a 6 well plate in triplicate and incubated in multiple drug concentrations for 14 days. Plates were washed with PBS, stained with crystal violet for 1 hour, and quantified.

CRISPR knockout

To create the CRISPR knockout cell line, a guide to exon 9: (5'-AAATGCATTCTACGCAACCT-3') was cloned into the MLM3636 plasmid (Addgene 43860). This plasmid along with a Cas9 plasmid were nucleofected into the cells and after at least 72 hours, successful Cas9 cleaving was validated using a T7 endonuclease assay. Cells were then

diluted to single cells into nine 96-well plates. Wells were then screened for colonies and replica plated to 96-well plates for imaging (Greiner screenstar 655866), and further passaged. Imaging plates were stained using the immunofluorescence protocol below. Cells with diminished ATRX foci were then chosen for further testing.

CRISPR Screen

To perform the CRISPR screen, cells were seeded in 15cm plates and transduced with CRISPR library (from Gupta Lab). Cells were selected in puromycin for three days and samples harvested periodically over 14 days. Genomic DNA was purified from samples and region with CRISPR insertion amplified. Each amplified PCR product was barcoded for each condition, and then pooled and sent for next generation sequencing (Genohub). Results were analyzed by Dr. Gregory Breuer to give beta scores for each gene.

Growth Rate

For determination of growth rate, cells were seeded at low densities (1000 or 2000 cells per well). In 1 column of a 96-well plate for 1 plate per day of study (typically 5 plates, 6, 24, 48, 72, 96 hours). Each plate was analyzed using short term viability assay protocol below.

Immunofluorescence

For immunofluorescence assays, cells were seeded in chamber slides (Millipore PEZGS0816) or 96 well plates (Greiner screenstar 655866). Cells were treated as indicated. For cyclin A (Santa cruz B-8 sc-271682), ATRX (Millipore), H2AX (Millipore 05-636) and 53BP1 (Novus NB100-904), cells were fixed in 4% PFA, 0.02% Triton in PBS for 15 minutes. Cells were then permeabilized/blocked for 1 hour in 5% BSA, 0.5% Triton in PBS and in primary overnight at 1:500 in blocking solution. Secondary (Alexa Fluor 647) was diluted 1:1000 for 1

hour. For pRPA32 S33 (Bethyl A300-246A) protocol was used as previous (Shiotani et al., 2013). Foci were analyzed using the Focinator (Oeck et al., 2017).

Neutral Comet Assay

Assay performed with manufactures protocol (Trevigen). In brief, cells were trypsinized and resuspended in LM Agarose (Trevigen). Slide was then left to dry, followed by lysis and incubated in neutral electrophoresis buffer at 21V for 45mins in the CometAssay Electrophoresis System (Trevigen). DNA was then precipitated and slides were dried overnight. After stained the following day with SYBR Gold; slides were then imaged on EVOS FL microscope (Advanced Microscopy Group), with 15 fields of view per replicate (greater than 100 cells). OpenComet was used to quantified comet tail moment (Gyori et al., 2014). Experiment performed in triplicate and data are means ± SEM.

Plasmid Reporter Assay

Cells were seeded at 40-60,000 cells in 24 well plate. Cells were transfected with 1μg of linearized Lux4 or PGL3 plasmid (from Glazer lab) and 250ng of Renilla control plasmid. After 24 (PGL3) or 48 (Lux4) hours, cells were harvested, lysed and analyzed with Promega Dual-Luciferase Reporter Assay System (Promega E1910).

Sequencing

Genomic DNA was purified from cells and CRISPR region was amplified. TOPO reaction was performed using TOPO TA cloning kit (Thermo Fisher 450071) and transformed into DH5α cells. DNA was amplified through colony PCR using SapphireAmp fast PCR (Takara Bio RR350), and PCR cleanup was performed with ExoSAP-IT™ (Applied Biosystems 75001). Sequencing was performed by the Yale Keck Biotechnology Resource Laboratory.

Short Term Viability Assay

Cells were plated at 2,000 cells per well of a 96-well plate. The following day cells were treated with various concentrations of drug as indicated. 96 hours after of drug treatment, cells were washed in 1X PBS, fixed in 4% formaldehyde, and stained with Hoechst at 1 μg/ml. Plates were imaged on a Cytation 3 (BioTek) and cells were counted using CellProfiler (http://cellprofiler.org/). For synergy assays, synergy was calculated using the Loewe method through Combenefit (Di Veroli et al., 2016).

Statistics

Student 2 tailed T test was performed to compare groups using GraphPad Prism unless otherwise described. Asterisks indicate levels of significance/p value (*≤0.05, **≤0.01,*** ≤0.001,**** ≤0.0001). Error bars indicate standard deviation.

3. Creation of ATRX knockout model

Parts of this chapter are adapted from work in publication:

Garbarino, J., Eckorate J., Jensen, R., and Bindra, R.. Loss of ATRX confers DNA repair defects and PARP inhibitor Sensitivity. *Translational Oncology* (***in revision***) 2021.

3.1. Introduction

When looking to characterize a specific protein, it is important to identify a relevant model cell line. In this case, I wanted to focus on identifying ATRX's role in brain cancers, and so focused on choosing models that are related to this system. The goal was to create an isogenic pair of cell lines to identify how ATRX loss alone impacts DNA repair and therefore changes sensitivity to different DNA damaging agents and repair inhibitors.

For this reason, I focused my efforts on the glioma cell lines LN229 and U87 as well as an immortalized astrocyte line. Each of these cell lines express ATRX, and have been used to model gliomas previously (Cai et al., 2015; Jackson et al., 2019; Sulkowski et al., 2020; Wang et al., 2019) and so would be good options for future characterization of this mutation.

I chose to use CRISPR/Cas9 to create the ATRX knockout cell lines. CRISPR (Clustered Regular Interspersed Short Palindromic Repeats)/Cas9 is a tool developed based on bacterial immunity. The Cas9 enzyme has ability to specifically target a region of the genome given to it as an RNA sequence, for cleavage. While this is used in bacteria to defend against viral DNA, it has now been repurposed for targeting the genomes of human cells. By expressing Cas9 and an RNA sequence of interest in cells, Cas9 can specifically cut genomic DNA and through DNA repair lead to the loss of that proteins expression. This relatively simple method has

revolutionized genomic editing, both for potential therapeutics and as a tool for research (Ahmad et al., 2018).

Creating this RNA sequence is an important component to utilizing the CRISPR/Cas9 system. These RNAs, called guide RNAs (gRNA) are what determine the exact place Cas9 will cut. For ATRX loss, there is no specific hotspot mutation in glioma, and mutation could be induced in any part of the genomic sequence. However, different sequences will have different affects, both in their ability to cut at the region of interest and to minimize chances of cutting in other locations. These have been quantified through on- and off-target scores.

On-target scores determine the ability of Cas9 to cleave DNA at the genomic loci. While all gRNAs need to be targeted to a 5′-NGG protospacer adjacent motif (PAM) site for cleavage to occur, the surrounding region can also dictate how efficient DNA cleavage will be. Through testing of over a thousand gRNAs, a model was able to be created by Doench and others to determine how successfully a gRNA will lead Cas9 to cleave (Doench et al., 2016). This model has been utilized to create an on-target score, which on a scale of 0-100 (higher indicates better cleavage) rates the ability of cleavage at a given site.

As important as an on-target score, the off-target score determines where else in the genome Cas9 could cleave given a specific gRNA. A similar model to off target score was created by the Zhang lab, allowing for a predicted score of how specific a gRNA will be (Hsu et al., 2013). This score, also a scale of 0-100, rates more specific gRNAs with numbers closer to 100. This allows a user to look for both a high off-target and on-target score as a predictor of successful cleavage.

These factors were utilized in the design of my CRISPR/Cas9 ATRX knockout clones. With these designs, I created three different knockout cell lines, LN229, U87 and immortalized

astrocytes to use for these experiments. During this process, I also developed a robust CRISPR knockout screening platform to allow me to readily analyze hundreds of clones. Identifying a successful method for ATRX KO creation was an important foundation for understanding the role of ATRX loss in glioma.

3.2. LN229 knockout creation through western blot screening:

To model the ATRX mutation, I first created 5 CRISPR gRNAs (Table 3.1). These gRNAs were chosen to be early in the ATRX sequence (exon 1-3) to ensure that no partially functional protein would be created.

gRNA	Exon	Sequence	On Target Score	Off Target Score
1	2	5'-CCACGACTTGCAATGAATCA-3'	63	87
2	2	5'-TGAAAGCAAGTTGAATACAT-3'	49	43
3	3	5'-TGGAAGTAACTCTGATATGA-3'	39	58
4	2	5'-TGCACACTCATCAGAAGAAT-3'	54	56
5	1	5'-ACATGACCGCTGAGCCCATG-3'	62	41

Table 3.1: CRISPR gRNA designs

Guides were designed to PAM sites in exons 1-3 and were chosen as those with the highest on and off target scores in this region.

These gRNAs had the highest on and off target cutting scores of this region. Each gRNA was then nucleofected along with Cas9 into the LN229 cell line. In this technique, Cas9 is only be transiently expressed, and not able to create further non-specific cuts over time. I then performed a T7 endonuclease assay which detects mismatches in DNA. After amplifying the genomic region surrounding the CRISPR gRNA site, the DNA is melted and reannealed. If

successful CRISPR cutting has led to mutation in a portion of the DNA, then these mutant DNA copies will mostly bind to the more prevalent wild-type copies. The T7 endonuclease will then cleave the DNA at the mismatch, which can be identified as lower bands on the gel. The amount of cleaved DNA visualized can qualitatively show how much cutting occurred and ensure that a high enough proportion of the population had successful cutting to be screened for effectively. Of these gRNAs, gRNA 2 had the most successful cleavage (Figure 3.1).

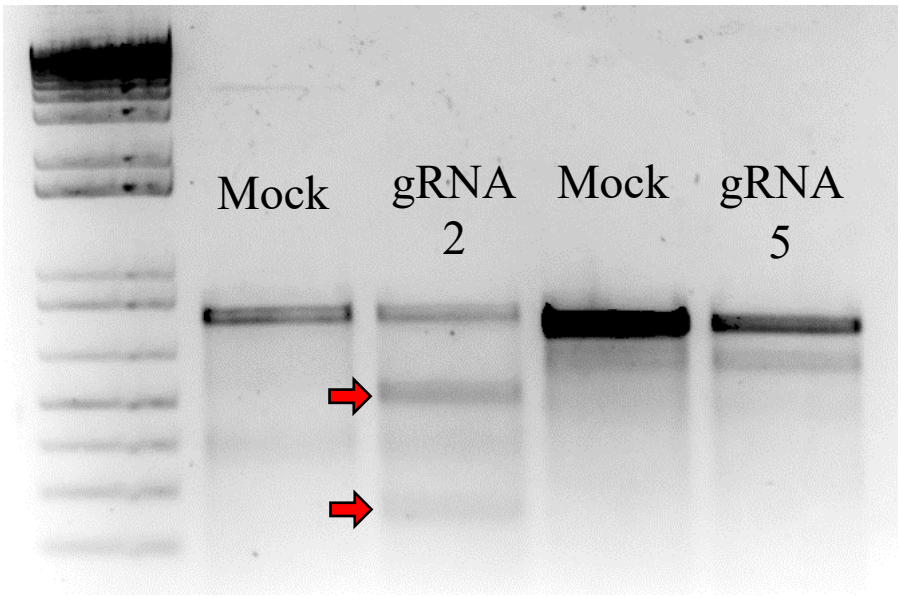

Figure 3.1: Successful cleavage with Cas9 and gRNA 2.

After transfection with Cas9 and gRNA 2, 5 or mock transfection, T7 endonuclease assay was performed on PCR amplified region of exon 2 of ATRX. Red arrows indicate bands created from mismatch at CRISPR cut site. For gRNA 5, while band was visualized, this band was also seen in the mock treatment and not specific to CRISPR cleavage.

Once this guide was selected as most successful, I diluted the cells to single cell colonies in 96 well plates. No antibiotic selection is used in this system and so many clones need to be analyzed. I, with assistance from an undergraduate researcher Jillian Eckorate, screened just over 200 LN229 clones through western blotting. Through this screening two clones were found to have no protein expression, 87 and 180 (Figure 3.2). This indicates that the efficiency for creating a CRISPR knockout using these cells and guide 2 was approximately 1%. After sequencing (see Chapter 4.2, Figure 4.1) it was found that these clones were identical and must have been duplicated at some point in the single cell cloning process.

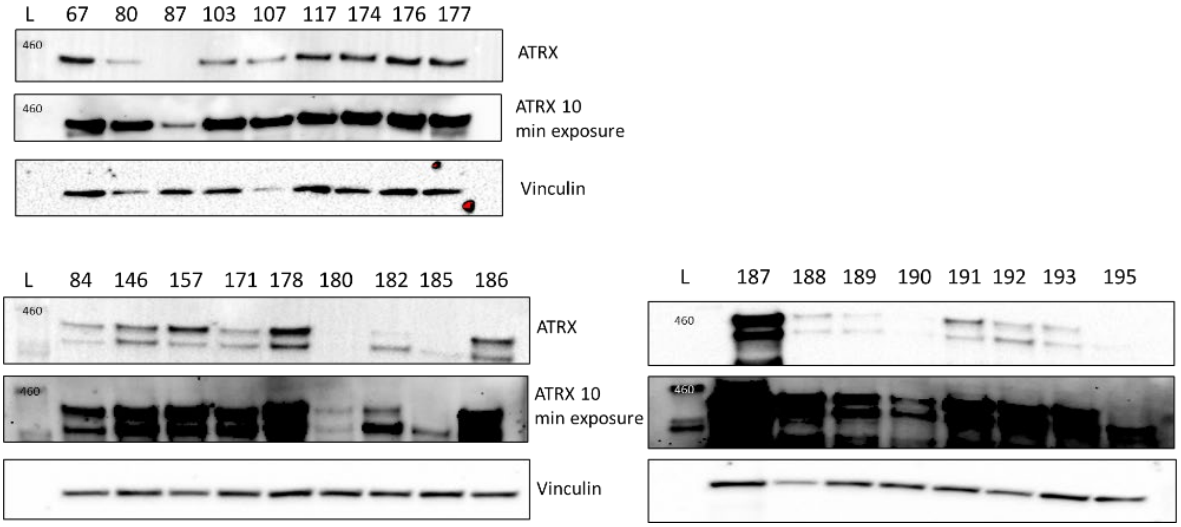

Figure 3.2: Representative western blots for LN229 ATRX clone screening

Western blots were performed on 200 potential ATRX knockout clones. Clones 87 and 180 were chosen for further analysis.

3.3. Development of foci screening pipeline

Screening the LN229 ATRX KO clones was a long, arduous process and required managing the expansion of many clones. To streamline this process, I began to develop a 96-well plate format for clone screening. I found from work initially characterizing cells with siATRX that ATRX foci are easily visualized through immunofluorescence in a 96-well plate imager (Figure 3.3B). This method was demonstrably improved to the traditional western blot screen by scaling up the screening process to 60 clones per 96 well plate and allowing for each plate to be read easily by an automatic plate imager.

In this method (Figure 3.3A), after initial dilution of approximately 1 cell per well of a 96 well plate, colonies that came from 1 cell are then moved into the inner 60 wells of a new 96 well plate. Inner 60 are used because the plate imager cannot read edge wells at 40X magnification. This plate is then split into 2, 1 traditional cell culture 96 well plate, and one imaging plate. After staining for ATRX, automatic imaging is performed to detect the ATRX foci. I then can quickly look through the images for those with low ATRX foci. Clones of potential interest can then be chosen off the replica plate for expansion and further characterization by western blot. This process was able to be utilized for the creation of new ATRX CRISPR knockout cell lines and allowed for a much more streamlined approach to screening.

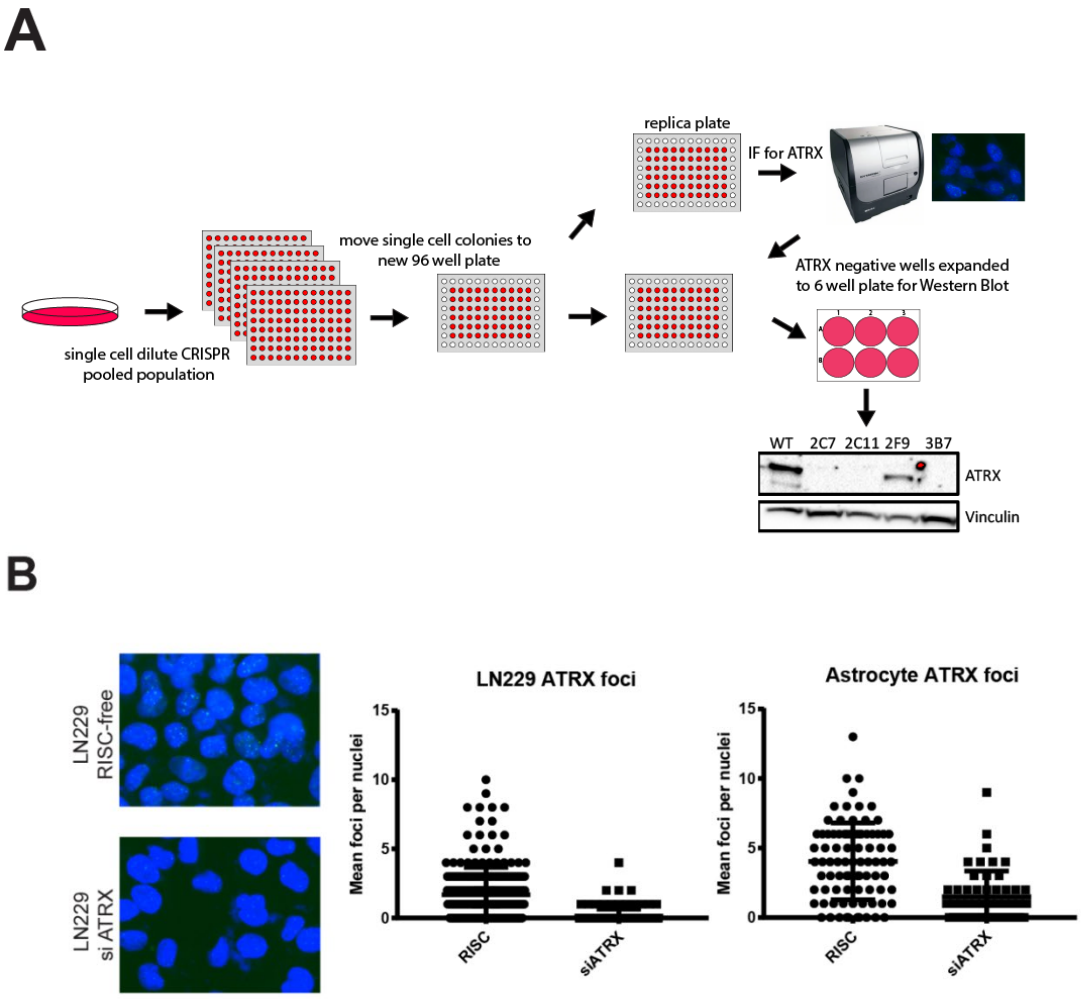

Figure 3.3: Immunofluorescence screening pipeline successful in identifying ATRX CRISPR knockout cells.

A) Schematic of immunofluorescence screening pipeline for CRISPR clones. B) Validation of immunofluorescence ATRX foci 96 hours after siRNA transfection.

3.4. U87 clone creation

After the low efficiency of gRNA 2 in the LN229s, I created new gRNAs in later exons of ATRX. Despite being later in the protein, they have much higher on and off target scores (Table 3.2). While exon 9 is further into the protein, ATRX is a large protein with 36 exons. Despite being several exons into the genomic sequence, this is still very early into the protein and importantly occurs before the completion of the first domain (Figure 3.4). This minimizes the chances of a partial formed protein expressing and binding to DNA, despite full-length expression not occurring.

gRNA	Exon	Sequence	On Target	Off Target
A	9	5'-AAATGCATTCTACGCAACCT-3'	70	87
B	9	5'-AGAACAAATAAAAGTACCGG-3'	72	74
C	9	5'-ACTCTTATTCCGCACTAATT-3'	64	74

Table 3.2: Improved guide RNAs to exon 9 for ATRX KO

Guides were designed to PAM sites from exons 1-15 and had the highest on and off target scores in this region.

Figure 3.4: gRNAs targeted to beginning of ATRX protein.

gRNAs 1-5 were designed to be in the first three exons which are very early in the ATRX gene. While the newly designed gRNAs are further down the genetic sequence, ATRX is a large protein and so these are still at the beginning of the ATRX protein. These gRNAs are also targeted to the ADD domain.

I then transfected each gRNA into the U87s as done in the LN229s and performed a T7 endonuclease assay with new PCR products from exon 9. gRNA A was found to be the most successful guide, and so was used for further analysis (Figure 3.6).

After dilution, instead of expanding clones to 6 well dishes for western blot, the foci pipeline described (Figure 3.3A) was used to screen U87 clones. Using this pipeline allowed for the screening of 120 clones at the 96 well level, saving the time of clone expansion and numerous western blots. Of these 5 had evidence of loss of ATRX expression (Figure 3.5). When validating through western blot 2 of the 5 clones were found to be ATRX negative. This increased the efficiency of the screen to 1.7%, but more importantly shortened the timespan to screen these clones considerably.

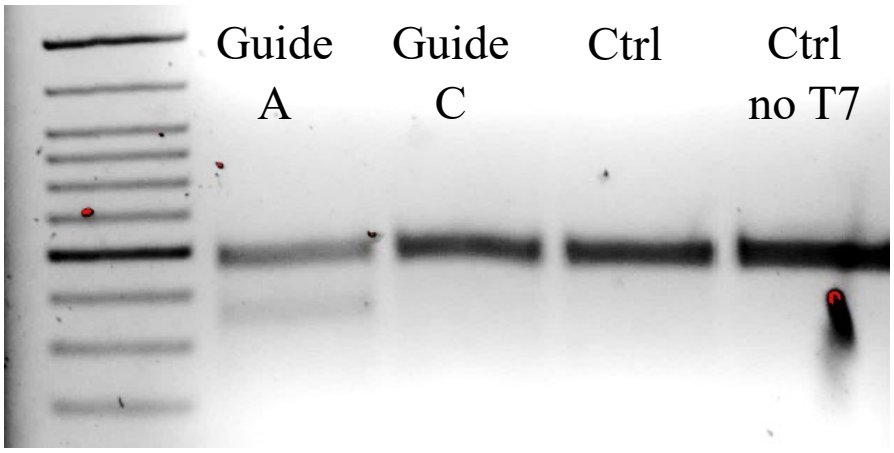

Figure 3.6: Successful cleavage with Cas9 and gRNA A in U87.

After transfection with Cas9 and gRNA A or C, or mock transfection, T7 endonuclease assay was performed on PCR amplified region of exon 9 of ATRX. gRNA C was unsuccessful in targeting Cas9 for cutting, while gRNA A was successful and used for further experiments.

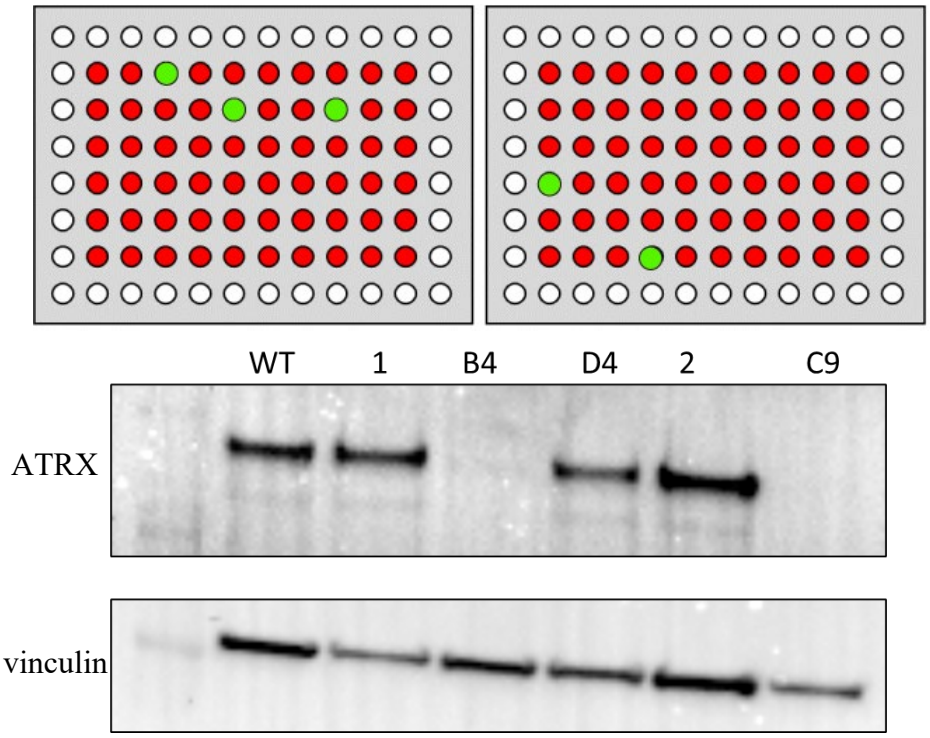

Figure 3.5: Utilization of immunofluorescence foci pipeline for U87 ATRX KO.

Representation of screen for U87 Parental clones. Potential hits labelled in green were expanded for further analysis. Representative western blots shown below of selected clones.

3.5. U87 R132H Clone Creation Attempt

While it is important to look at ATRX knockout alone, it is also very interesting to determine how it interacts with other mutations it commonly co-occurs with, such as IDH1 R132H. As a U87 R132H model already existed in the Bindra Lab, adding the ATRX KO seemed like an excellent way to characterize this double mutation.

I transfected U87 IDH1 mutant cells with Cas9 and the same gRNA A used in the U87 parental cells. I found that my efficiency of editing, determined by T7 endonuclease assay, seemed to be much lower than my U87 parental cell knockout, as the gel needed to be exposed much longer to see the band indicating Cas9 cleavage (Figure 3.7). Since cutting was seen I proceeded forward with growing single cell clones for screening as I could increase my number of clones screened more readily with my foci screening platform.

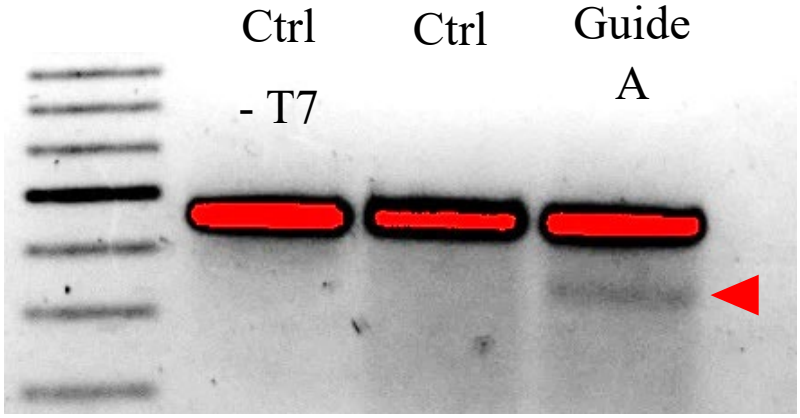

Figure 3.7: Successful cleavage with Cas9 and gRNA A in U87 R132H cells.

After transfection with Cas9 and gRNA A or C, or mock transfection, T7 endonuclease assay was performed on PCR amplified region of exon 9 of ATRX. Red indicates oversaturation of signal for uncut bands. While gRNA A was successful, the efficiency of cleavage was much lower than with the parental U87 cell line (Figure 3.6).

I screened approximately 240 clones via immunofluorescence and found only 4 clones that seemed promising (Figure 3.8). However, of the 4, only 1 was able to effectively grow, but was found to still retain ATRX expression through western blot (data not shown). The lack of successful clones could be due to the deficiencies already present in the IDH1 mutated cells, such as their high levels of the oncometabolite 2-hydroxygluarate (see Chapter 1.8). Because of this, U87 R132H cells were not used as a cell line model.

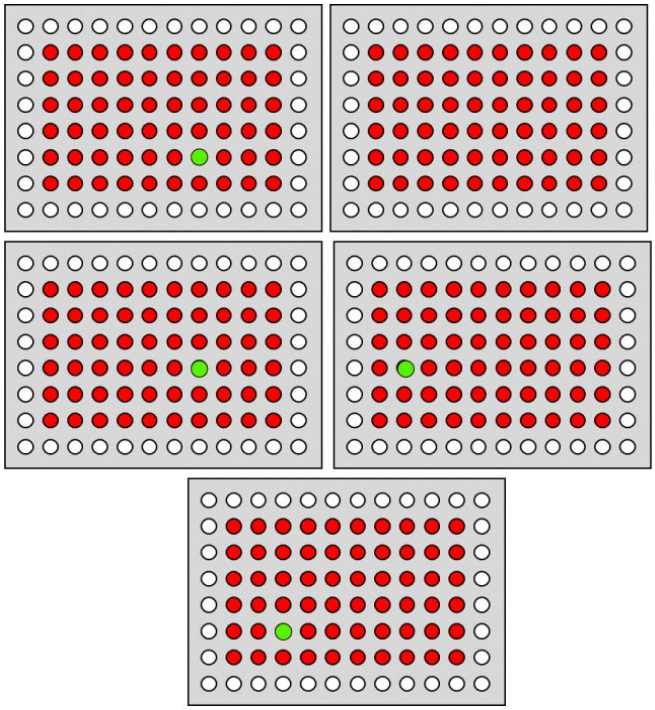

Figure 3.8: Schematic of foci platform results for U87 R132H screen.

Potential hits labelled in green were attempted to be expanded for further analysis. No hits were successfully expanded that have ATRX knockout.

3.6. Immortalized Astrocyte clone screening

In addition to using glioma cell lines, I also wanted to compare in a cell line that had less background mutations but was still relevant to the brain cancer setting. I chose immortalized astrocytes as this model. Immortalized astrocytes are normal human astrocytes with only a few mutations that keep them growing in cell culture (Wang et al., 2019).

The same gRNA A from Table 3.2 was used and successful cleavage at the cut site was seen using the same T7 endonuclease assay (Figure 3.9).

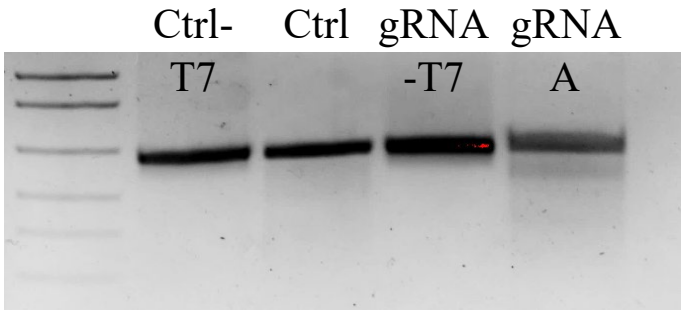

Figure 3.9 Successful cleavage with Cas9 and gRNA A in immortalized astrocytes. After transfection with Cas9 and gRNA A or mock transfection, T7 endonuclease assay was performed on PCR amplified region of exon 9 of ATRX.

I then employed the foci screening platform used to screen of the U87 cell lines, this time with increased success. With 14 clones of interest in the initial screening, nearly 6% of the clones tested had evidence of ATRX knockout (Figure 3.10). Of these five were found to have no ATRX expression through western blot. This could be because these cells grow more readily from a single cell than the U87, and that they also had more efficient Cas9 cleavage. Clone 3-B7 was chosen to be used for further characterization.

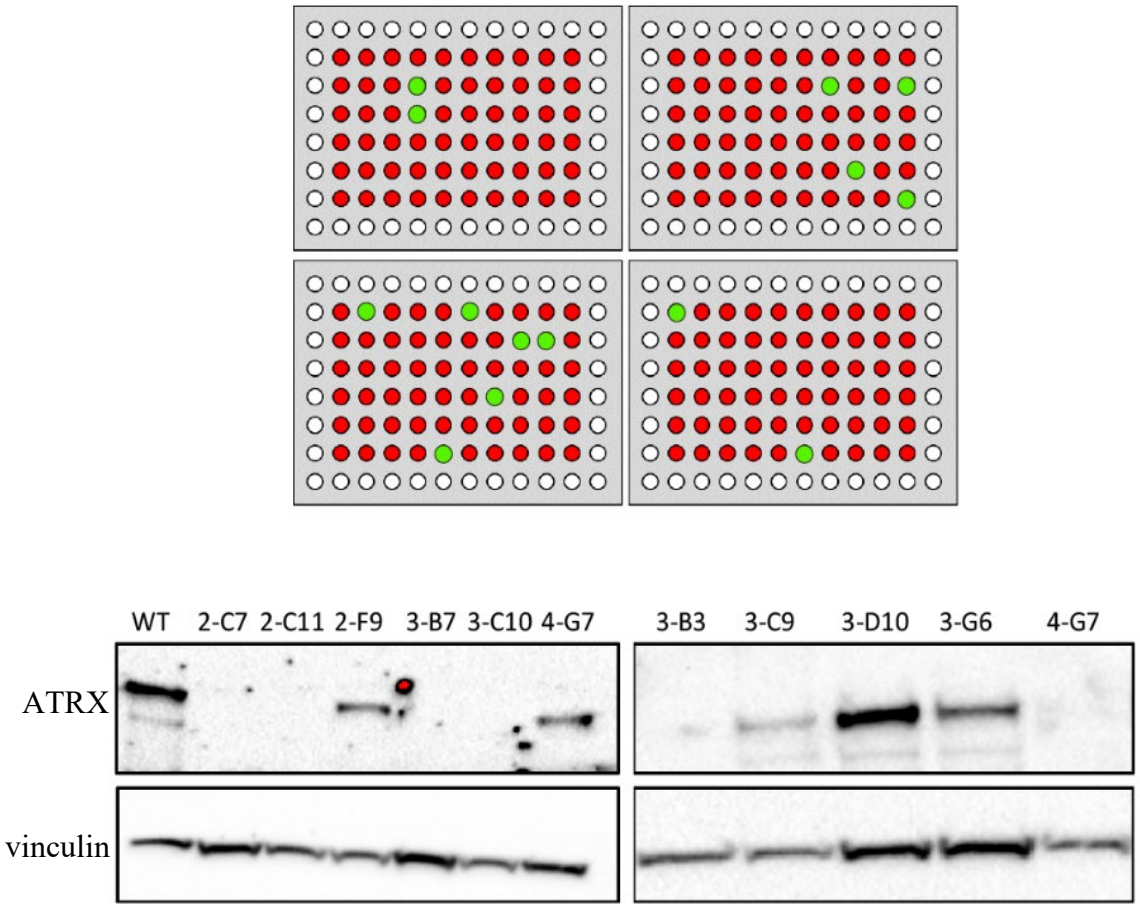

Figure 3.10 Utilization of immunofluorescence foci pipeline.

Representation of screen for immortalized astrocyte clones. Potential hits labelled in green were expanded for further analysis. Representative western blots shown below of selected clones. Clone 3B7 was chosen for further characterization.

3.7. Discussion

CRISPR is a valuable tool for the creation of isogenic cell lines. These cell lines give the ability to compare as similar conditions as possible, with only the gene of interest differing between them. However, there are many important factors to the success of these CRISPR knockout cell lines.

One important element to the creation of these cell lines, is the design of the CRISPR gRNA. While at first I focused on ensuring the knockout location being as close to the beginning of the protein as possible, this severely limited my options of strongly scored gRNAs. These first gRNAs I designed were the relatively better gRNAs, but did not have very high scores when compared to typical ideal CRISPR guide RNAs (Table 3.1 vs Table 3.2). While the gRNA I first chose (gRNA 2) was successful, the screening of clones was a very inefficient process, probably in part due to the low on-target score. This was why creating new guides was a crucial step to the eventual creation of the other cell lines.

I also found that certain cell lines are more adapted to the CRISPR screening process than others. For example, I was unable to find any U87 IDH1 R132H clones to successfully knockout ATRX. I screened double the number of clones that was used for the U87 parental cell line, and yet had very few potential options, nearly all of which died during attempted expansion (Figure 3.8). This suggests a biological difficulty in creating this cell line, despite the frequency of co-occurrence in tumors. While out of scope for this work, a way to determine if this was the case would be to try to create the cell line again but in the presence of an R132H inhibitor. The inhibitor would block 2HG production and essentially allow the cell line to behave more like wild type until expanded and 2HG production could be allowed to continue.

In the literature there have been two creations of this double mutant cell line (Mukherjee et al., 2018; Núñez et al., 2019). In both, ATRX knockout/knockdown was performed first, then IDH1 R132H overexpression. This could perhaps indicate that this order of mutation is necessary in patients for tumor growth. This further supports the necessity of further study of the interplay of these two mutations.

Overall, the CRISPR knockout method I chose can be inefficient, as transfection has a lower success rate than other methods such as transduction. However, I used this method because I wanted to ensure that Cas9 was not constitutively expressed in my cell line. As I am studying DNA repair capacity, I wanted to ensure that Cas9 was not nonspecifically cleaving DNA, even at low levels while my experiments were performed. I also did not want my cells to require antibiotic selection, as this is another variable that could affect how the cells behave. This method minimized the changes to the genome and helped create as ideal an isogenic pair as possible for my studies.

To help increase the efficiency of using this method, I developed a foci-based screening platform instead of screening through western blotting. This allows for many more clones to be screened at once before expansion, which can help making up for the inefficiency of transfection and no selection. The pipeline in its currently form relies on the fact that ATRX readily form foci at in the absence of damage (Figure 3.3). However, this method could be utilized for other proteins that do not form foci by instead quantifying intensity of staining. As long as proper optimization is done to ensure that there is a difference in visualization of a protein based on whether or not it is present, this method can be applied to many other proteins.

When utilizing all the information learned from this endeavor, many successful CRISPR knockout models can be created. Identifying ideal guide RNAs, cell lines and screening methods

are all important in the efficient creation of a strong model system to use for future studies. Once model cell lines are created, many different experiments can be performed to analyze the specific differences caused by loss of a protein, such as ATRX.

4. Characterization of LN229 and U87 ATRX knockout

4.1. Introduction

Understanding the DNA repair capacity of the LN229 and U87 knockout cells is important for learning how to treat these mutations in the clinic. As there are many DNA damaging agents and repair inhibitors already used therapeutically, being able to use ATRX status as a biomarker would be very advantageous. Since DNA repair defects can often lead to increased mutational rate, many believe inhibiting these mutations is the solution to halting cancer growth. However, exploiting these defects instead can be a powerful tool to kill cancer cells. By analyzing a mutations specific DNA repair defect, inhibitors to alternative repair mechanisms can be utilized to overwhelm the cell with DNA damage.

To identify how DNA damage is repaired in a cell, investigating the signaling components is often a key step. This is often done through foci analysis for specific DNA repair factors. DNA damage sites recruit many copies of repair factors that can be identified through immunofluorescence, called foci. The number of foci at various times can be used to determine the amount of DNA damage and repair is occurring. Two major markers of DNA damage signaling are γH2AX and 53BP1.

γH2AX is the phosphorylation of histone H2 variant H2AX at residue serine 139. This phosphorylation can be performed by ATR, ATM and DNA-PKcs to signal the chromatin location of a DNA break. This is one of the earliest signals for a DNA break, and so is a great tool to determine how many breaks are occurring throughout the genome (Kuo and Yang, 2008; Paull et al., 2000). This signal is propagated around the region of damage to create a platform for the recruitment of repair factors, whether homologous recombination (HR) or

nonhomologous end joining (NHEJ) factors (Collins et al., 2020). This phosphorylation event is now readily studied as an early stage indicator of DNA damage and can be used to compare differences in amounts and response to damage.

53BP1 is another factor well studied in the DNA repair field. A signal downstream from γH2AX, 53BP1 is important for pathway choice and recruitment of many other DDR factors. Its recruitment favors nonhomologous end joining and alternative end joining (Mirza-Aghazadeh-Attari et al., 2019; Ward et al., 2003; Xiong et al., 2015). This factor along with γH2AX can show how much DNA damage and repair is occurring in a cell.

Another way to determine a DNA repair defect in cells is to compare the survival of cells in the presence of DNA damaging agents and repair inhibitors. By screening different compounds, a synthetic lethal interaction can be identified. Synthetic lethality is the concept that while knocking out one gene (in this case ATRX) allows for cell survival as well as the independent inhibition of another protein, but when both are lost cells are no longer able to survive. A classic example of this is BRCA loss and PARP inhibitor sensitivity (Bryant et al., 2005). While BRCA loss and PARP inhibitor are tolerated by cells, the combination is much more lethal than either action alone. Since this work much has been done to understand the relationship between BRCA1/2 and PARP, furthering knowledge of DNA repair mechanisms as well as providing a therapeutic option for patients with BRCA mutant tumors. Finding other synthetic lethality combinations for other cancer proteins, such as ATRX, is a promising strategy to discover other potential treatments.

By focusing on DNA repair capacity in ATRX knockout cells, it is possible to get mechanistic insights into the DNA repair process as well as potential therapeutic options for patients with these mutations. With the LN229 and U87 ATRX KO cell lines I showed a

decrease in homologous recombination and an increase in replication stress. While outside factors may have led to only minor differences in drug screen sensitivities, future study could widen these differences and allow for better options for further study.

4.2. LN229 and U87 ATRX KO Clone Validation

LN229 ATRX knockout was validated through three methods: western blot, immunofluorescence, and sequencing. As seen in Figure 4.1A-B, there is no detectable ATRX expression in these cells by western blot or through immunofluorescence staining.

Since there are multiple copies of ATRX in LN229, I performed TOPO cloning to amplify and sequence genomic PCR products individually. Out of 65 products sequenced, there were 22 copies of a 136 base pair insertion and 43 copies of a 1 base pair deletion (Figure 4.1C). The uneven amounts of each sequence type could be due to different integration rate of the different sized PCR products.

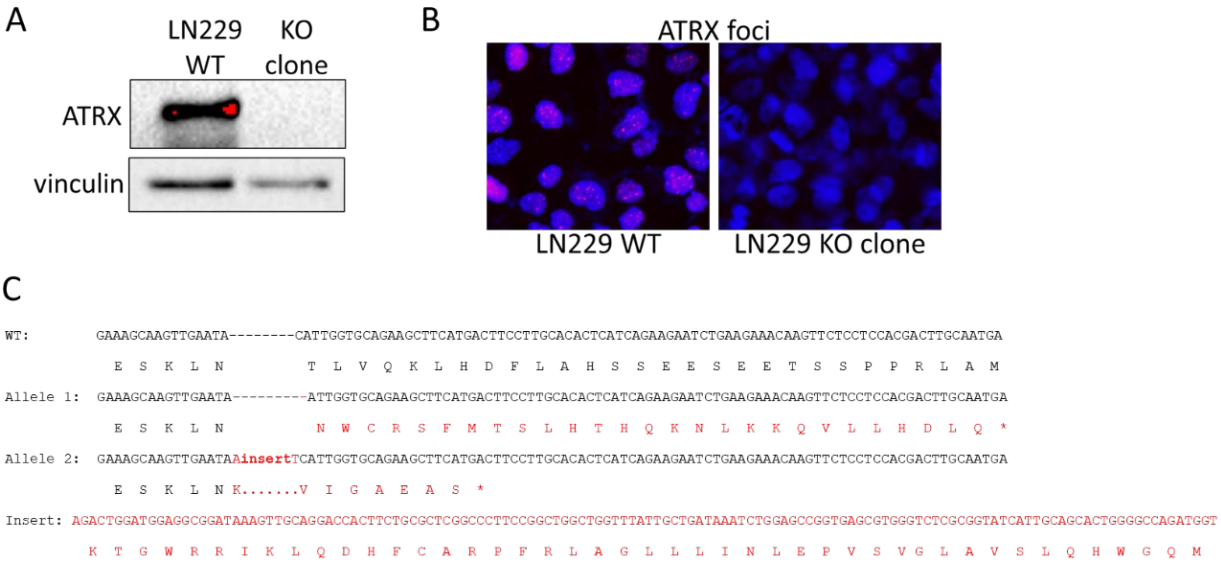

Figure 4.1: LN229 ATRX knockout clone validation

A) Western blot showing ATRX levels in WT vs ATRX knockout (KO) clone. B) Immunofluorescence staining for ATRX in WT and KO cell lines. Cells were stained with Hoescht dye for nuclear staining as well as ATRX antibody C) Sequencing data from the ATRX KO clone. Mutation is shown in red. While allele 1 has a 1 base pair deletion, allele 2 has a 136 base pair insertion. Insertion sequence is listed below so alignments between KO alleles and WT can be compared.

While validating ATRX KO, I noticed that there were typically more cells in my ATRX knockout plates than in the parental LN229 ones. To quantify this difference, I seeded equal numbers of both cell lines and tracked their growth overtime. I determined that there were more cells in the ATRX knockout wells at each time point, including the initial time point. Since this could be due to an increase in cell adherence or initial seeding, I then repeated the experiment using 1,000 and 2,000 cells per cell line. I found that despite having fewer cells by 24 hours, ATRX knockout cells had more cells than the parental line by 96 hours (Figure 4.2). This suggests that ATRX knockout cells proliferate at a higher rate than the parental cells.

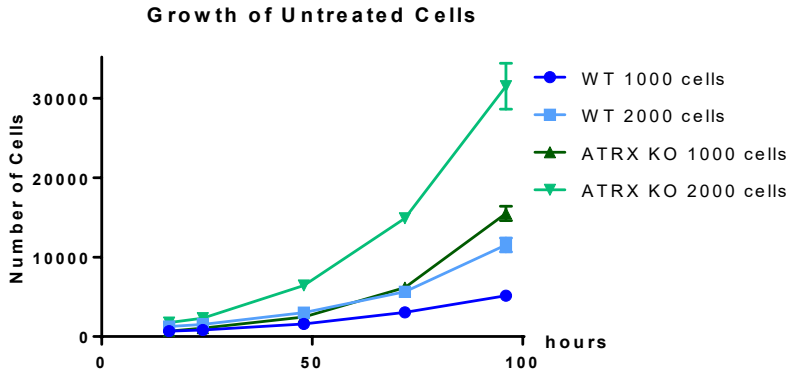

Figure 4.2: Growth rate of LN229 WT vs ATRX KO cells

1,000 or 2,000 cells per well were plated in multiple 96 well plates. At each time point over 96 hours, one plate was fixed and number of cells were counted. WT counts are shown in blues and ATRX KO cell counts are shown in greens.

I validated the U87 ATRX KO cell lines in a similar manner. First confirmation of knockout was shown through western blot and immunofluorescence in clone B4 and clone C9 (Figure 4.3A-B). Then TOPO sequencing was performed to attain allele sequences on both clones. For clone C9, 13 sequences had a 26 base pair deletion and 18 sequences had a 1 base pair insertion. Both mutations lead to a stop codon and a lack of functional protein (Figure 4.3C).

For Clone B4, while one 18 sequences contained a 2 base pair deletion, 6 sequences led to a 9 base pair deletion (Figure 4.3C). The 9 base pair deletion leads to a loss of 3 amino acids and remains in frame for the rest of the protein. However, since there is a lack of detectable expression, this could still be leading to lack of expression. This could occur because the mutation deletes three amino acids in an alpha helix in the ADD domain of the protein. This deletion could lead to misfolding and degradation of the mutant protein. Additionally, as ATRX is located on the X chromosome, this second allele could be inactivated with the rest of the X chromosome, leaving only the non-functional first allele to be expressed. However, since this mutant protein could be expressed at low levels, I primarily focused my work on clone C9.

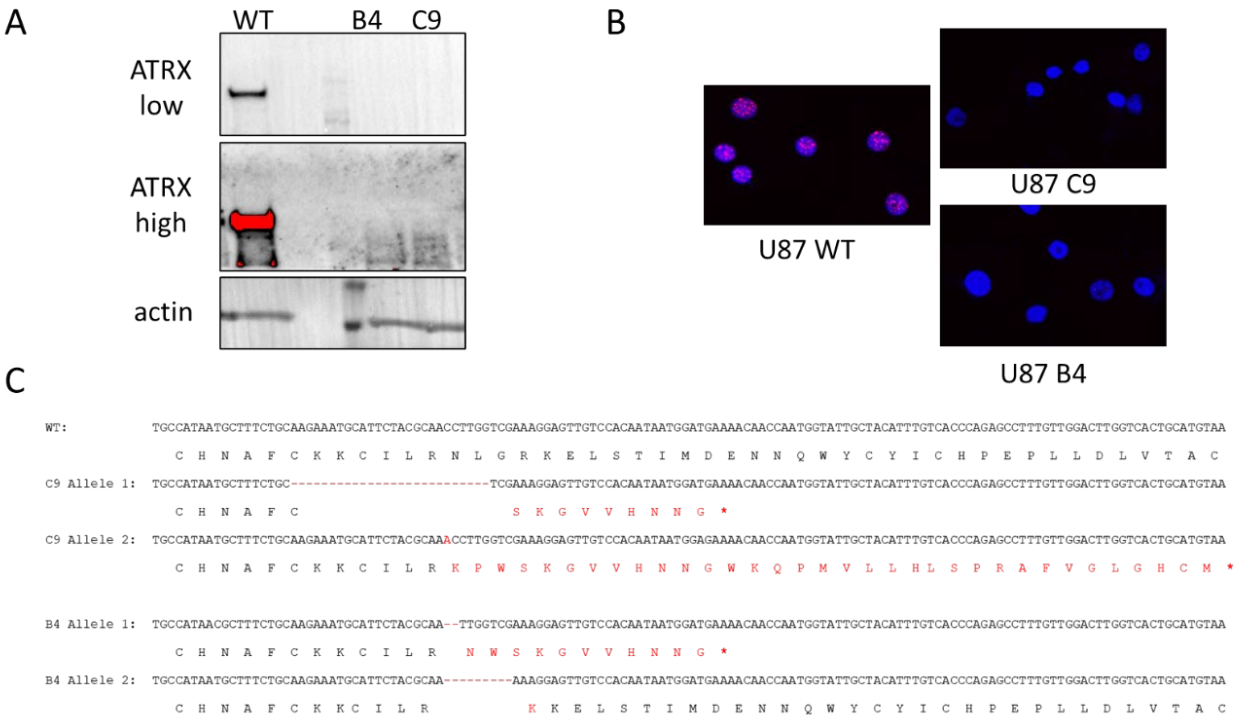

Figure 4.3: U87 ATRX knockout clone validation

A) Western blot showing ATRX levels in WT and ATRX knockout cells for both U87 clones. B) Immunofluorescence staining for ATRX in WT and KO cell lines. Cells were stained with Hoescht dye for nuclear staining as well as ATRX antibody C) Sequencing data from the ATRX KO clone. Mutation is shown in red for both DNA and amino acid sequence.

I then began to characterize the C9 ATRX knockout cell line. These cells have a different morphology that causes them to not form the same structures as the wild type cells (Figure 4.4B). This leads to these cells becoming confluent on the plate with less cells present (Figure 4.4A). This change could be due to a cloning artifact, as many of the single cell clones observed had different morphologies regardless of ATRX status, or from ATRX loss itself.

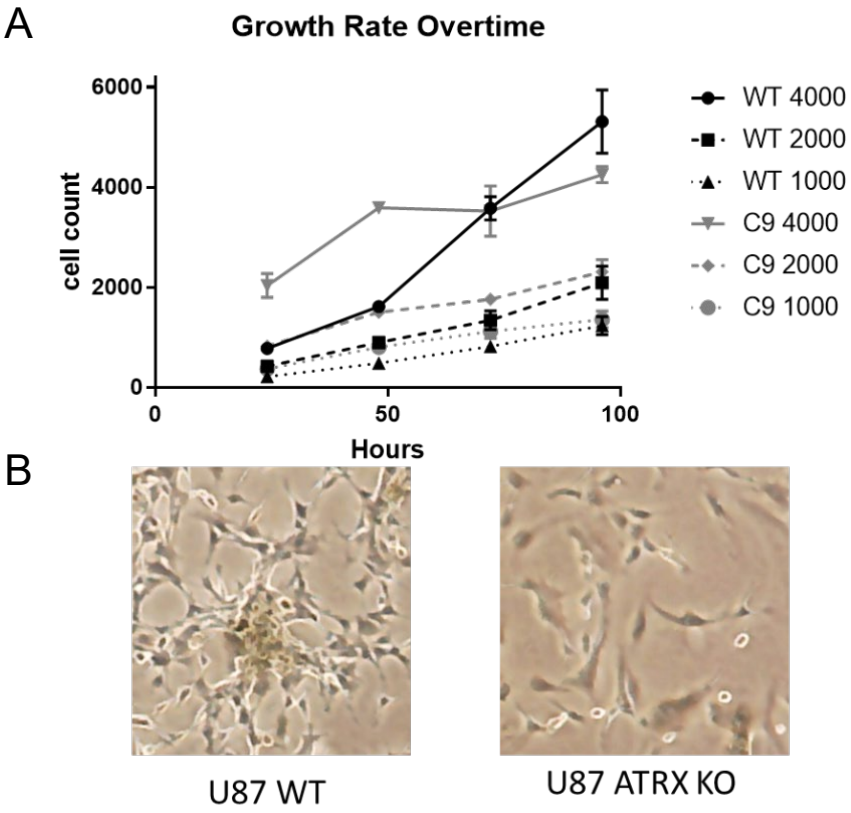

Figure 4.4: Growth of U87 ATRX KO clone altered from WT

A) 1,000, 2,000 cells or 4,000 cells per well were plated in multiple 96 well plates. At each time point over 96 hours, one plate was fixed and number of cells were counted. WT counts are shown in black and ATRX KO cell counts are shown in gray. Solid line indicates 4000 cells plated, dashed line is 2,000 cells and dotted line is 1,000. B) Visualization of changes in morphology between WT and ATRX KO cells. Typical U87 cell clustering is abrogated in ATRX KO cells

4.3. DNA repair capacity

After these clones were established, the next step was to determine their DNA repair capacity. These glioma lines were characterized by their ability to perform homologous recombination, signal for damage and propensity for double strand breaks. Overall, I found a modest but consistent DNA repair defect in these cell lines, specifically suggesting deficiencies with homologous recombination and increased replication stress.

The ability of these cells to repair DNA through homologous recombination or nonhomologous end joining was investigated through a luciferase reporter assay. In this assay a linearized plasmid is transfected into cells and repair leads to luminescence. For HR, luminescence only occurs when a template further down on the plasmid is used to repair the break and for NHEJ luminescence occurs if the repair causes a frame shift leading to expression (Figure 4.5D).

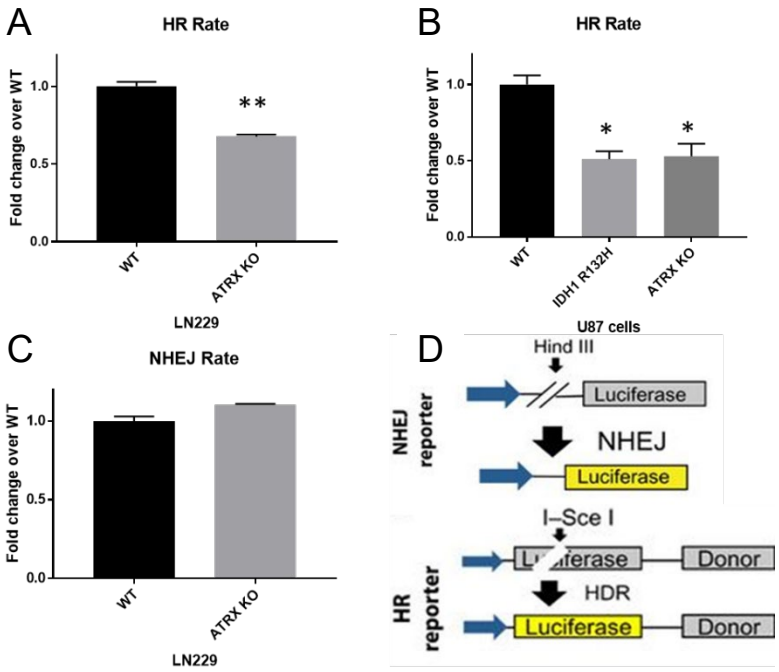

Figure 4.5: Homologous Recombination rate decreased in ATRX KO cells

A) Homologous recombination rate in LN229 cells compared between WT and ATRX KO B) Homologous recombination rate in U87 cells with ATRX KO or IDH1 R132H mutation compared to WT. For A) and B) Cells were analyzed 48 hours after transfection and normalized to Renilla luciferase signal before normalization to fold change over WT. C) Nonhomologous end joining rate in LN229s using NHEJ reporter plasmid. Cells were analyzed 24 hours after transfection and normalized as above. D) Schematic depicting the repair needed for luciferase to be expressed in both reporter assays.

I have found that in both LN229 and U87 cells the reporter plasmid is unable to be repaired by homologous recombination as readily in the ATRX KO cells as in comparison to their WT counterparts (Figure 4.5A-B). I have also found that the LN229s have no change in the ability to perform NHEJ repair of the transfected plasmid (Figure 4.5C). The NHEJ assay in the U87s was too toxic to determine the luciferase rate, but U87s were able to be compared to the U87 R132H cell line which has a known homologous recombination defect (Sulkowski et al., 2017). I see a similar rate of homologous recombination in these two mutant cell lines (Figure 4.5C), which suggest that ATRX KO has equivalent DNA repair defect to the IDH1 mutant cell line.

In addition to identifying changes in homologous recombination, I also wanted to investigate increases in replication stress in the ATRX KO cells. Following evidence in the literature of replication stress, I first looked at the effect of hydroxyurea treatment overtime (Leung et al., 2013). I found that at 18 and 24 hours after treatment there was an increase in γH2AX foci, a marker for DNA damage in ATRX deficient cells (Figure 4.6). To ensure that this was not due to the cells becoming confluent faster due to their faster growth rate, I repeated this experiment with different amounts of cells and achieved the same results (data not shown). This could suggest that ATRX knockout cells have increased levels of replication stress, as well as the homologous recombination defects seen above (Figure 4.5).

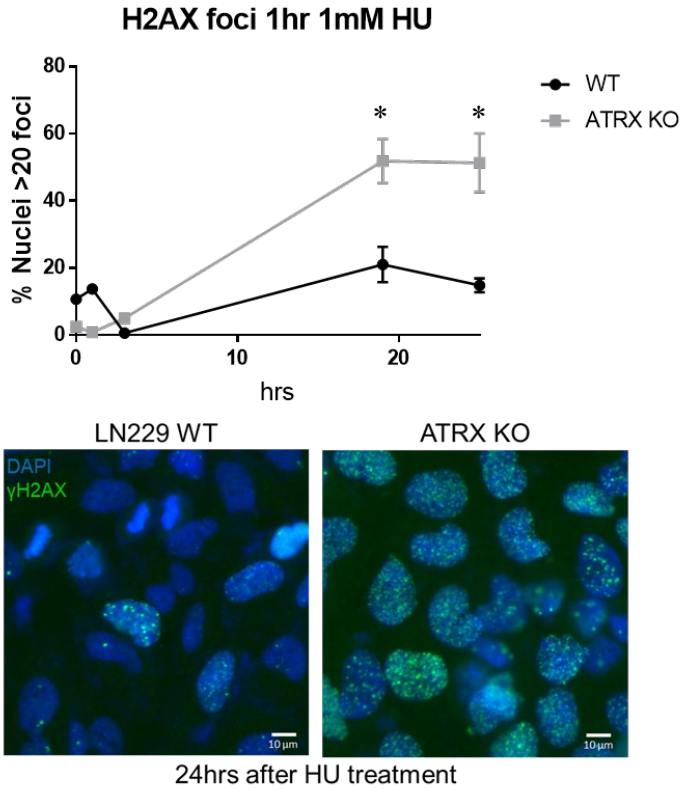

Figure 4.6: LN229 ATRX KO has increased levels of γH2AX foci after HU treatment

LN229 WT and ATRX KO cells were analyzed at 1, 3, 18 and 24 hours after 1mM HU treatment. Percentage of cells with greater than 20 γH2AX foci were quantified for each condition. Representative image shows γH2AX levels 24 hours HU treatment.

Once the U87 ATRX KO cell line was created, I also investigated its response to hydroxyurea. I found that the ATRX KO U87 cells showed similar increase in γH2AX levels after 18-24 hours of hydroxyurea treatment to their LN229 counterparts (Figure 4.7). Additionally, this was similarly elevated in the U87 R132H parental cell line, which has been shown to have these increases in these foci previously at baseline (Sulkowski et al., 2017). This suggests that there is also increased replication stress in both the U87 and LN299 ATRX KO cell lines. Interestingly, the U87 cell line also had large increase in untreated γH2AX and 53BP1 levels. I hypothesize that ATRX knockout lead to increases in accumulated DNA damage, as DNA repair capacity is lowered in these cells.

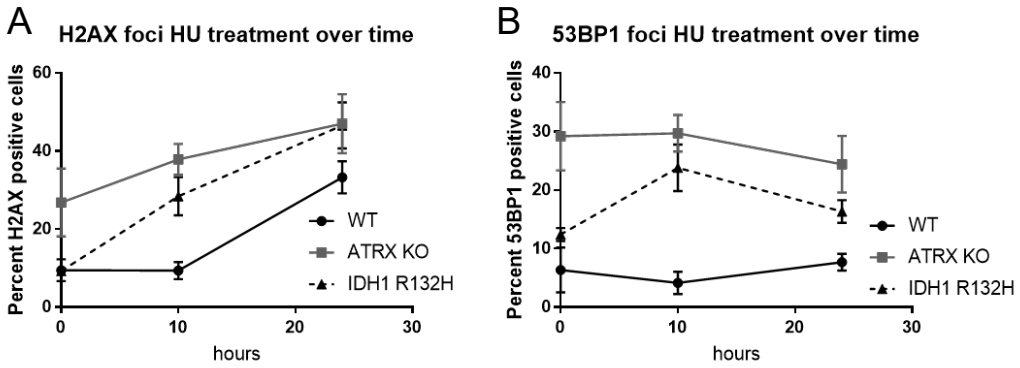

Figure 4.7: U87 ATRX KO cells have increased γH2AX and 53BP1 levels

U87 cells were analyzed at 0, 10 and 24 hours after 1mM HU treatment. Cells were counted as positive with greater than 20 γH2AX and 10 53BP1 foci. ATRX KO is shown in gray and IDH1 R132H is shown with a dashed line.

I then performed a comet assay to determine if an increase in DNA breaks was occurring in the LN229 cells. I found that there were trending increases in both baseline DNA breaks as well as breaks after radiation (Figure 4.8). This could also indicate an increase in double strand breaks, and further work could expand to more time points to better understand this result. It would be interesting for future work to see if this repeated in the U87 cell line.

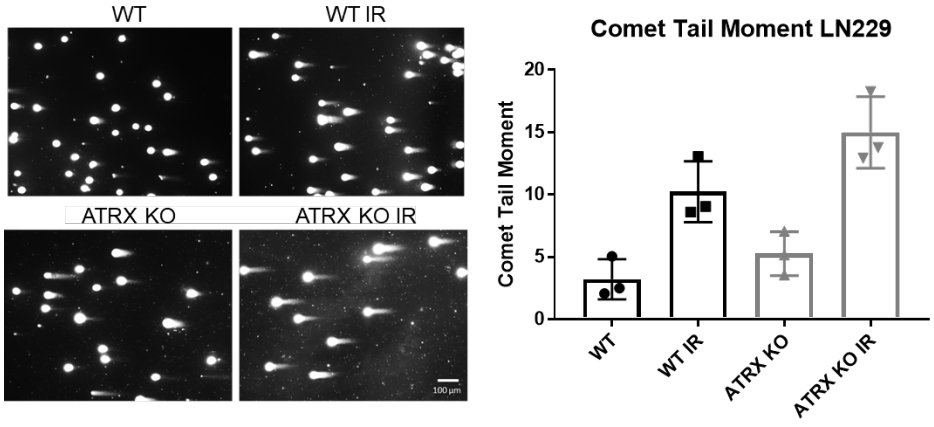

Figure 4.8: Increase in double strand breaks in LN229 ATRX KO cells

Comet assay was performed to identify double strand breaks in LN229 cells. Cells were harvested 1 hour after 10 Gy radiation, or no treatment. Average comet tail moment over 3 independent experiments were graphed. In each experiment at least 50 comet tails were analyzed using Open Comet (Gyori et al., 2014).

4.4. Drug Screen

Since ATRX loss leads to a DNA repair defect I then performed a drug screen aimed to exploit this deficiency. This was done by focusing the screen on DNA damaging agents and repair inhibitors. In addition to therapeutic relevance, the specific targets of inhibitors that show differential sensitivity can be further studied to provide mechanistic insights into the DNA repair defect in ATRX KO cells.

I performed a preliminary drug screen using 24 DNA repair related compounds. Each compound was used at 7 concentrations in a 96 well plate and fixed 96 hours after treatment (Figure 4.9). After counting Hoechst dye-stained nuclei, I was able to determine whether ATRX knockout cells were more sensitive to any of the compounds tested (Figure 4.9A). In this drug screen, I tested both of the identical clones from my clone screen as a control (Figure 3.2), listed as ATRX KO and ATRX KO repeat (Figure 4.9B).

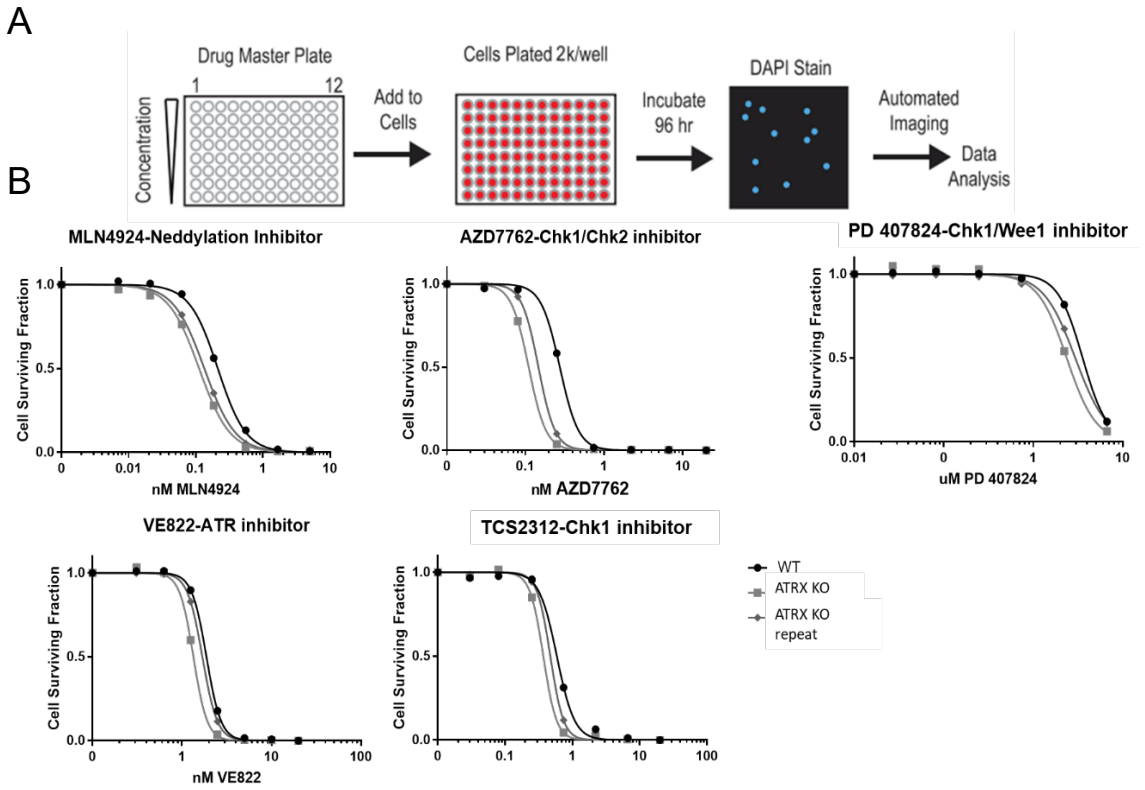

Figure 4.9: Drug Screen in LN229 ATRX KO cells shows sensitivity to Chk1 inhibitors

A) Schematic of drug screen technique. Each column of a 96 well plate has a different drug to allow for screening of multiple compounds. B) Representative images of successful hits from the screen, showing that nearly all hits inhibit CHK1. ATRX KO and ATRX KO repeat are the two identical clones 87 and 180 found in the screening process (Chapter 3.2)

Most compounds did not show sensitivity differences between WT and ATRX KO cells. However, few did show approximately two-fold differences in IC_{50}. Interestingly, three of the five compounds with these differences inhibited CHK1 (Figure 4.9B). This could also imply increased replication stress such as seen with the foci data, as CHK1 is an important component of the ATR pathway that signals for replication stress (Saldivar et al., 2017). However, since

these differences were small, it appears that adding DNA damaging agents will be needed to enlarge the differences between the parental and ATRX knockout cells.

Additionally, adding other common mutations in genes such as IDH1 may be necessary to find larger differences. To investigate this, I overexpressed the R132H mutant in the ATRX KO cell line (Figure 4.10).

I then screened compounds in the LN229s to identify ones that specifically target these double mutant cells. I have compared the doxycycline inducible R132H LN229 cells with and without ATRX KO to determine changes in sensitivity to DNA repair inhibitors and DNA damaging agents. I tested 20 compounds and found a few possible changes in sensitivity in the double mutants (Figure 4.11).

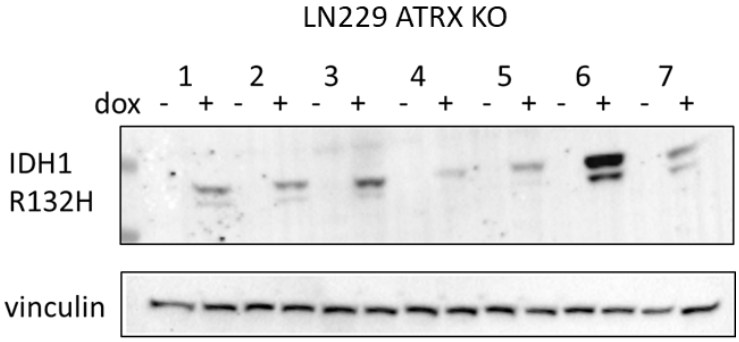

Figure 4.10: Expression of IDH1 R132H in LN229 ATRX KO cells

Screen of multiple single cell clones of LN229 ATRX KO with IDH1 R132H overexpression. Mutant IDH1 expression was induced with 2μg/ml of doxycycline for at least 48 hours before analysis. Clone 3 and 6 were chosen for further study.

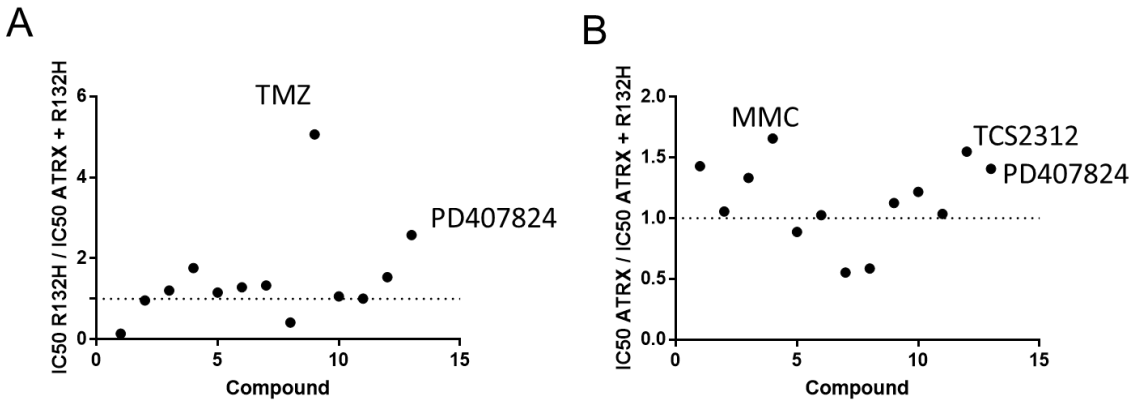

Figure 4.11: Drug screen comparing WT, ATRX KO, IDH1 R132H and double mutants

Drug screen was performed as seen in Figure 4.9A. IC_{50} of each drug was compared between the four cell lines. The IC_{50} between A) R132H and B) ATRX KO and the double mutant were divided and the ratio plotted. Ratios greater than 1 indicate greater sensitivity in the double mutant cells than the individual mutations. A) shows compounds sensitive specific to ATRX KO and B) shows compounds sensitive to R132H addition. PD407824 is a Wee1/CHK1 inhibitor and TCS2312 is a CHK1 inhibitor

While TMZ appeared to have a difference in sensitivity (Figure 4.11A), this was found to be an artifact of the screen and unable to be repeated. However, it is interesting that two of the CHK1 inhibitors (PD407824 and TCS2312) were found to be slightly more sensitive to double mutant sensitivity than ATRX KO alone. As these hits were found in the previous drug screen (Figure 4.9B) it is promising that CHK1 is an interesting target in ATRX KO cells as well as the double mutant cells.

4.5. Discussion

The investigation of DNA repair capacity in the LN229 and U87 ATRX KO cell lines provides great evidence that ATRX KO can be exploited therapeutically. There is evidence of both homologous recombination defect as well as increased replication stress in these cells. This

was found through plasmid reporter assays, increases in γH2AX and 53BP1 foci after hydroxyurea treatment and sensitivity to CHK1 inhibitors.

While the decrease in homologous recombination is interesting, further work could be done to explore this mechanism. Difficulties with the toxicity of the assay led to variations in results and an inability to combine with control siRNAs to central DNA repair proteins such as BRCA1 for HR and Ku80 for NHEJ. A great assay to minimize these toxicities would be the EJ-DR reporter assay that has both HR and NHEJ assays integrated into the cell line so no transfection is necessary (Bindra et al., 2013). Unfortunately, this assay is in the U2OS cell line, which already lacks ATRX expression (Lovejoy et al., 2012). Over expression of ATRX using a plasmid has so far been unsuccessful, perhaps due to IS10 insertion (Valle-García et al., 2014) and is currently being optimized. Additional studies that could be done to look at homologous repair deficiency are foci studies of HR markers (BRCA1, RAD51, BRCA2). However, it was decided to prioritize the replication stress phenotypes in these cells for future work.

The increase in γH2AX and 53BP1 foci after hydroxyurea treatment indicates an increase in replication stress. While this was seen at later timepoints than in the literature (Leung et al., 2013), this could suggest that the ATRX KO cells are stalling in S phase as they have more difficulties with the stress caused by the lack of nucleotides due to hydroxyurea. This implies that ATRX KO cells are more sensitive to changes during replication, as they may already have low levels of replication stress that are heightened with damage. It is interesting that damage at baseline is seen in the U87 cell lines but not in the LN229. This could indicate that LN299s have increased capacity to handle replication stress than the U87s but this capacity is not enough to counteract the stress from hydroxyurea treatment.

To further investigate if increases in double strand breaks are occurring in the LN229s, I performed a comet assay. While not statistically significant, there is a trend for an increase in double strand breaks not only at baseline but also 1 hour after radiation. This further supports the idea that as these cells have an inability to repair DNA, especially when damage levels are increased by DNA damaging agents such as radiation. Further work could be done to identify if this occurs in the U87 cell line as well as later time points to increase the number of cells going through replication after radiation. It would also be interesting to see if this would be in enhanced in the double mutant IDH1 and ATRX KO cells. IDH1 R132H mutant cells have been shown previously to have increased comet tails and so the addition of ATRX knockout could lead to further differences (Sulkowski et al., 2017)

While the work in DNA repair capacity showed some differences between WT and mutant, very little differences were seen in the drug screen. This could be partially due to the increase in growth rate seen in the ATRX KO masking the differences in survival with these compounds. It is interesting however that despite the differences only being slight that they consistently showed sensitivity to CHK1 inhibition. As CHK1 is an important factor in the signaling of replication stress (Saldivar et al., 2017), this further supports that replication stress could be occurring in these cells. However, it seems that the differences in growth rate as well as unknown background mutations in these cell lines are making them resistant to different DNA repair inhibitors, and so focus was shifted to the immortalized astrocyte cell line for further drug screens.

5. LN229 ATRX KO CRISPR Screen

5.1. Introduction

CRISPR/Cas9 is a powerful molecular tool that can be used for additional purposes than creating model cell lines as described in Chapter 3. This technique can also be used to identify key genes related to a gene of interest. Referred to as a CRISPR screen, this assay has been used countless times to further identify mechanisms of survival in different cell lines and potential therapeutic targets for cancer cells.

In this method, numerous CRISPR/Cas9 gRNAs are created to make a library of potential gene knockouts. These are transduced into cells at a low multiplicity of infection, so that cells receive at most one CRISPR gRNA from the library. The cells are then put under selection and studied overtime by harvesting samples of cells periodically for next generation sequencing. This can be done with untreated cells, or while treating with a compound of interest. Each sample is then barcoded through PCR amplification and next generation sequencing is performed to identify each individual gRNA present in each sample. If a gRNA decreases in representation over time, this implies that cells with this gRNA have a growth disadvantage and so are sensitive to the loss of that gene. Conversely gRNAs that increase in representation give a growth advantage compared to controls which can also be studied mechanistically. Comparing how these population changes occur between drug treatments or cell lines gives targets of interest for further study.

For my work, I chose to do a targeted CRISPR screen focused on DNA damage response using a library from the Gupta lab (Feng et al., 2019). This library contains 284 genes that are known or suspected to be involved in DNA repair. Many of these proteins are involved in

multiple pathways, creating a very interconnected map of genes in this study (Figure 5.1). Using a more targeted approach for this CRISPR screen allows for increased coverage for each gene (10 or more gRNAs per gene). These and over 1000 non targeting control gRNAs give a total of nearly 4000 gRNAs in the library. The gRNAs for each gene can then be pooled and their representation in the population can be compared to the non-targeting controls over time.

KEGG Pathway	Genes
Fanconi anemia	42
Nucleotide excision repair	34
Homologous recombination	31
Base excision repair	29
Cellular senescence	25
Cell cycle	22
Chromosome and associated proteins	22
p53 signaling pathway	17
Mismatch repair	16
Metabolic pathways	16
DNA replication	14
Ubiquitin mediated proteolysis	12
Non-homologous end-joining	11
Lysine degradation	11
Basal transcription factors	9

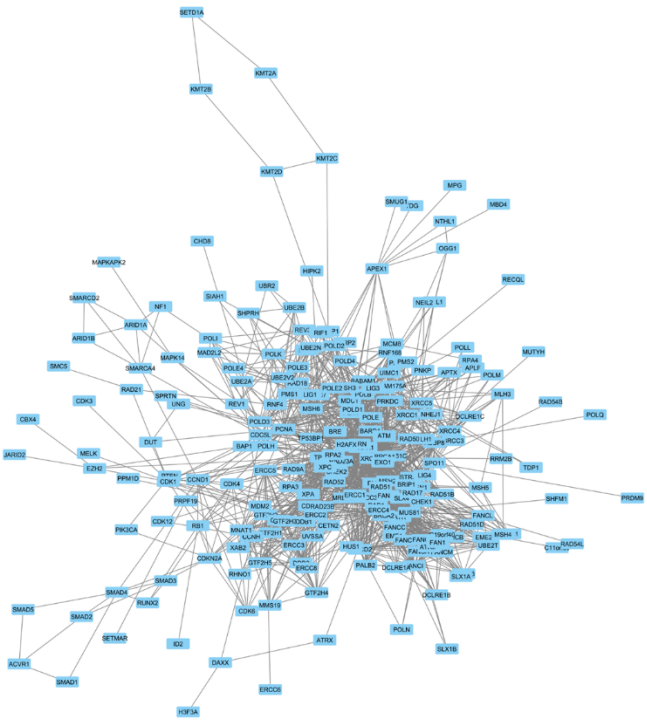

Figure 5.1: Genes in CRISPR screen library

284 genes in multiple DNA damage response pathways were tested in this screen (left). Many genes overlap in these pathways, leading to a complex network (right).

I performed this screen in duplicate, with the second screen being more robust than the first through increased cell sample size. These screens gave multiple interesting hits to further pursue, such as XPC, KDM2A, and UHRF1 that are more sensitive to ATRX loss compared to WT. Further mechanistic insights into ATRX's role in DNA repair can be elucidated with future work understanding these CRISPR screen hits.

5.2. Initial CRISPR Screen

I performed a CRISPR screen to identify targets that are synthetically lethal (see Chapter 3.1) with ATRX knockout. I transduced both cell lines with the CRISPR library pool targeting 284 DNA repair related genes. After puro selection, I harvested the cells over two weeks and purified the genomic DNA. I then performed a PCR of the CRISPR guide sequence incorporated into the genome and barcoded each sample through a second PCR (Figure 5.2). While there are large bands from the primers annealing to each other, it was possible to isolate the top band and send for next generation sequencing. Round 3 PCR was also performed to validate the success of the amplifications from the first two rounds.

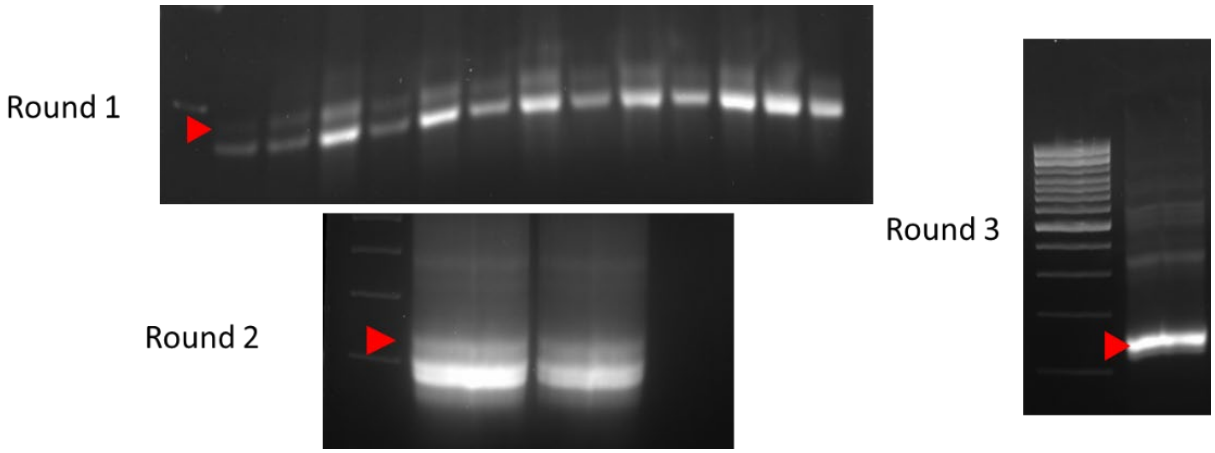

Figure 5.2: Representative CRISPR Screen PCR

CRISPR insertion region is amplified in round 1 and barcoded in round 2. Round 3 is performed to confirm successful amplification.

The next generation sequencing data was then processed by Dr. Gregory Breuer. I received the beta scores for each gene tested, which combines the effect of the gene as well as the confidence in that effect. To increase the power of the experiment, he pooled each of the different day results into one beta score per gene. By looking at the difference between these scores I can determine potential synthetic lethal targets with ATRX (Figure 5.3).

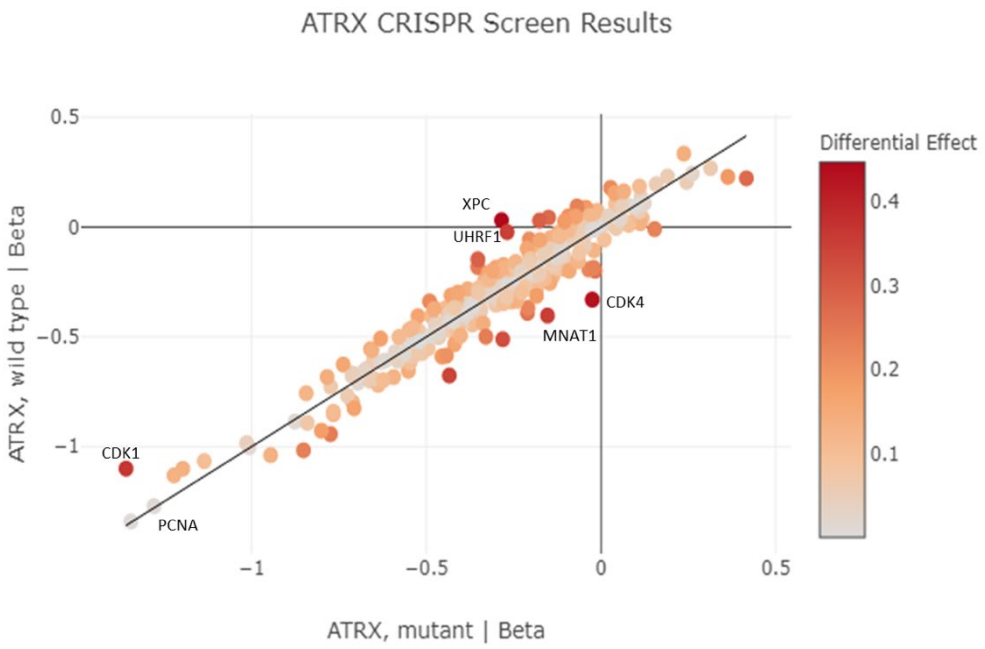

Figure 5.3: First CRISPR Screen beta scores

Beta scores were calculated as -log10(p-value)*(effect size). Plot shows the deviation of the WT and ATRX mutant score from each other (y=x). An increased differential effect is highlighted with a darker point. Beta scores were calculated by Greg Breuer and plot was created by Sam Friedman.

In Figure 5.3, the color of each point indicates how far each gene of interest deviated from equal sensitivity in WT and ATRX KO cells. Points above the line indicate gRNAs that were more represented in the WT than the ATRX KO. This suggests that the ATRX KO cells were more likely to lose this gene through the experiment as these cells were less likely to survive. These genes such as XPC and UHRF1 could be potential targets for synthetic lethality with ATRX loss. While less therapeutically relevant, the points below the equal sensitivity line can also give insight to mechanistically what genes are less relied on when ATRX is lost. These could be genes that are in the same pathways as ATRX, as their loss is epistatic with ATRX loss. In this screen CDK4 and MNAT1 are both cell cycle proteins, suggesting that there are already

irregularities in cell cycle when ATRX is knocked out, making these genes less necessary for survival.

5.3. Improved CRISPR Screen

After performing the initial screen, I learned many ways to increase the robustness of the screen. I repeated the screen and greatly scaled up the cells, harvesting 8 million cells for each cell line instead of the 1-2 million from the initial screen. This larger input size allowed for that the days harvested to be analyzed independently, and so differences over time were able to be analyzed. The overall trends can be seen in Table 5.1. The difference calculation is now able to involve the representation over time due to the increased power.

Gene	sgRNA	WT_D4	WT_D7	WT_D10	WT_D14	ATRX_D4	ATRX_D7	ATRX_D10	ATRX_D14	diff
XRCC3	10	0.10	-0.04	-0.27	-0.71	-0.25	-0.48	-0.94	-1.47	-1.43
POLD2	10	0.15	-0.25	-0.33	-0.57	-0.37	-0.63	-0.92	-1.24	-1.27
CCNH	10	0.00	-0.52	-0.80	-1.00	-0.14	-0.93	-1.28	-1.71	-1.20
UHRF1	10	-0.12	-0.28	-0.71	-1.14	-0.23	-0.60	-1.23	-1.70	-1.07
PARP3	10	0.09	0.14	-0.01	-0.04	-0.15	-0.41	-0.51	-0.61	-1.07
CLK2	10	0.10	0.08	-0.12	-0.05	-0.25	-0.35	-0.59	-0.65	-1.07
UNG	10	0.13	0.09	0.11	0.01	-0.08	-0.32	-0.44	-0.50	-1.06
POLD1	10	0.12	-0.16	-0.50	-0.88	-0.29	-0.76	-1.05	-1.36	-1.03
GTF2H3	9	-0.04	-0.11	-0.47	-0.62	-0.10	-0.67	-0.94	-1.15	-1.01
XAB2	10	-0.16	-0.43	-0.64	-0.52	-0.70	-0.91	-1.05	-1.10	-0.99
KDM2A	10	-0.02	-0.08	-0.14	-0.39	-0.28	-0.48	-0.67	-0.83	-0.97
FANCC	10	0.03	0.08	-0.06	-0.05	-0.31	-0.36	-0.40	-0.68	-0.96
GTF2H1	10	0.01	-0.38	-0.59	-0.78	-0.07	-0.62	-1.09	-1.22	-0.93
DCLRE1B	10	-0.09	-0.20	-0.29	-0.53	-0.03	-0.44	-0.81	-0.94	-0.93
LIG1	10	0.44	0.37	0.24	0.14	-0.09	-0.14	-0.21	-0.34	-0.93
NUDT1	10	0.28	0.32	0.22	0.12	-0.20	-0.15	-0.30	-0.28	-0.92
EXO1	10	-0.06	-0.19	0.03	-0.14	0.16	-0.30	-0.53	-0.50	-0.92
CUX1	10	0.01	0.15	0.14	0.11	-0.29	-0.19	-0.37	-0.29	-0.92

Table 5.1: Top hits from repeat CRISPR screen

Genes with greatest difference between WT and ATRX KO cells. Difference was calculated as the sum of WT day 10 and 14 subtracted from ATRX KO day 10 and 14. Negative values indicate loss in representation in the screen.

In this screen, the top results were genes such as the Rad51 paralog XRCC3, replication and repair polymerase polδ and the chromatin modifier UHRF1. The top overrepresented gene in the ATRX KO cells was BRCA1, which can indicate that there is a homologous recombination defect in the ATRX KO cells that causes them to less reliant on BRCA1. These genes occurred in many repair pathways, but most were in the nucleotide and base excision repair pathways (

Table 5.2). Since many genes are in multiple pathways, many pathways had multiple hits.

KEGG Pathway	**Genes**
Nucleotide excision repair	6
Base excision repair	5
Mismatch repair	4
DNA replication	3
Basal transcription factors	3
Chromosome and associated proteins	3
Homologous recombination	3
Cell cycle	1
Fanconi anemia pathway	1

Table 5.2: Top pathways for CRISPR screen hits

CRISPR screen hits were seen in many repair pathways as well as DNA replication and some chromatin associated factors.

5.4. Comparison of Screens

When comparing the hits from the two screens, it quickly becomes apparent how the change in initial cell number helped strengthen the results. As seen in Figure 5.4, the overall range in difference in beta scores is much higher in the second screen than the first. Due to this, different thresholds were used to determine the top scoring gRNAs, which can be seen as a red line in Figure 5.4.

Despite the differences in robustness, 25% of the top 40 hits from both screened overlapped, showing the validity of even the smaller screen (Figure 5.5). These overlapping top genes tend to fall into the nucleotide and base excision repair pathways as well as chromosome and associated proteins. However, those in bold (CLK2, KD2A and UHRF1) were the genes with the greatest difference in both screens and were chosen for preliminary validation.

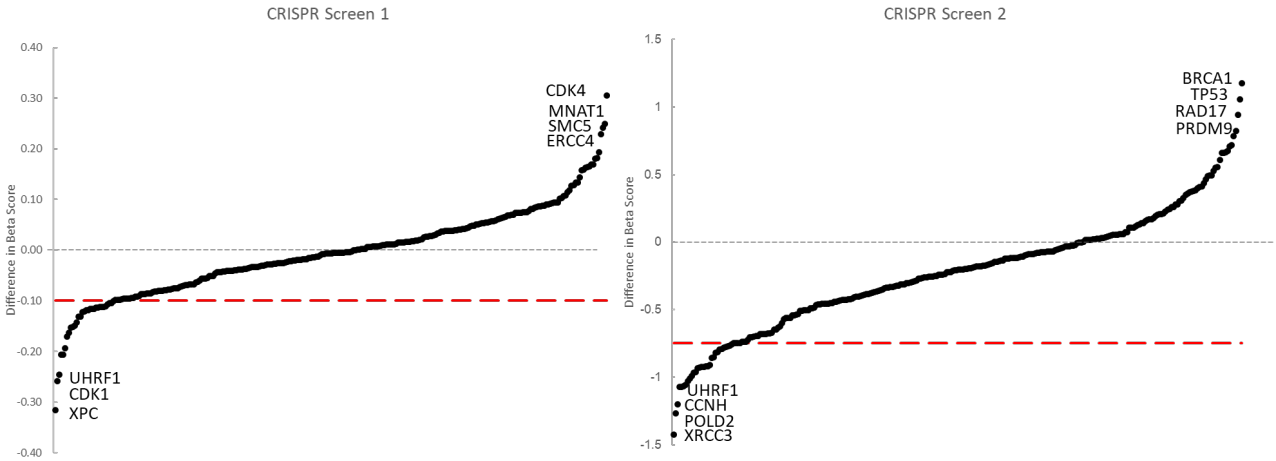

Figure 5.4: Comparing differences in beta scores between screens

Differences in beta scores as indicated in Figure 5.3 and Table 3.2 were plotted from lowest to highest. Red dashed line indicates cut off for hits chosen for further analysis.

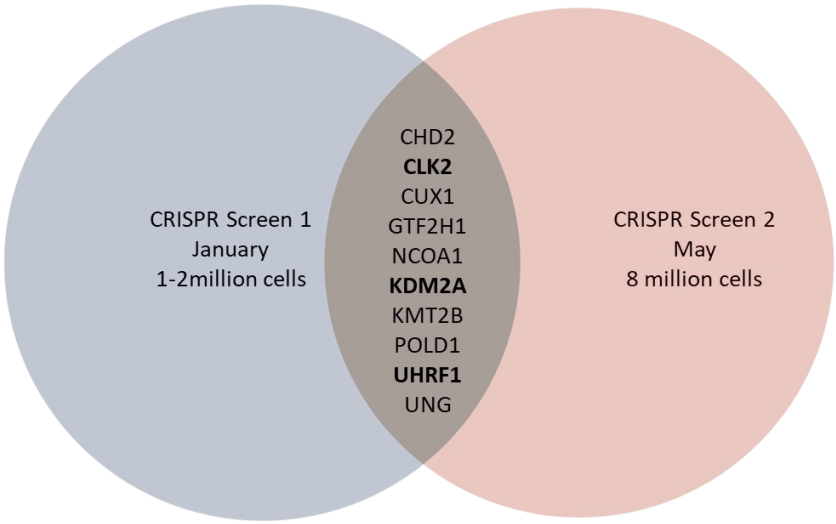

Figure 5.5: Overlap of hits between CRISPR screens

While both CRISPR screens differed in sample size, 25% of the top hits overlapped between screens. Genes in bold were at the very top of both screens and selected to be validated first.

5.5. Hit Validation

To begin validating these hits, I began by first testing the top result from the first screen, XPC. XPC is known for its role in the sensing of large legions for nucleotide excision repair but has also been found to have a role in chromatin modification and metabolism (Nemzow et al., 2015). To investigate if XPC is required for ATRX KO cell survival, I compared cell growth in WT and ATRX KO cells with siXPC. Despite the screen being performed in LN229s, I also repeated this in the U87 cell lines to control for a cell line specific sensitivity.

XPC siRNA was toxic in both WT and KO cell lines compared to the RISC free control. However when comparing the normalized growth in each cell line, it can be seen that siXPC is significantly more toxic in the ATRX KO than the WT (Figure 5.6) This suggests that ATRX

KO is more sensitivity to loss of XPC, which preliminarily validates the result from the CRISPR screen.

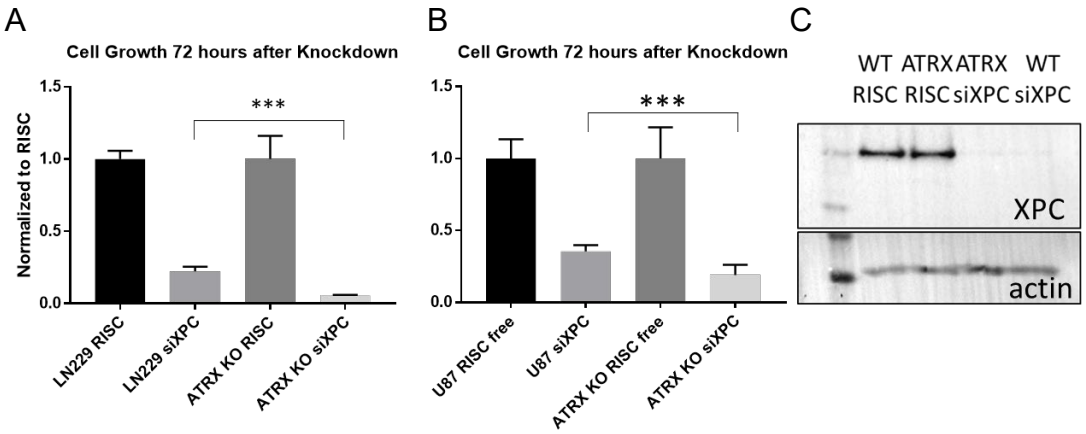

Figure 5.6: XPC knockdown leads to greater sensitivity in ATRX KO cells than WT

A-B) Normalized cell growth after 72 hours of siXPC or RISC free control. Cells were transfected in 6 well dish with siRNA 72 hours before cells were split into 96 well plate and remaining used for western blot analysis. Growth normalized to RISC free for each cell line. Experiment performed in both A) LN229s and B)U87 cells. C) Western blot showing XPC levels in the LN229 cells. U87 cells did not have enough cells for XPC levels to be tested.

After the second screen the top result, XRCC3, as well as the three top genes that overlapped in both screens (CLK2, KDM2A and UHRF1) were tested using siRNA in a similar manner to the siXPC. siXRCC3 was found to be very toxic and so no clear difference was seen between cell lines (Figure 5.7). siKDM2A had the greatest difference between WT and ATRX KO while siCLK2 had a minor difference (Figure 5.7). Further study of KDM2A's role as a histone demethylase and its role in ATRX KO cells would be interesting for further study.

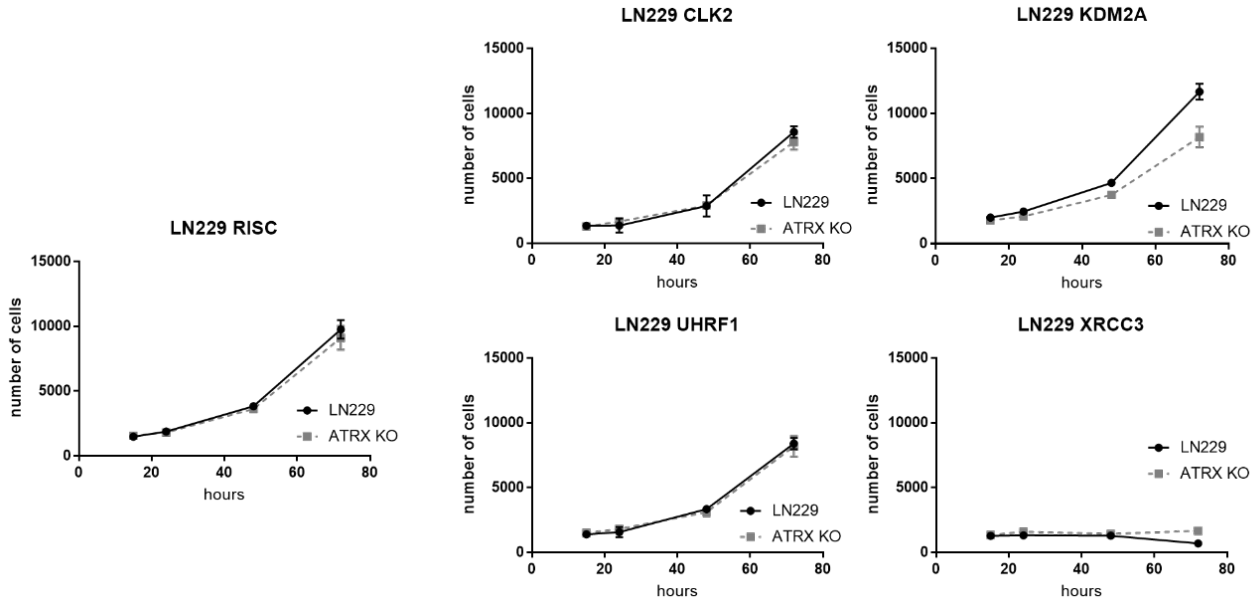

Figure 5.7: siRNA validation of top CRISPR screen hits

Normalized cell growth after 72 hours of siRNA or RISC free control. Cells were transfected in 6 well dish with siRNA 72 hours before cells were split into 96 well plate for growth rate analysis.

To more robustly validate the CRISPR screen, I chose single gRNAs from the pool to create new cell lines for long term clonogenic survival assays. Using the beta scores of each individual guide RNA (supplied by Dr. Gregory Breuer), I chose gRNAs that represented the second-best result to avoid generally toxic or nonfunctional guides without biasing the validation to the best available gRNA. For example, for CLK2 I chose gRNA 2 (shown in green) as the second-best gRNA in the pool for further analyze (Figure 5.8 left). This representation can also show the overall trend in survival. For BRCA1 (Figure 5.8 right) you can see while each gRNA decreased in representation overtime, this was much more variable in the ATRX KO cells. This is what caused BRCA1 to be the most overrepresented gRNA in the ATRX KO cells compared to WT.

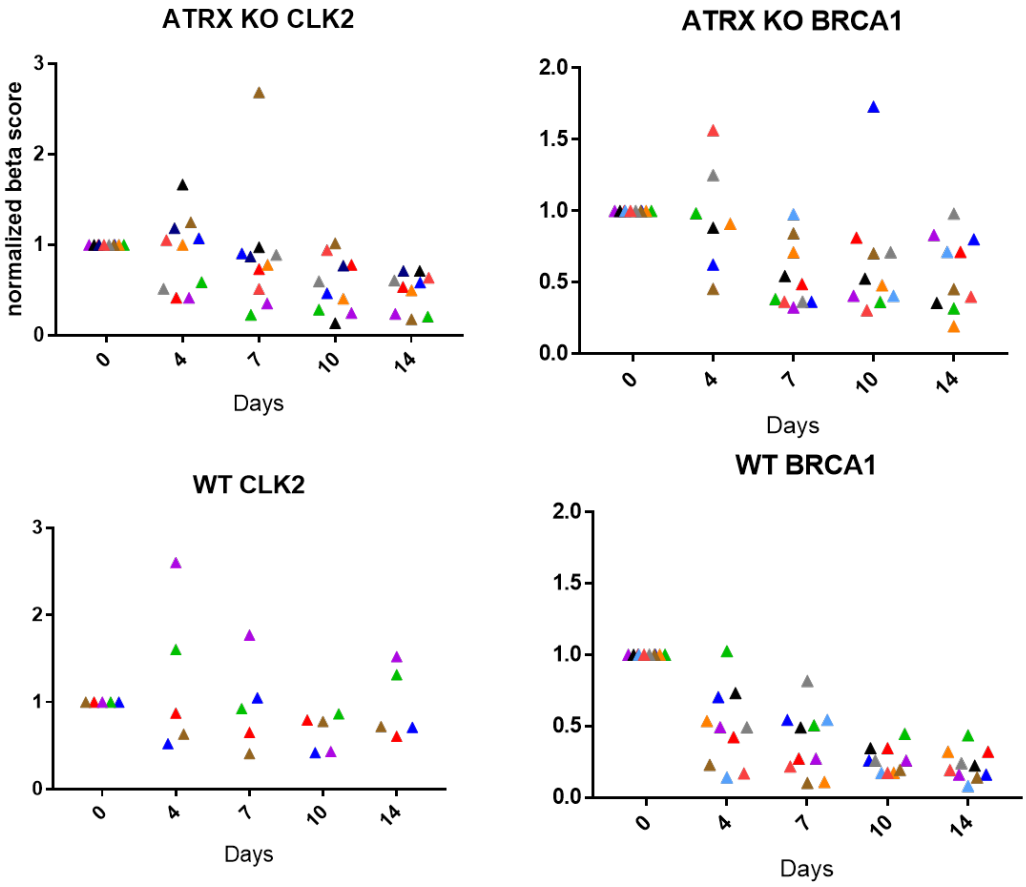

Figure 5.8: Representative individual gRNA results used for validation

Each triangle color represents a different gRNAs representation in the screen overtime. Comparison of trends in both WT and ATRX KO cells were done to choose the ideal gRNA for repeat validation. For CLK2 the green gRNA was chosen and for BRCA1 the brown gRNA was chosen for further study.

Once these gRNAs were chosen, they were cloned into the LCV2 system for transduction into the LN229s (Sanjana et al., 2014). After much optimization of the cloning process, CUX4, CCNH and UHRF1 were the first genes with gRNAs successfully cloned into the LCV2 plasmid and to be tested through a clonogenic survival assay.

As seen in Figure 5.9, while there was no significant difference in survival between CUX4 and CCNH there is a nearly-significant difference with UHRF1. UHRF1, which binds H3K9 methylation to maintain DNA methylation after mitosis (Rothbart et al., 2012), was very toxic to both cell lines despite not seeing this toxicity in the siRNA experiment (Figure 5.7). Further validation of this result would be very interesting especially if toxicity can be reduced with an inhibitor instead of complete knockout.

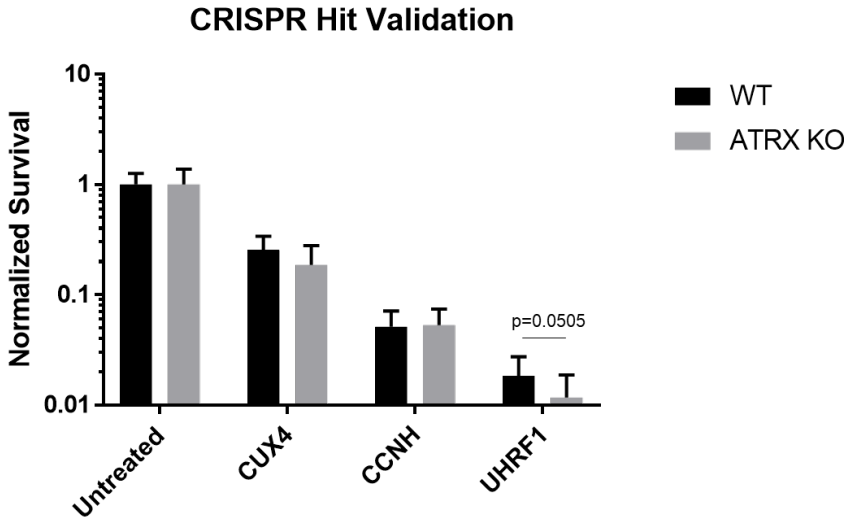

Figure 5.9: Validation of CRISPR Screen hits through clonogenic survival assay

Survival of each cell line after two weeks. Growth was normalized to the parental WT or ATRX KO untreated survival.

5.6. Discussion

CRISPR screens are a great tool for probing for specific genes that interact with or rely on a gene of interest. Using a specific screen of only genes in certain pathways allows for better coverage of each gene and allows for a smaller, more robust screen. After performing two duplicate CRISPR screens, I have several hits that can be further validated. These include the top hit from the first screen, XPC and two that were seen at the top of both screens KDM2A and UHRF1. These genes all could be involved with ATRX function, and perhaps could be inhibited to cause selective sensitivity to ATRX loss.

XPC (xeroderma pigmentosum complementation group C) is a protein involved in recognizing DNA legions and recruiting additional repair factors for nucleotide excision repair (Nemzow et al., 2015). While this might seem independent of ATRX function, XPC has been implicated in other DNA repair process as well. XPC has been found to be required for ATM/ATR activation after UV legions (Ray et al., 2009, 2013). As there is evidence in my work of ATRX loss leading to increased ATR activation and γH2AX increases (Chapter 6.4 and 4.3), further disruption of this signaling pathway could lead to increased sensitivity in ATRX KO cells. Additionally, there is some evidence that the XPC is required for telomere stability (Stout and Blasco, 2013). Since ATRX loss is associated with telomere stability as well (Clynes et al., 2015), losing both XPC and ATRX might lead to heightened telomere instability, which in turn leads to cell death. Either of these hypotheses of mechanism of selective sensitivity would be very interesting to further analyze.

Another interesting hit from the siRNA growth validation experiments is KDM2A. KDM2A is a histone demethylase that targets H3K36 methylation (Vacík et al., 2018). KDM2A is also associated with similar structured repetitive sections of chromatin as ATRX such as centromeric

heterochromatin (Frescas et al., 2008) and rRNA (Tanaka et al., 2010). As ATRX is also a chromatin modifier in these regions (Udugama et al., 2015, 2018; Voon et al., 2015), it would be interesting to investigate how the histone methylation changes after KDM2A depletion when ATRX KO has already caused epigenetic changes in these regions. The chromatin at these more structured regions may no longer be able to be properly maintained leading to greater DNA damage and increased cell death.

UHRF1 and ATRX also have interesting overlapping functions. Similar to KDM2A, UHRF1 also acts on histone H3. Specifically, UHRF1 binds to H3K9 methylation and recruits DNA methylation machinery to methylate the daughter strand during replication (Rothbart et al., 2012). Since ATRX loss is also modulating H3 levels and binds to H3K9 methylation (Iwase et al., 2011) it would be interesting to identify how these two proteins interact. Perhaps the lack of both of these proteins binding will lead to increased genomic instability. Additionally, the frequently cooccurring mutation with ATRX, IDH1 R132H, causes increases in H3K9 methylation levels (Sulkowski et al., 2020). Understanding the chromatin state with each of these mutations would be very interesting to further elucidate their mechanisms.

Each of these hits leads to very interesting mechanistic questions that could allow for a better understanding of ATRX's function. Additionally, inhibitors to any of these proteins would be potential therapeutic targets in ATRX mutant cancers to future explore. While more validation needs to be done, these hits are very promising and would be fascinating to pursue further.

6. ATRX KO immortalized astrocytes have sensitivity to PARP inhibitors due to increased replication stress

This chapter is adapted from work to be published:

Garbarino, J., Eckorate J., Jensen, R., and Bindra, R.. Loss of ATRX confers DNA repair defects and PARP inhibitor Sensitivity. *Translational Oncology* (***in revision***) 2021.

6.1. Introduction

ATRX (Alpha Thalassemia Retardation syndrome X-linked) has been studied extensively for its role in the syndrome it is named after, but was only recently found to have importance in cancers such as pancreatic neuroendocrine tumors (PanNet) (Chan et al., 2018) and gliomas (Reifenberger et al., 2016). ATRX is a ATP dependent chromatin modifier that helps deposit histone 3.3 (H3.3) into the genome at heterochromatin (Voon et al., 2015), pericentromic regions (Iwase et al., 2011), rDNA (Udugama et al., 2018) and other structured regions. ATRX is now a diagnostic marker for gliomas due to its frequency and distinguishing characteristics, as nearly 30% of younger glioma patients have an ATRX mutation (Haase et al., 2018). ATRX loss is also necessary but not sufficient for the Alternative-Lengthening of Telomeres pathway, which occurs in 10-15% of tumors (Voon et al., 2016). Since its discovery in cancer, ATRX has been implicated in a number of DNA damage response (DDR) pathways, including replication stress response (Clynes et al., 2015; Huh et al., 2016; Leung et al., 2013; Wang et al., 2019), homologous recombination (HR) (Juhász et al., 2018; Raghunandan et al., 2019) and non-homologous end joining (NHEJ) (Koschmann et al., 2016). However, it has yet to be determined whether loss of ATRX confers sensitivity to DDR inhibitors in glioma models.

An important pathway studied in these processes is the signaling of replication stress. This is done through ATR activation. Ataxia telangiectasia and Rad3-related (ATR) is a kinase that is recruited to single strand breaks by Replication Protein A (RPA). ATR phosphorylates RPA (at S33) as well as other proteins to activate DNA repair pathways (Murphy et al., 2014; Saldivar et al., 2017; Vassin et al., 2009). CHK1 is another of these proteins activated by ATR phosphorylation (at S317 and S345) which halts the cell cycle for replication stress to be resolved as well as activating downstream, DNA repair factors (Smith et al., 2010). Investigating the signaling in this pathway allows for better understanding for the levels of replication stress in a cell.

Additionally, ATRX loss often co-occurs with glioma-associated mutations in other genes, such as isocitrate dehydrogenase-1 and -2 (IDH1/2). IDH1/2 encode citric acid cycle enzymes which convert isocitrate into alpha-ketoglutarate (αKG), and neomorphic mutations in these genes converts alpha-ketoglutarate into the oncometabolite, 2-hydroxyglutarate (2-HG). 2HG competitively inhibits αKG-dependent dioxygenase proteins, which induces profound epigenetic alterations and impaired differentiation (Lu et al., 2012; Xu et al., 2011). Previous work recently demonstrated that 2HG induces HR defects and sensitivity to poly(ADP)-ribose polymerase (PARP) inhibitors (Lu et al., 2017; Molenaar et al., 2018; Sulkowski et al., 2017, 2020; Wang et al., 2020). However, it has yet to be fully elucidate how ATRX and IDH1/2 mutations interact with regard to modulation of the DDR. One study reported that loss of ATRX induces impaired NHEJ (Koschmann et al., 2016), but a subsequent study from the same group suggested that ATRX loss actually increases DDR activity specifically in the context of IDH1/2 mutations (Núñez et al., 2019). These studies were largely performed in rodent models, and thus additional data are required in human glioma models.

To further investigate the function of ATRX function in the DDR, I created isogenic wild-type (WT) and knockout (KO) ATRX model cell lines using CRISPR-based gene targeting and performed a focused drug screen for novel synthetic lethal interactions with DDR inhibitors and DNA damaging agents. These studies revealed that loss of ATRX confers sensitivity to poly(ADP)-ribose polymerase (PARP) inhibitors, which was linked to an increase in replication stress, as detected by increased activation of the ATR signaling axis. I found that the magnitude of PARP inhibitor sensitivity was equal in cell line models with ATR loss and IDH1 mutations alone, although no further sensitization was observed in combination, suggesting an epistatic interaction. Finally, I observed enhanced synergistic tumor cell killing in ATRX KO cells with combined ATR and PARP inhibition, which is commonly seen in HR-defective cells (Kim et al., 2017; Lloyd et al., 2020; Schoonen et al., 2019). Taken together, these data reveal that ATRX may be used as a molecular marker for DDR defects and PARP inhibitor sensitivity, which is independent of IDH1/2 mutations.

6.2. Validation of ATRX knockout

Using the platform discussed in Chapter 3.3, I found human astrocyte clones with successful ATRX knockout (Figure 3.10). To further validate knockout in this clone, I performed western blots to confirm loss of the ATRX protein (Figure 6.1A). I then used sequencing analysis combined with TOPO cloning to confirm biallelic loss of ATRX through a 26 and 11 base pair deletion (Figure 6.1B).

ATRX loss has been associated with cell cycle changes (Leung et al., 2013), so I further characterized the growth patterns and patterns of cell cycle phase distribution in the WT and ATRX KO models. I determined that the ATRX KO cell line grew at the same rate as the parental astrocytes, as seen previously with ATRX KO in HeLa cells, and did not detect any

differences in plating efficiencies (Juhász et al., 2018; Leung et al., 2013) (Figure 6.1C). This differs from the LN229 and U87 clones that have growth rate and morphology differences between WT and ATRX KO which made the astrocytes a more robust isogenic pair for comparison (Figure 4.2 and Figure 4.4). I also found that a significantly larger percentage of ATRX knockout cells were cyclin A-positive in comparison to their wild-type counterparts (Figure 6.1D), which suggests an increased S/G2 population in ATRX KO cells.

I also found that these cells have similar functional defects similar to those previously reported in ATRX-deficient cells, such as pyridostatin (PDS) sensitivity (Figure 6.1E). As a G-quadruplex stabilizer, PDS has been found to specifically target ATRX deficient cells as H3.3 deposition is important for resolution of this DNA structure (see Chapter 1.7) (Wang et al., 2019). Taken together, these data confirm the ability to characterize, and functionally validate ATRX WT and KO isogenic GBM model cell line pairs.

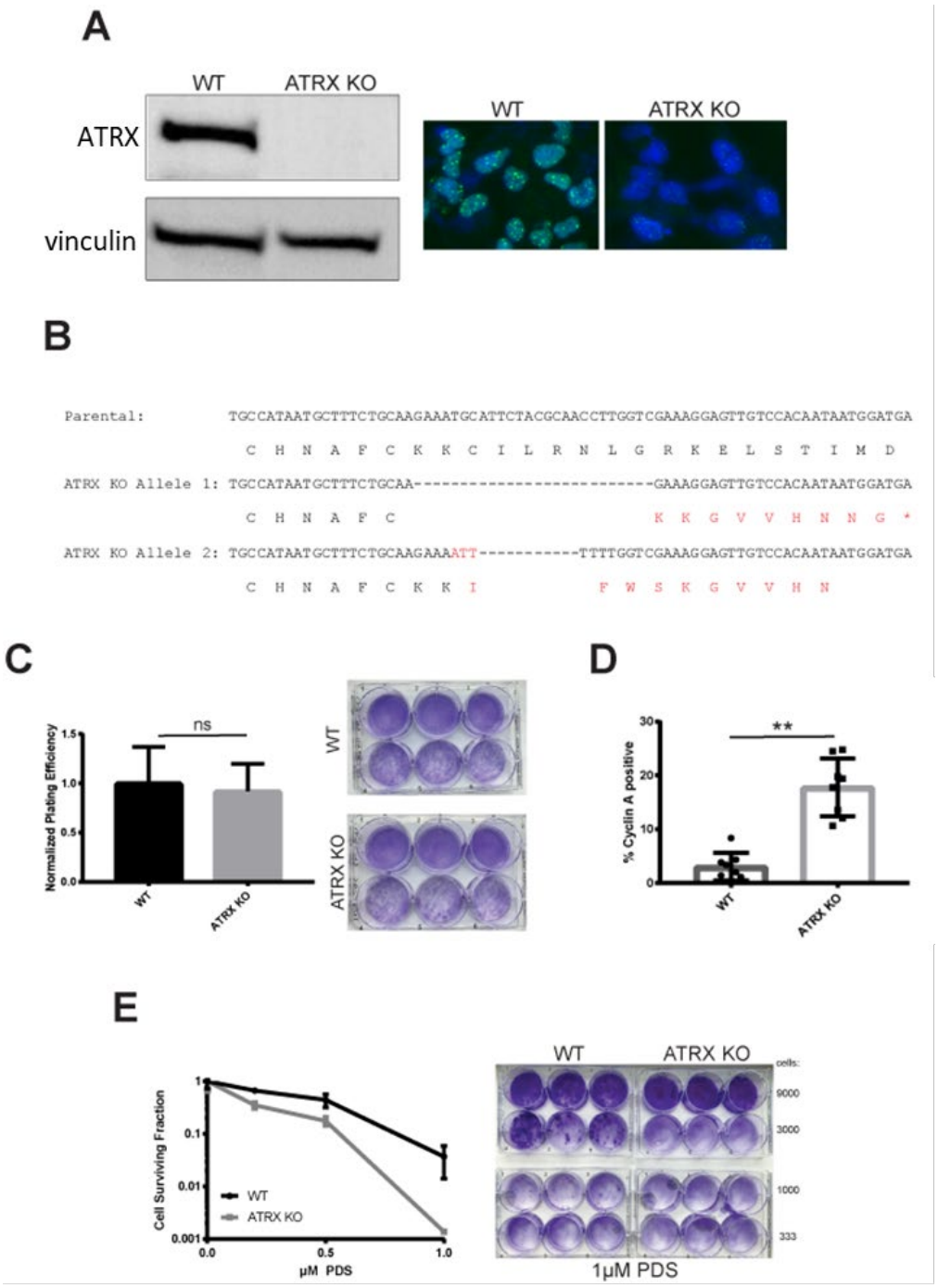

Figure 6.1 Validation of immortalized astrocyte ATRX KO cell line

A) ATRX KO clone in immortalized astrocytes further validated through western blot and immunofluorescence. B) Sequencing data showing biallelic knockout of ATRX. C) Representative plating efficiency in parental and wildtype cell lines. D) Sensitivity to pyridostatin after 14 day Clonogenic survival assay. Cells were treated with 0.1, 0.5 and 1μM pyridostatin. E) Cyclin A staining was performed, and positive cells were scored through immunofluorescence intensity greater than 20,000 in 16-bit images.

6.3. Drug screen with ATRX KO cells shows PARP inhibitor sensitivity

Given previous evidence of a possible role for ATRX in the DDR, I performed a focused screen with unique DNA damaging agents and repair inhibitors to identify potential synthetic lethal interactions that are associated with ATRX loss. Screening was performed in the active dose ranges for the molecules, and ATRX WT and KO cell lines were analyzed in parallel. Screening data is shown in Figure 6.2, along with a summary table of the calculated IC50s for each drug in the ATRX WT and KO cell lines. I included pyridostatin as a positive control because of the known selectivity for ATRX KO cells. I observed a detectable selectivity (albeit modest) against ATRX KO versus WT cells, which had also been seen in the clonogenic survival assays during the initial validation studies with these model lines (shown in Figure 6.1). I also found that treatment with the Wee1 inhibitor, MK1775, also selectively targeted ATRX KO cells, which is consistent with previously published studies (Liang et al., 2019). I detected a robust synthetic lethal interaction between two PARPi's, olaparib and BMN673 (talazoparib) and loss of ATRX, with olaparib having an almost 5-fold reduction in IC_{50} in ATRX KO cells compared to WT (Figure 6.2).

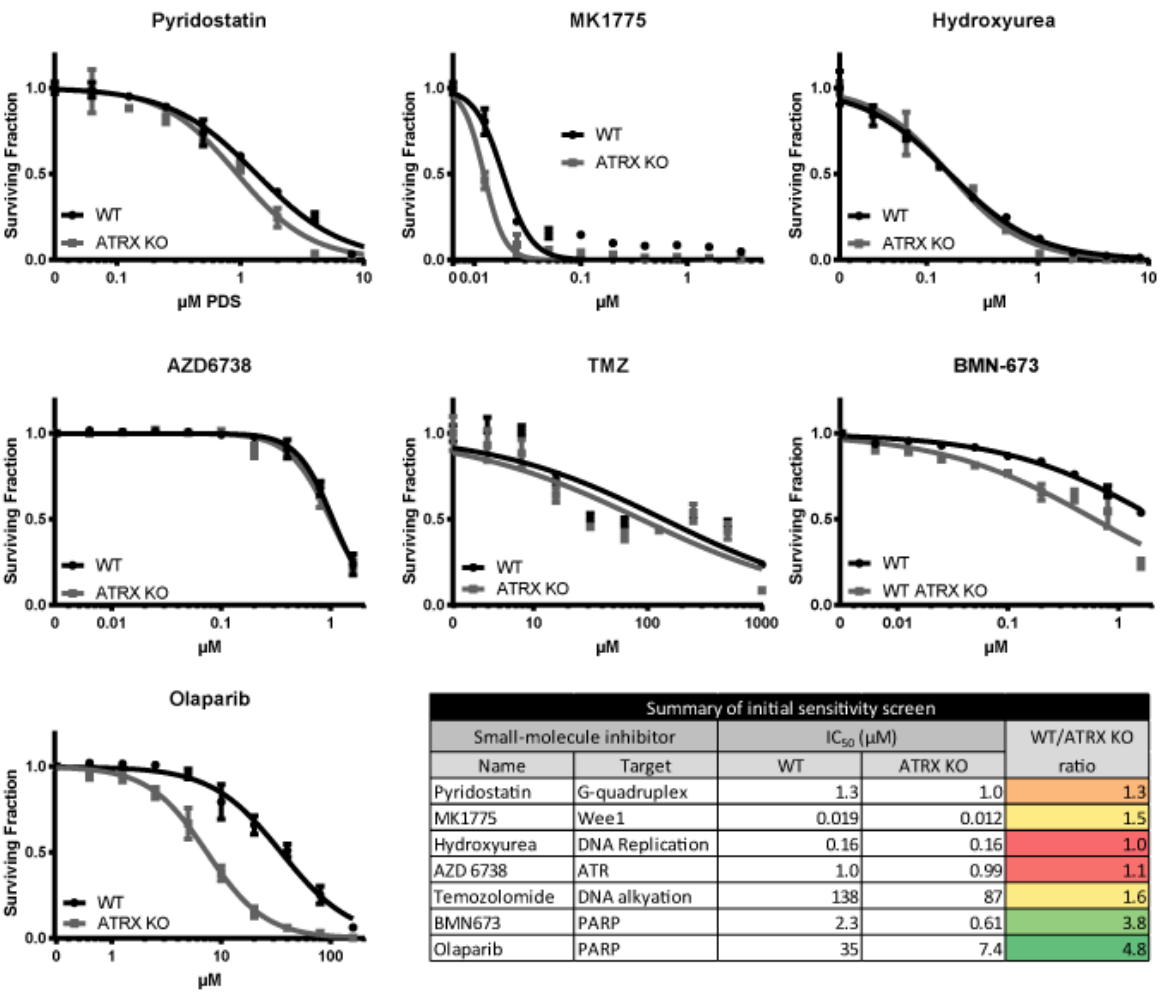

Summary of initial sensitivity screen				
Small-molecule inhibitor		IC_{50} (μM)		WT/ATRX KO
Name	Target	WT	ATRX KO	ratio
Pyridostatin	G-quadruplex	1.3	1.0	1.3
MK1775	Wee1	0.019	0.012	1.5
Hydroxyurea	DNA Replication	0.16	0.16	1.0
AZD 6738	ATR	1.0	0.99	1.1
Temozolomide	DNA alkyation	138	87	1.6
BMN673	PARP	2.3	0.61	3.8
Olaparib	PARP	35	7.4	4.8

Figure 6.2: ATRX KO astrocytes shows PARP inhibitor sensitivity in DNA repair focused drug screen.

Representative IC_{50} plots of short-term viability assays 96 hours after drug treatment. Table shows ratio of WT/KO IC_{50} to identify greatest differences in sensitivities.

I further validated this synthetic lethal interaction in clonogenic survival assays with olaparib (Figure 6.3A). As shown in the representative crystal violate-stained plates, there are nearly no surviving ATRX KO colonies at 5μM of treatment with olaparib, despite many colonies still present with the WT cells.

I then validated this differential PARP inhibitor sensitivity in a glioma cell line, U251, which I engineered for doxycline (dox)-inducible ATRX knockdown using shRNAs (Figure 6.3B). These ATRX knockdown cells also show sensitivity to olaparib (Figure 6.3C) and BMN-673 (Figure 6.3D). PARP inhibitor sensitivity was also further confirmed in a clonogenic survival assay with olaparib in this dox-inducible shATRX knockdown model (Figure 6.3E). Collectively, these data suggest that loss of ATRX confers significant sensitivity to PARP inhibitors.

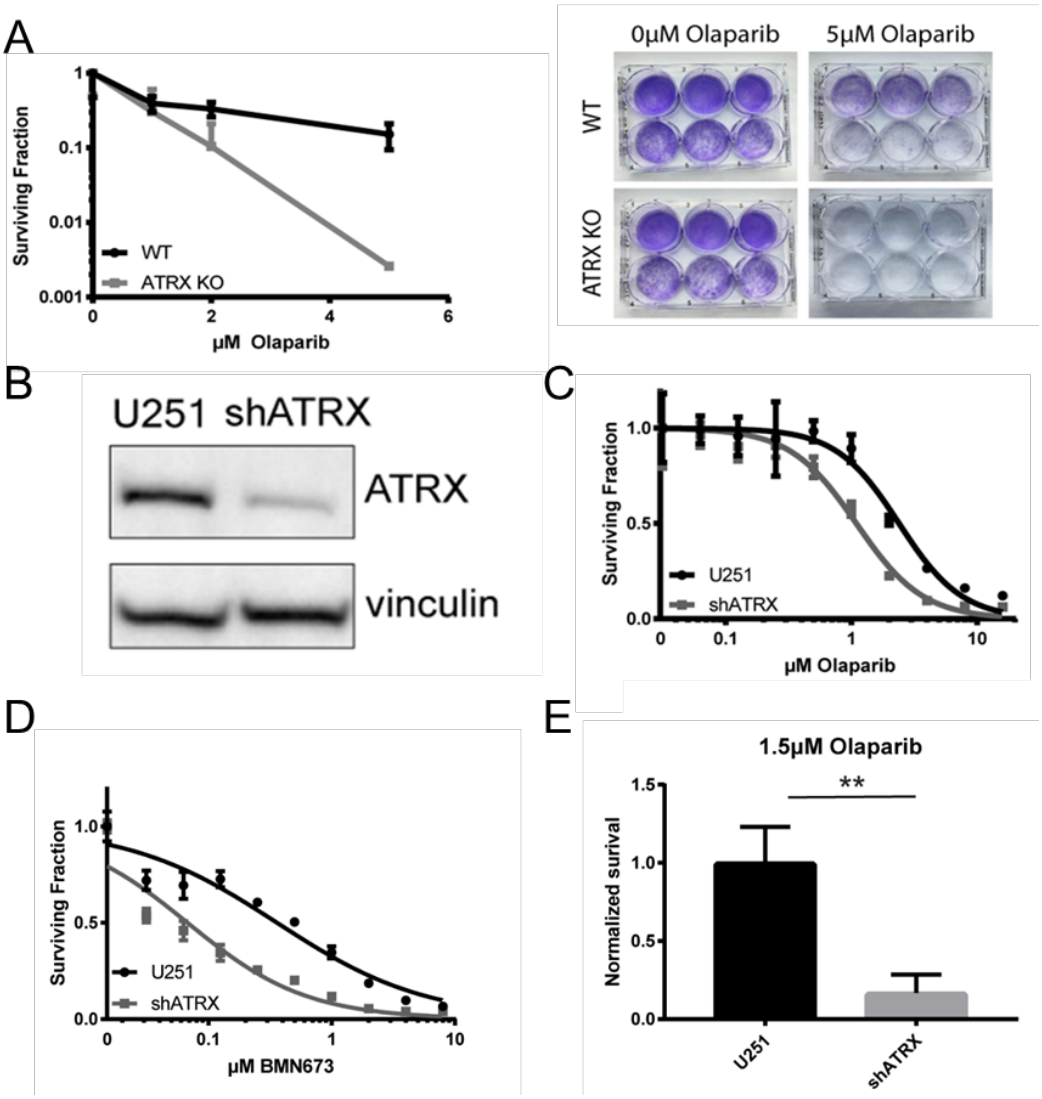

Figure 6.3: PARPi sensitivity from drug screen validated in astrocytes and U251s

A) Sensitivity to olaparib in ATRX KO cells after 14 day clonogenic survival assay. B) Western blot show knockdown of ATRX also leads to PARPi sensitivity in U251s. sATRX induced with 1 µg/ml of doxycycline for greater than 96 hours prior to experiment. C) Short term viability assay with olaparib 96 hours after treatment. D) Short term viability assay with BMN673 96 hours after treatment. E) Clonogenic survival assay with 1.5µM olaparib 14 days after treatment.

6.4. Olaparib leads to increased replication stress in ATRX KO cells

Given the findings that loss of ATRX is associated with a higher fraction of S-phase cells (Figure 6.1E), and increased sensitivity to PARP inhibitors (Figure 6.3), I considered the possibility that ATRX KO cells have baseline elevated levels of replication stress. Phosphorylated RPA (pRPA) foci is a well-established marker for elevated replication stress, as pRPA coats single-stranded DNA at stalled/collapsed replication forks in direct response to ATR activation (Murphy et al., 2014; Vassin et al., 2009). I observed elevated levels of pRPA foci at in untreated cells (Figure 6.4A). These levels were increased after olaparib exposure, and the induction was significantly greater in ATRX KO versus WT cells (Figure 6.4B). I validated this phenotype in the dox-inducible U251 shATRX cell line as well (Figure 6.4C). Enhanced pRPA foci after olaparib exposure also correlated with phosphorylation of another ATR target, Chk1 (Smith et al., 2010), as detected by western blot analysis in ATRX KO cells (Figure 6.4D).

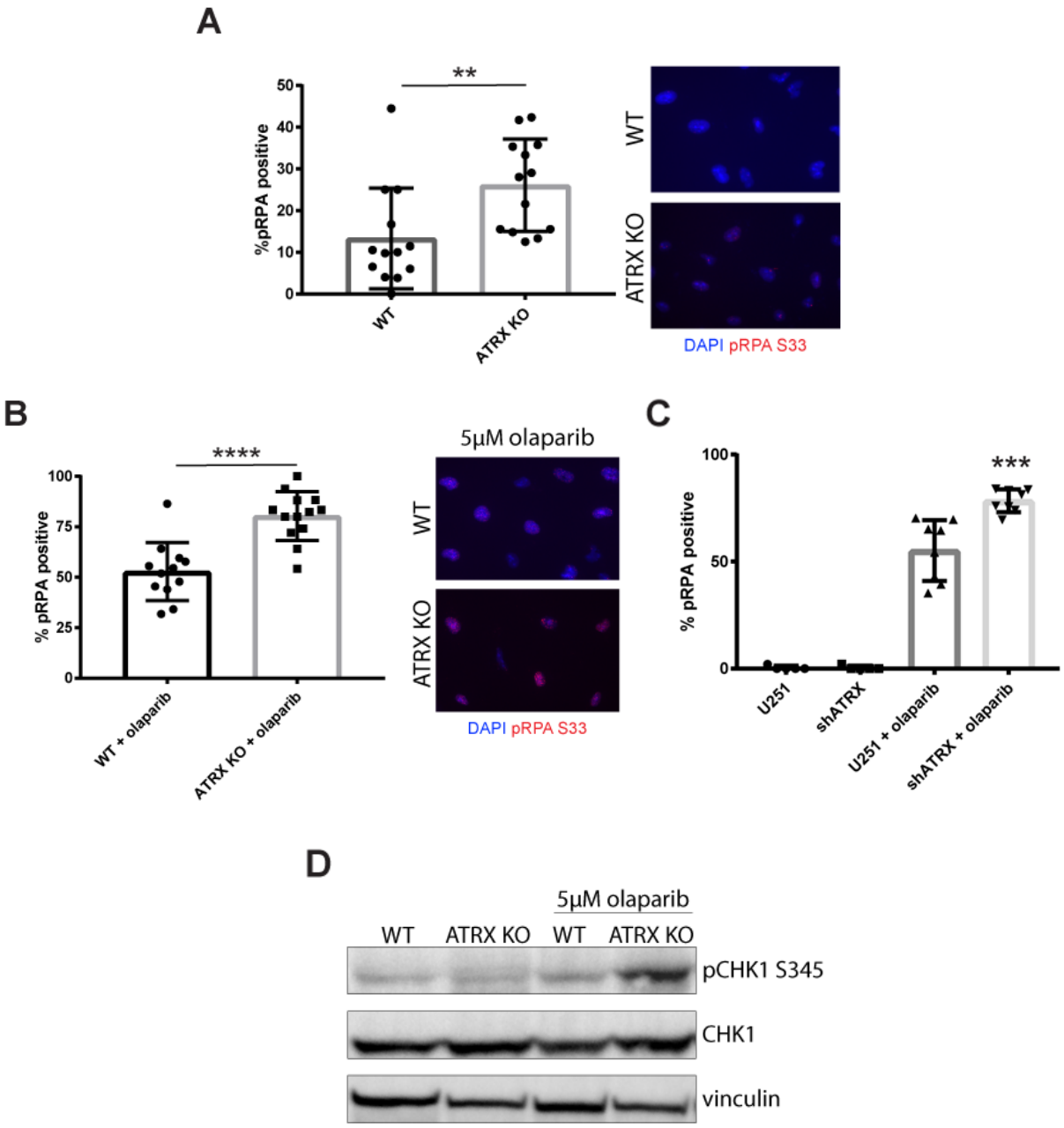

Figure 6.4: Olaparib leads to increased replication stress in ATRX KO cells.

A) pRPA32 S33 foci in ATRX KO cells compared to WT. Cells with greater than 5 foci were marked positive. B) pRPA32 S33 foci in immortalized astrocytes. Studies were performed at 24 hours after 5 μM olaparib treatment. Cells with greater than 10 foci were marked positive. C) pRPA32 S33 foci in U251 cells. Studies were performed at 24 hours after 2 μM olaparib treatment and in the presence of 1μg/ml doxycycline. Cells with greater than 10 foci were marked positive. D) pCHK1 S345 western blot was performed 24 hours after 5 μM olaparib treatment

As described earlier, ATRX and IDH1/2 mutations co-occur frequently in glioma, and many have reported that the latter induce HR defects and PARP inhibitor sensitivity (Lu et al., 2017; Molenaar et al., 2018; Sulkowski et al., 2017, 2020; Wang et al., 2020). After identifying ATRX KO PARPi sensitivity (Figure 6.3), I wanted to understand how PARPi sensitivity would change in the context of IDH1/2 mutations. I engineered the immortalized astrocyte ATRX WT and KO cell line models to contain a dox-inducible IDH1-mutant (R132H) expression vector, and single cell clones were selected and validated by western blot analysis (Figure 6.5A). In these cells, the double mutant cells behaved similarly to ATRX deficiency alone with olaparib treatment (Figure 6.5B) as well as BMN-673 (Figure 6.5C).

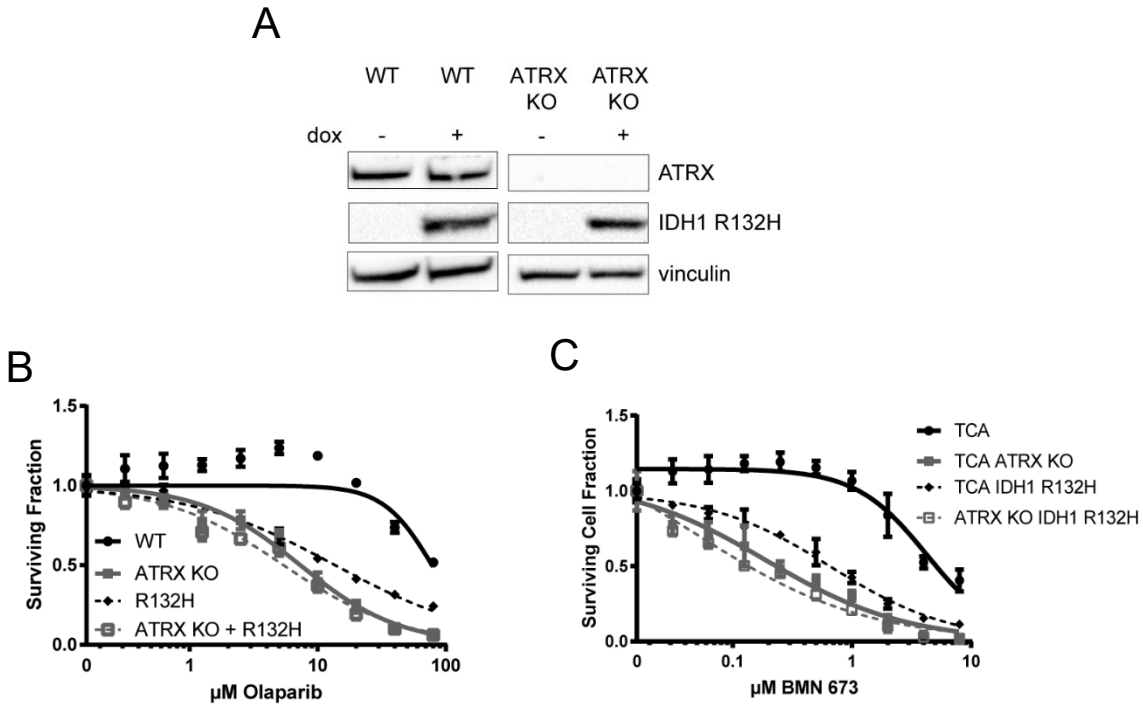

Figure 6.5: ATRX KO and IDH1 R132H double mutation leads to equivalent PARPi sensitivity as either mutation alone.

A) Western blot showing ATRX KO and IDH1 R132H over expression individually and in combination in astrocytes. R132H induced with 1μg/ml for at least 96 hours. B) Short term viability assay with olaparib comparing the combination of ATRX KO and IDH1 R132H mutation to each mutation alone and wild type 96 hours after treatment. C) Short term viability assay with additional PARPi, BMN673

Additionally, I also created the combination mutants in the U251 shATRX cell line (Figure 6.6A), and validated that olaparib sensitivity is equivalent in the shATRX, IDH1-mutant and double mutant models (Figure 6.6B). The findings in immortalized astrocyte model with olaparib were also validated in clonogenic survival assays in the U251 model (Figure 6.6C).

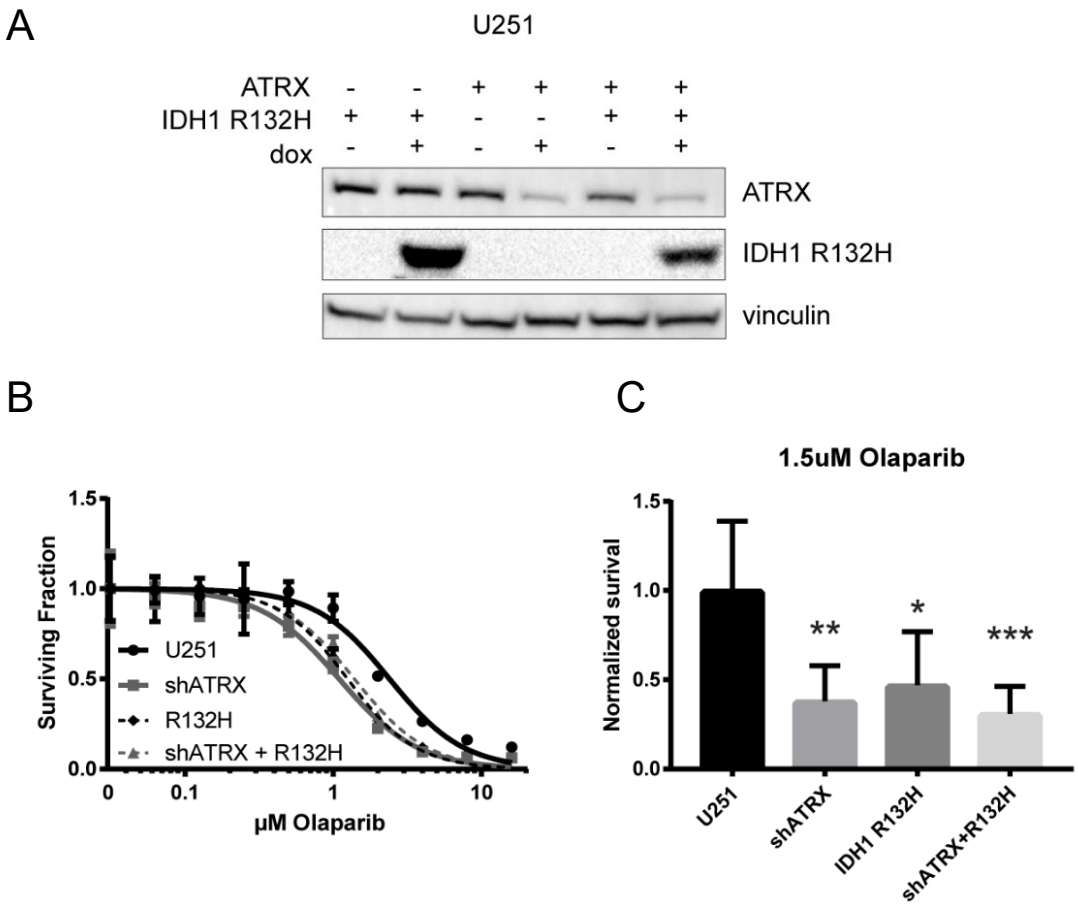

Figure 6.6 ATRX shATRX and IDH1 R132H double mutation leads to equivalent PARPi sensitivity pattern as immortalized astrocytes.

A) Western blot showing induction of ATRX knockdown and IDH1 R132H over expression individually and in combination. 1 μg/ml of doxycycline was used for induction. B) Short term viability assay with olaparib comparing the combination of shATRX and IDH1 R132H overexpression to each mutation alone and wild type. C) Clonogenic survival assay with 1.5μM olaparib comparing all four U251 cells lines. Significance was calculated compared to WT. For B) and C) All four cells lines were treated with 1 μg/ml of doxycycline for at least 96 hours prior to experiment.

Finally, ATR and PARP inhibitor combinations have enhanced synergy in tumors with replication stress and/or HR defects (Kim et al., 2017; Lloyd et al., 2020; Schoonen et al., 2019), and unpublished work from our laboratory suggests that this combination is particularly effective against IDH1/2-mutant tumors (Sule *et. al.*, manuscript in revision). In parallel, the data presented here suggest that loss of ATRX activates the ATR signaling axis and induces replication stress. These findings lead me to test for synergy with ATR and PARP inhibition. I observed robust synergy with this combination in the immortalized astrocyte models, with maximal synergy seen in the ATRX KO cells as compared to WT (Figure 6.7). These data further highlight the dependence of ATRX KO cells on ATR signaling, and support the use of a PARP and ATR inhibitor combination against tumors with these mutations.

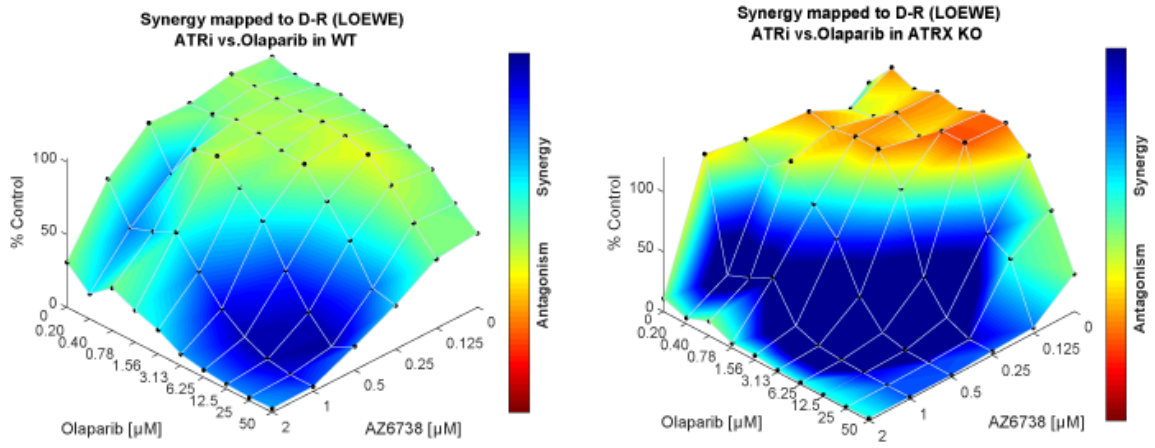

Figure 6.7: Synergy experiments were performed with olaparib and AZD 6738 (ATR inhibitor) in both WT and ATRX KO cells. Cells were treated for 96 hours and the Loewe method was used to calculate synergy.

6.5. Discussion

I created an isogeneic pair of cell lines in immortalized astrocytes using CRISPR/Cas9-based gene editing to knockout ATRX. I investigated their DNA repair efficiency through a focused drug screen of DNA damaging agents and repair inhibitors and discovered that ATRX KO cells have increased sensitivity to poly(ADP)-ribose polymerase (PARP) inhibitors than WT. I showed that this was due to increased replication stress as identified through increased activation of the ATR signaling pathway. In both immortalized astrocytes and U251 cells, I found that IDH1 mutation and ATRX deficiency combined lead to similar levels of PARPi sensitivity compared to the individual mutations, suggesting an overlap in function leading to an epistatic interaction. Additionally, I determined that ATRX KO leads to even greater PARP and ATR inhibitor synergy than wild-type cells. Overall, this suggests that ATRX is a potential biomarker for PARP inhibitor sensitivity and DDR deficiencies, independent of IDH1/2 mutation.

This work shows that in different model systems, combined ATRX and IDH1 mutation still leads to DNA repair defect, despite previous literature suggesting otherwise (see Chapter 1.8) (Núñez et al., 2019). Interestingly, both the IDH1 and ATRX mutations are known lead to chromatin aberrations as well as DNA repair defects. IDH1 mutation leads to an increase in H3K9 trimethylation, an important signal for recruitment of DNA repair proteins (Sulkowski et al., 2020). ATRX is required for the deposition of H3.3, which can carry this epigenetic mark and require it for its localization (Iwase et al., 2011; Udugama et al., 2015). Further work is needed to understand the mechanism of the interplay of these two mutations, but the combination's equal sensitivity to olaparib suggests that they affect similar repair pathways.

7. Discussion

7.1. Conclusions

ATRX is a vital protein for genomic integrity. There is growing evidence of its role in DNA replication and repair but more work is needed to further characterize this protein. As ATRX is mutated frequently in cancers such as gliomas, it is also important to identify potential therapeutic options for patients with this mutation. I created a platform for screening numerous CRISPR knockout clones and created ATRX knockout in three different cell lines. I then characterized the DNA repair capacity of each of these cell lines and found DNA repair defects in each of them linked to homologous recombination and replication stress. I also performed a CRISPR screen which highlighted the importance of the chromatin modifications made by ATRX and that ATRX KO cells are more susceptible to increased deregulation of the chromatin. I also determined that the astrocyte cell line ATRX KO is sensitive to PARP inhibition, which is caused by increased replication stress in these cells. This sensitivity was epistatic with the commonly co-occurring IDH1 R132H mutation, which would suggest they act in similar pathways. There are many possible avenues of future work with these model cell lines, such as further mechanistic exploration of PARP sensitivity, continued characterization of the CRISPR screen, analysis of G-quadruplex sensitivity, and understanding the role of ALT in these cell lines.

7.2. Exploration of possible mechanism for PARP sensitivity

I determined that immortalized astrocytes cell line ATRX KO has sensitivity to PARP inhibitors in both short- and long-term assays (Figure 6.3). I then investigated the cause of this sensitivity to be due to increased replication stress. This was supported by increase in pRPA and

CHK1 levels indicating increase in ATR activation in the ATRX KO cells. Further work can be done to investigate the mechanism of increased replication stress in these cells.

Multiple groups have shown that ATRX can bind the MRN complex (see Chapter 1.6) (Clynes et al., 2015; Huh et al., 2016; Leung et al., 2013). Clynes and Huh both hypothesize that ATRX sequesters the MRN complex to prevent fork degradation and decrease fork stalling. Without ATRX, this increase in fork degradation leads to increased overall replication stress.

To determine if this is also occurring in my ATRX KO cells, I will perform DNA fiber combing experiments to investigate fork stalling in these cells in the presence of PARPi. In DNA fiber combing, nucleotide analogs are incorporated into the genome and the amount of each analog can be analyze to understand changes in replication. By comparing the lengths of each analog in the DNA, the amount of stalled or degraded forks can be compared. Then, these experiments can be repeated in the presence of mirin, an MRE11 inhibitor to determine if changes in ATRX KO fork stalling no longer occur. This would support that the inhibition of MRN by ATRX is important for fork protection when PARP is inhibited. I have also begun optimizing other foci markers to identify stalled forks, such as SMARCAL1, which I hope to also use to support the hypothesis of increased fork stalling in ATRX mutant cells (Cicconi et al., 2020). Additionally, I will perform a synergy short term viability assay similar to the one performed with olaparib and ATR inhibitor (Figure 6.7) but instead with mirin and olaparib. I hypothesize that mirin will antagonize the increased sensitivity seen with olaparib in the ATRX KO cells, as it would mimic the inhibition of the MRN complex through ATRX binding. This would further support that fork protection from MRE11 is necessary for survival from PARP inhibitor in these cells.

Another interesting avenue for further investigation is the differences in PARPi sensitivity between cell lines. While the immortalized astrocytes and U251 cell lines show PARPi sensitivity, this is not seen in the LN229 and U87 cell lines (data not shown). This could be due to the changes in morphology and growth rate in these cells masking any differences in cell growth in the presence of olaparib. However, these cells did show sensitivity to CHK1 inhibition, suggesting they do also rely on CHK1 activation. This indicate that a CHK1 or ATR inhibitor could potentially sensitize these cell lines to PARPi.

These more PARP resistant glioma lines could have other currently unknown mutations that lead to PARP inhibitor resistance. For example, even though IDH1 R132H mutation leads to marked sensitivity to PARPi in other cell lines (Sulkowski et al., 2017; Wang et al., 2020), LN229s with IDH1 R132H overexpression only have a mild sensitivity to olaparib. Other mutations in the cells could be compensating for the DNA repair defect. Further understanding of the overall genetic landscape of each of these cell lines would be needed to better understand the differences in these cell lines.

7.3. Further validation for CRISPR screen

An additional direction for future study is continued validation of the CRISPR screen results. While my hypotheses for certain hits are outlined in Chapter 5.6, I also would like to validate these hits in the more sensitive immortalized astrocyte cell line. As they have a more prominent sensitivity to PARPi, they might also show greater effects from loss of the different CRISPR hits than the LN229 cell line shows. It may in fact be beneficial to repeat the screen entirely in the astrocytes, using the knowledge gained in the original screens to ensure robustness. I can also further validate these hits in the U87 cell line. I had made attempts to repeat this screen in U87 ATRX KO cell line, however it became very difficult to have enough cells for the assay due to

their changes in morphologies leading to high confluency at lower cell numbers. Priority for future study could be given to hits that are validated by all three cell lines, whether or not a CRISPR screen is completed in all three lines.

Additionally, to focus specifically on PARP inhibition, this screen could instead be done in the presence of olaparib. In the astrocytes and the U251s, this would allow for more specific targeting of the factors involved in PARP sensitivity in these lines and could further support the hypothesis of replication stress in these cells. The LN229s and U87s could also be screened in the presence of PARP inhibitor and the results compared to those from the astrocytes and U251s. This could help determine differences in these cell lines to further characterize the components besides ATRX KO necessary for PARP inhibitor sensitivity in these cells.

7.4. Analysis of G-quadruplex sensitivity in ATRX KO cells

An additional way to characterize these cell lines is further investigation into G-quadruplex sensitivity. G-quadruplex stabilization was shown to lead to sensitivity in the astrocyte cell line (Figure 6.1) as well as the U251 cell line (data not shown). I would be very interested to see if increases in G-quadruplex levels are seen in my ATRX deficient models, as shown by others (Clynes et al., 2015; Wang et al., 2019). I additionally want to investigate to see if DNA repair markers after olaparib treatment co-localize with these G-quadruplexes, such as pRPA foci, to indicate if that these are the sites of replication stress. I also plan to investigate these same replication stress markers in the presence of G-quadruplex stabilization with and without PARP inhibitor to identify the importance of G-quadruplex formation in PARPi sensitivity for ATRX mutant cells.

7.5. Understanding the role of ALT in ATRX KO model cell lines

Another way to further characterize these cell lines would be to investigate their ability to perform ALT to extend their telomeres. For example, the immortalized astrocyte line was created by overexpression telomerase and so would not need ALT for telomere maintenance (Sonoda et al., 2001). The other glioma cell lines tested, LN229, U87 and U251 have also been shown to express telomerase, with LN229 having low telomerase expression compared to the others (Vietor et al., 2000). This makes sense, as all of these cell lines initially expressed ATRX, and so would be less likely to be using the ALT pathway. However, telomerase expression could be preventing ALT to occur in these cells, as they do not need to utilize the pathway to maintain telomere length.

Despite this, initial levels of ALT in these cells will be tested in collaboration with the Chang Lab, who study telomeres extensively (Chen et al., 2011; Cicconi et al., 2020; He et al., 2009; Rai et al., 2011). It would be interesting to identify if some ALT phenotypes are present, even in the presence of telomerase. It will be especially fascinating to see if the double mutant IDH1 R132H and ATRX deficient cell lines have increased ALT phenotype compared to either mutation alone, as this has been as seen in a previous study (Mukherjee et al., 2018). Telomerase could also be silenced in these cells and then ALT capacity could be studied further. ALT is an important pathway in cancer characterized by ATRX loss, and so the ability to test these models for ALT activity would be a valuable tool for further understanding this process.

8. References

Ahmad, H.I., Ahmad, M.J., Asif, A.R., Adnan, M., Iqbal, M.K., Mehmood, K., Muhammad, S.A., Bhuiyan, A.A., Elokil, A., Du, X., et al. (2018). A Review of CRISPR-Based Genome Editing: Survival, Evolution and Challenges. Curr. Issues Mol. Biol. *28*, 47–68.

Bindra, R.S., Goglia, A.G., Jasin, M., and Powell, S.N. (2013). Development of an assay to measure mutagenic non-homologous end-joining repair activity in mammalian cells. Nucleic Acids Res. *41*, e115.

Brosnan-Cashman, J.A., Yuan, M., Graham, M.K., Rizzo, A.J., Myers, K.M., Davis, C., Zhang, R., Esopi, D.M., Raabe, E.H., Eberhart, C.G., et al. (2018). ATRX loss induces multiple hallmarks of the alternative lengthening of telomeres (ALT) phenotype in human glioma cell lines in a cell line-specific manner. PLoS One *13*, e0204159.

Bryant, H.E., Schultz, N., Thomas, H.D., Parker, K.M., Flower, D., Lopez, E., Kyle, S., Meuth, M., Curtin, N.J., and Helleday, T. (2005). Specific killing of BRCA2-deficient tumours with inhibitors of poly(ADP-ribose) polymerase. Nature *434*, 913–917.

Cai, J., Chen, J., Zhang, W., Yang, P., Zhang, C., Li, M., Yao, K., Wang, H., Li, Q., Jiang, C., et al. (2015). Loss of ATRX, associated with DNA methylation pattern of chromosome end, impacted biological behaviors of astrocytic tumors. Oncotarget *6*, 18105–18115.

Cerami, E., Gao, J., Dogrusoz, U., Gross, B.E., Sumer, S.O., Aksoy, B.A., Jacobsen, A., Byrne, C.J., Heuer, M.L., Larsson, E., et al. (2012). The cBio cancer genomics portal: an open platform for exploring multidimensional cancer genomics data. Cancer Discov. *2*, 401–404.

Chan, C.S., Laddha, S. V., Lewis, P.W., Koletsky, M.S., Robzyk, K., Da Silva, E., Torres, P.J.,

Untch, B.R., Li, J., Bose, P., et al. (2018). ATRX, DAXX or MEN1 mutant pancreatic neuroendocrine tumors are a distinct alpha-cell signature subgroup. Nat. Commun. *9*.

Chen, Y., Rai, R., Zhou, Z.R., Kanoh, J., Ribeyre, C., Yang, Y., Zheng, H., Damay, P., Wang, F., Tsujii, H., et al. (2011). A conserved motif within RAP1 has diversified roles in telomere protection and regulation in different organisms. Nat. Struct. Mol. Biol. *18*, 213–223.

Chu, H.-P., Cifuentes-Rojas, C., Kesner, B., Aeby, E., Lee, H., Wei, C., Oh, H.J., Boukhali, M., Haas, W., and Lee, J.T. (2017). TERRA RNA Antagonizes ATRX and Protects Telomeres. Cell *170*, 86-101.e16.

Cicconi, A., Rai, R., Xiong, X., Broton, C., Al-Hiyasat, A., Hu, C., Dong, S., Sun, W., Garbarino, J., Bindra, R.S., et al. (2020). Microcephalin 1/BRIT1-TRF2 interaction promotes telomere replication and repair, linking telomere dysfunction to primary microcephaly. Nat. Commun. *11*.

Clynes, D., Jelinska, C., Xella, B., Ayyub, H., Scott, C., Mitson, M., Taylor, S., Higgs, D.R., and Gibbons, R.J. (2015). Suppression of the alternative lengthening of telomere pathway by the chromatin remodelling factor ATRX. Nat. Commun. *6*, 7538.

Collins, P.L., Purman, C., Porter, S.I., Nganga, V., Saini, A., Hayer, K.E., Gurewitz, G.L., Sleckman, B.P., Bednarski, J.J., Bassing, C.H., et al. (2020). DNA double-strand breaks induce H2Ax phosphorylation domains in a contact-dependent manner. Nat. Commun. *11*, 1–9.

Dang, L., White, D.W., Gross, S., Bennett, B.D., Bittinger, M.A., Driggers, E.M., Fantin, V.R., Jang, H.G., Jin, S., Keenan, M.C., et al. (2009). Cancer-associated IDH1 mutations produce 2-hydroxyglutarate. Nature *462*, 739–744.

Danussi, C., Bose, P., Parthasarathy, P.T., Silberman, P.C., Van Arnam, J.S., Vitucci, M., Tang, O.Y., Heguy, A., Wang, Y., Chan, T.A., et al. (2018). Atrx inactivation drives disease-defining phenotypes in glioma cells of origin through global epigenomic remodeling. Nat. Commun. *9*, 1057.

Doench, J.G., Fusi, N., Sullender, M., Hegde, M., Vaimberg, E.W., Donovan, K.F., Smith, I., Tothova, Z., Wilen, C., Orchard, R., et al. (2016). Optimized sgRNA design to maximize activity and minimize off-target effects of CRISPR-Cas9. Nat. Biotechnol. *34*, 184–191.

Dyer, M.A., Qadeer, Z.A., Valle-Garcia, D., and Bernstein, E. (2017). ATRX and DAXX: Mechanisms and Mutations. Cold Spring Harb. Perspect. Med. *7*, a026567.

Feng, W., Simpson, D.A., Carvajal-Garcia, J., Price, B.A., Kumar, R.J., Mose, L.E., Wood, R.D., Rashid, N., Purvis, J.E., Parker, J.S., et al. (2019). Genetic determinants of cellular addiction to DNA polymerase theta. Nat. Commun. *10*.

Flynn, R.L., Cox, K.E., Jeitany, M., Wakimoto, H., Bryll, A.R., Ganem, N.J., Bersani, F., Pineda, J.R., Suvà, M.L., Benes, C.H., et al. (2015). Alternative lengthening of telomeres renders cancer cells hypersensitive to ATR inhibitors. Science *347*, 273–277.

Frescas, D., Guardavaccaro, D., Kuchay, S.M., Kato, H., Poleshko, A., Basrur, V., Elenitoba-Johnson, K.S., Katz, R.A., and Pagano, M. (2008). Cell Cycle KDM2A represses transcription of centromeric satellite repeats and maintains the heterochromatic state. Cell Cycle *7*, 3539–3547.

Gibbons, R.J., Picketts, D.J., Villard, L., and Higgs, D.R. (1995). Mutations in a putative global transcriptional regulator cause X-linked mental retardation with α-thalassemia (ATR-X syndrome). Cell *80*, 837–845.

Goldberg, A.D., Banaszynski, L.A., Noh, K.-M., Lewis, P.W., Elsaesser, S.J., Stadler, S., Dewell, S., Law, M., Guo, X., Li, X., et al. (2010). Distinct Factors Control Histone Variant H3.3 Localization at Specific Genomic Regions. Cell *140*, 678–691.

González-Billalabeitia, E., Seitzer, N., Song, S.J., Song, M.S., Patnaik, A., Liu, X.S., Epping, M.T., Papa, A., Hobbs, R.M., Chen, M., et al. (2014). Vulnerabilities of PTEN-TP53-deficient prostate cancers to compound PARP-PI3K inhibition. Cancer Discov. *4*, 896–904.

Gyori, B.M., Venkatachalam, G., Thiagarajan, P.S., Hsu, D., and Clement, M.V. (2014). OpenComet: An automated tool for comet assay image analysis. Redox Biol. *2*, 457–465.

Haase, S., Garcia-Fabiani, M.B., Carney, S., Altshuler, D., Núñez, F.J., Méndez, F.M., Núñez, F., Lowenstein, P.R., and Castro, M.G. (2018). Mutant ATRX: uncovering a new therapeutic target for glioma. Expert Opin. Ther. Targets *22*, 599–613.

Hänsel-Hertsch, R., Beraldi, D., Lensing, S. V, Marsico, G., Zyner, K., Parry, A., Di Antonio, M., Pike, J., Kimura, H., Narita, M., et al. (2016). G-quadruplex structures mark human regulatory chromatin. Nat. Genet. *48*, 1267–1272.

He, H., Wang, Y., Guo, X., Ramchandani, S., Ma, J., Shen, M.-F., Garcia, D.A., Deng, Y., Multani, A.S., You, M.J., et al. (2009). Pot1b Deletion and Telomerase Haploinsufficiency in Mice Initiate an ATR-Dependent DNA Damage Response and Elicit Phenotypes Resembling Dyskeratosis Congenita. Mol. Cell. Biol. *29*, 229–240.

He, J., Mansouri, A., and Das, S. (2018). Alpha Thalassemia/Mental Retardation Syndrome X-Linked, the Alternative Lengthening of Telomere Phenotype, and Gliomagenesis: Current Understandings and Future Potential. Front. Oncol. *7*, 322.

Heyer, W.-D., Ehmsen, K.T., and Liu, J. (2010). Regulation of homologous recombination in eukaryotes. Annu. Rev. Genet. *44*, 113–139.

Higgs, D.R., Gibbons, R.J., McDowell, T.L., Raman, S., O'Rourke, D.M., Garrick, D., and Ayyub, H. (2000). Mutations in ATRX, encoding a SWI/SNF-like protein, cause diverse changes in the pattern of DNA methylation. Nat. Genet. *24*, 368–371.

Hsu, P.D., Scott, D.A., Weinstein, J.A., Ran, F.A., Konermann, S., Agarwala, V., Li, Y., Fine, E.J., Wu, X., Shalem, O., et al. (2013). DNA targeting specificity of RNA-guided Cas9 nucleases. Nat. Biotechnol. *31*, 827–832.

Huh, M., Ivanochko, D., Hashem, L., Curtin, M., Delorme, M., Goodall, E., Yan, K., and Picketts, D. (2016). Stalled replication forks within heterochromatin require ATRX for protection. Cell Death Dis. *7*.

Iwase, S., Xiang, B., Ghosh, S., Ren, T., Lewis, P.W., Cochrane, J.C., Allis, C.D., Picketts, D.J., Patel, D.J., Li, H., et al. (2011). ATRX ADD domain links an atypical histone methylation recognition mechanism to human mental-retardation syndrome. Nat. Struct. Mol. Biol. *18*, 769–776.

Jackson, C.B., Noorbakhsh, S.I., Sundaram, R.K., Kalathil, A.N., Ganesa, S., Jia, L., Breslin, H., Burgenske, D.M., Gilad, O., Sarkaria, J.N., et al. (2019). Temozolomide sensitizes MGMT-deficient tumor cells to ATR inhibitors. Cancer Res. *79*, 4331–4338.

Jette, N., and Lees-Miller, S.P. (2015). The DNA-dependent protein kinase: A multifunctional protein kinase with roles in DNA double strand break repair and mitosis. Prog. Biophys. Mol. Biol. *117*, 194–205.

Johnson, N., Li, Y.C., Walton, Z.E., Cheng, K.A., Li, D., Rodig, S.J., Moreau, L.A., Unitt, C., Bronson, R.T., Thomas, H.D., et al. (2011). Compromised CDK1 activity sensitizes BRCA-proficient cancers to PARP inhibition. Nat. Med. *17*, 875–882.

Juhász, S., Elbakry, A., Mathes, A., and Löbrich, M. (2018). ATRX Promotes DNA Repair Synthesis and Sister Chromatid Exchange during Homologous Recombination. Mol. Cell *71*, 11-24.e7.

Kim, H., George, E., Ragland, R.L., Rafail, S., Zhang, R., Krepler, C., Morgan, M.A., Herlyn, M., Brown, E.J., and Simpkins, F. (2017). Targeting the ATR/CHK1 axis with PARP inhibition results in tumor regression in BRCA-mutant ovarian cancer models. Clin. Cancer Res. *23*, 3097–3108.

Kim, J., Sun, C., Tran, A.D., Chin, P.-J., Ruiz, P.D., Wang, K., Gibbons, R.J., Gamble, M.J., Liu, Y., and Oberdoerffer, P. (2019). The macroH2A1.2 histone variant links ATRX loss to alternative telomere lengthening. Nat. Struct. Mol. Biol. *26*, 213–219.

Kolinjivadi, A.M., Sannino, V., de Antoni, A., Técher, H., Baldi, G., and Costanzo, V. (2017). Moonlighting at replication forks - a new life for homologous recombination proteins BRCA1, BRCA2 and RAD51. FEBS Lett. *591*, 1083–1100.

Koschmann, C., Calinescu, A.-A., Nunez, F.J., Mackay, A., Fazal-Salom, J., Thomas, D., Mendez, F., Kamran, N., Dzaman, M., Mulpuri, L., et al. (2016). ATRX loss promotes tumor growth and impairs nonhomologous end joining DNA repair in glioma. Sci. Transl. Med. *8*, 328ra28.

Kotsantis, P., Petermann, E., and Boulton, S.J. (2018). Mechanisms of oncogene-induced replication stress: Jigsaw falling into place. Cancer Discov. *8*, 537–555.

Kuo, L.J., and Yang, L.-X. (2008). γ-H2AX - A Novel Biomarker for DNA Double-strand Breaks. In Vivo (Brooklyn). *22*.

Lamarche, B.J., Orazio, N.I., and Weitzman, M.D. (2010). The MRN complex in double-strand break repair and telomere maintenance. FEBS Lett. *584*, 3682–3695.

Law, M.J., Lower, K.M., Voon, H.P.J., Hughes, J.R., Garrick, D., Viprakasit, V., Mitson, M., De Gobbi, M., Marra, M., Morris, A., et al. (2010). ATR-X Syndrome Protein Targets Tandem Repeats and Influences Allele-Specific Expression in a Size-Dependent Manner. Cell *143*, 367–378.

Leung, J.W.-C., Ghosal, G., Wang, W., Shen, X., Wang, J., Li, L., and Chen, J. (2013). Alpha thalassemia/mental retardation syndrome X-linked gene product ATRX is required for proper replication restart and cellular resistance to replication stress. J. Biol. Chem. *288*, 6342–6350.

Lewis, P.W., Elsaesser, S.J., Noh, K.-M., Stadler, S.C., and Allis, C.D. (2010). Daxx is an H3.3-specific histone chaperone and cooperates with ATRX in replication-independent chromatin assembly at telomeres. Proc. Natl. Acad. Sci. U. S. A. *107*, 14075–14080.

Liang, J., Zhao, H., Diplas, B.H., Liu, S., Liu, J., Wang, D., Lu, Y., Zhu, Q., Wu, J., Wang, W., et al. (2019). Genome-Wide CRISPR-Cas9 Screen Reveals Selective Vulnerability of ATRX - Mutant Cancers to WEE1 Inhibition . Cancer Res.

Lloyd, R.L., Wijnhoven, P.W.G., Ramos-Montoya, A., Wilson, Z., Illuzzi, G., Falenta, K., Jones, G.N., James, N., Chabbert, C.D., Stott, J., et al. (2020). Combined PARP and ATR inhibition potentiates genome instability and cell death in ATM-deficient cancer cells. Oncogene *39*, 4869–4883.

Lovejoy, C.A., Li, W., Reisenweber, S., Thongthip, S., Bruno, J., de Lange, T., De, S., Petrini, J.H.J., Sung, P.A., Jasin, M., et al. (2012). Loss of ATRX, genome instability, and an altered DNA damage response are hallmarks of the alternative lengthening of telomeres pathway. PLoS Genet. *8*, e1002772.

Lovejoy, C.A., Takai, K., Huh, M.S., Picketts, D.J., and de Lange, T. (2020). ATRX affects the repair of telomeric DSBs by promoting cohesion and a DAXX-dependent activity. PLoS Biol. *18*, e3000594.

Lu, C., Ward, P.S., Kapoor, G.S., Rohle, D., Turcan, S., Abdel-Wahab, O., Edwards, C.R., Khanin, R., Figueroa, M.E., Melnick, A., et al. (2012). IDH mutation impairs histone demethylation and results in a block to cell differentiation. Nature *483*, 474–478.

Lu, Y., Kwintkiewicz, J., Liu, Y., Tech, K., Frady, L.N., Su, Y.T., Bautista, W., Moon, S.I., MacDonald, J., Ewend, M.G., et al. (2017). Chemosensitivity of IDH1-mutated gliomas due to an impairment in PARP1-mediated DNA repair. Cancer Res. *77*, 1709–1718.

Maya-Mendoza, A., Moudry, P., Merchut-Maya, J.M., Lee, M., Strauss, R., and Bartek, J. (2018). High speed of fork progression induces DNA replication stress and genomic instability. Nature *559*, 279–284.

Mirza-Aghazadeh-Attari, M., Mohammadzadeh, A., Yousefi, B., Mihanfar, A., Karimian, A., and Majidinia, M. (2019). 53BP1: A key player of DNA damage response with critical functions in cancer. DNA Repair (Amst). *73*, 110–119.

Molenaar, R.J., Radivoyevitch, T., Nagata, Y., Khurshed, M., Przychodzen, B., Makishima, H., Xu, M., Bleeker, F.E., Wilmink, J.W., Carraway, H.E., et al. (2018). Idh1/2 mutations sensitize acute myeloid leukemia to parp inhibition and this is reversed by idh1/2-mutant inhibitors. Clin.

Cancer Res. *24*, 1705–1715.

Mukherjee, J., Johannessen, T.-C.A., Ohba, S., Chow, T.T., Jones, L.E., Pandita, A., and Pieper, R.O. (2018). Mutant IDH1 cooperates with ATRX loss to drive the alternative lengthening of telomere (ALT) phenotype in glioma. Cancer Res. canres.2269.2017.

Murai, J., Huang, S.Y.N.S. -y. N., Das, B.B., Renaud, A., Zhang, Y., Doroshow, J.H., Ji, J., Takeda, S., and Pommier, Y. (2012). Trapping of PARP1 and PARP2 by Clinical PARP Inhibitors. Cancer Res. *72*, 5588–5599.

Murphy, A.K., Fitzgerald, M., Ro, T., Kim, J.H., Rabinowitsch, A.I., Chowdhury, D., Schildkraut, C.L., and Borowiec, J.A. (2014). Phosphorylated RPA recruits PALB2 to stalled DNA replication forks to facilitate fork recovery. J. Cell Biol. *206*, 493–507.

Nemzow, L., Lubin, A., Zhang, L., and Gong, F. (2015). XPC: Going where no DNA damage sensor has gone before. DNA Repair (Amst). *36*, 19–27.

Núñez, F.J., Mendez, F.M., Kadiyala, P., Alghamri, M.S., Savelieff, M.G., Garcia-Fabiani, M.B., Haase, S., Koschmann, C., Calinescu, A.A., Kamran, N., et al. (2019). IDH1-R132H acts as a tumor suppressor in glioma via epigenetic up-regulation of the DNA damage response. Sci. Transl. Med. *11*.

Oeck, S., Malewicz, N.M., Hurst, S., Al-Refae, K., Krysztofiak, A., and Jendrossek, V. (2017). The Focinator v2-0-Graphical Interface, Four Channels, Colocalization Analysis and Cell Phase Identification. Radiat. Res. *188*, 114–120.

Oppel, F., Tao, T., Shi, H., Ross Id, K.N., Zimmerman Id, M.W., Heid, S., Tong, G., Aster, J.C., and Lookid, A.T. (2019). Loss of atrx cooperates with p53-deficiency to promote the

development of sarcomas and other malignancies.

Panzarino, N.J., Krais, J.J., Cong, K., Peng, M., Mosqueda, M., Nayak, S.U., Bond, S.M., Calvo, J.A., Doshi, M.B., Bere, M., et al. (2020). Replication Gaps Underlie BRCA-deficiency and Therapy Response. Cancer Res. canres.1602.2020.

Parsons, D.W., Jones, S., Zhang, X., Lin, J.C.-H., Leary, R.J., Angenendt, P., Mankoo, P., Carter, H., Siu, I.-M., Gallia, G.L., et al. (2008). An integrated genomic analysis of human glioblastoma multiforme. Science *321*, 1807–1812.

Paull, T.T., Rogakou, E.P., Yamazaki, V., Kirchgessner, C.U., Gellert, M., and Bonner, W.M. (2000). A critical role for histone H2AX in recruitment of repair factors to nuclear foci after DNA damage. Curr. Biol. *10*, 886–895.

Pehrson, J.R., and Fried, V.A. (1992). MacroH2A, a core histone containing a large nonhistone region. Science (80-.). *257*, 1398–1400.

Raghunandan, M., Yeo, J.E., Walter, R., Saito, K., Harvey, A.J., Ittershagen, S., Lee, E.-A., Yang, J., Hoatlin, M.E., Bielinsky, A.K., et al. (2019). Functional crosstalk between the Fanconi anemia and ATRX/DAXX histone chaperone pathways promotes replication fork recovery. Hum. Mol. Genet. *00*, 1–13.

Rai, R., Li, J.M., Zheng, H., Lok, G.T.M., Deng, Y., Huen, M.S.Y., Chen, J., Jin, J., and Chang, S. (2011). The E3 ubiquitin ligase Rnf8 stabilizes Tpp1 to promote telomere end protection. Nat. Struct. Mol. Biol. *18*, 1400–1407.

Ramamoorthy, M., and Smith, S. (2015). Loss of ATRX Suppresses Resolution of Telomere Cohesion to Control Recombination in ALT Cancer Cells. Cancer Cell *28*, 357–369.

Ratnakumar, K., Duarte, L.F., LeRoy, G., Hasson, D., Smeets, D., Vardabasso, C., Bönisch, C., Zeng, T., Xiang, B., Zhang, D.Y., et al. (2012). ATRX-mediated chromatin association of histone variant macroH2A1 regulates α-globin expression. Genes Dev. *26*, 433–438.

Ray, A., Mir, S.N., Wani, G., Zhao, Q., Battu, A., Zhu, Q., Wang, Q.-E., and Wani, A.A. (2009). Human SNF5/INI1, a Component of the Human SWI/SNF Chromatin Remodeling Complex, Promotes Nucleotide Excision Repair by Influencing ATM Recruitment and Downstream H2AX Phosphorylation. Mol. Cell. Biol. *29*, 6206–6219.

Ray, A., Milum, K., Battu, A., Wani, G., and Wani, A.A. (2013). NER initiation factors, DDB2 and XPC, regulate UV radiation response by recruiting ATR and ATM kinases to DNA damage sites. DNA Repair (Amst). *12*, 273–283.

Reifenberger, G., Wirsching, H.-G., Knobbe-Thomsen, C.B., and Weller, M. (2016). Advances in the molecular genetics of gliomas — implications for classification and therapy. Nat. Rev. Clin. Oncol. *14*, 434–452.

Rothbart, S.B., Krajewski, K., Nady, N., Tempel, W., Xue, S., Badeaux, A.I., Barsyte-Lovejoy, D., Martinez, J.Y., Bedford, M.T., Fuchs, S.M., et al. (2012). Association of UHRF1 with methylated H3K9 directs the maintenance of DNA methylation. Nat. Struct. Mol. Biol. *19*, 1155–1160.

Saldivar, J.C., Cortez, D., and Cimprich, K.A. (2017). The essential kinase ATR: Ensuring faithful duplication of a challenging genome. Nat. Rev. Mol. Cell Biol. *18*, 622–636.

Sanjana, N.E., Shalem, O., and Zhang, F. (2014). Improved vectors and genome-wide libraries for CRISPR screening. Nat. Methods *11*, 783–784.

Schoonen, P.M., Kok, Y.P., Wierenga, E., Bakker, B., Foijer, F., Spierings, D.C.J., and van Vugt, M.A.T.M. (2019). Premature mitotic entry induced by ATR inhibition potentiates olaparib inhibition-mediated genomic instability, inflammatory signaling, and cytotoxicity in BRCA2-deficient cancer cells. Mol. Oncol. *13*, 2422–2440.

Shibata, A., and Jeggo, P.A. (2014). DNA double-strand break repair in a cellular context. Clin. Oncol. (R. Coll. Radiol). *26*, 243–249.

Shiotani, B., Nguyen, H.D., Håkansson, P., Maréchal, A., Tse, A., Tahara, H., and Zou, L. (2013). Two Distinct Modes of ATR Activation Orchestrated by Rad17 and Nbs1. Cell Rep. *3*, 1651–1662.

Smith, J., Mun Tho, L., Xu, N., and A. Gillespie, D. (2010). The ATM-Chk2 and ATR-Chk1 pathways in DNA damage signaling and cancer. In Advances in Cancer Research, (Academic Press Inc.), pp. 73–112.

Sonoda, Y., Ozawa, T., Hirose, Y., Aldape, K.D., Mcmahon, M., Berger, M.S., and Pieper, R.O. (2001). Formation of Intracranial Tumors by Genetically Modified Human Astrocytes Defines Four Pathways Critical in the Development of Human Anaplastic Astrocytoma 1.

Stewart, E., Goshorn, R., Bradley, C., Griffiths, L.M., Benavente, C., Twarog, N.R., Miller, G.M., Caufield, W., Freeman, B.B., Bahrami, A., et al. (2014). Targeting the DNA repair pathway in Ewing sarcoma. Cell Rep. *9*, 829–840.

Stout, G.J., and Blasco, M.A. (2013). Telomere length and telomerase activity impact the UV sensitivity syndrome xeroderma pigmentosum C. Cancer Res. *73*, 1844–1854.

Sulkowski, P.L., Corso, C.D., Robinson, N.D., Scanlon, S.E., Purshouse, K.R., Bai, H., Liu, Y.,

Sundaram, R.K., Hegan, D.C., Fons, N.R., et al. (2017). 2-Hydroxyglutarate produced by neomorphic IDH mutations suppresses homologous recombination and induces PARP inhibitor sensitivity. Sci. Transl. Med. *9*, eaal2463.

Sulkowski, P.L., Oeck, S., Dow, J., Economos, N.G., Mirfakhraie, L., Liu, Y., Noronha, K., Bao, X., Li, J., Shuch, B.M., et al. (2020). Oncometabolites suppress DNA repair by disrupting local chromatin signalling. Nature *582*, 586–591.

Szenker, E., Ray-Gallet, D., and Almouzni, G. (2011). The double face of the histone variant H3.3. Cell Res. *2114*.

Tanaka, Y., Okamoto, K., Teye, K., Umata, T., Yamagiwa, N., Suto, Y., Zhang, Y., and Tsuneoka, M. (2010). JmjC enzyme KDM2A is a regulator of rRNA transcription in response to starvation. EMBO J. *29*, 1510–1522.

Turner, N.C., Lord, C.J., Iorns, E., Brough, R., Swift, S., Elliott, R., Rayter, S., Tutt, A.N., and Ashworth, A. (2008). A synthetic lethal siRNA screen identifying genes mediating sensitivity to a PARP inhibitor. EMBO J. *27*, 1368–1377.

Udugama, M., Chang, F.T.M., Chan, F.L., Tang, M.C., Pickett, H.A., Mcghie, J.D.R., Mayne, L., Collas, P., Mann, J.R., and Wong, L.H. (2015). Histone variant H3.3 provides the heterochromatic H3 lysine 9 tri-methylation mark at telomeres. Nucleic Acids Res. *43*, 10227–10237.

Udugama, M., Sanij, E., Voon, H.P.J., Son, J., Hii, L., Henson, J.D., Chan, F.L., Chang, F.T.M., Liu, Y., Pearson, R.B., et al. (2018). Ribosomal DNA copy loss and repeat instability in ATRX-mutated cancers. Proc. Natl. Acad. Sci. U. S. A. *115*, 4737–4742.

Vacík, T., Lađinović, D., and Raška, I. (2018). KDM2A/B lysine demethylases and their alternative isoforms in development and disease. Nucleus *9*, 431–441.

Valle-García, D., Griffiths, L.M., Dyer, M.A., Bernstein, E., and Recillas-Targa, F. (2014). The ATRX cDNA is prone to bacterial IS10 element insertions that alter its structure. Springerplus *3*, 1–7.

Vassin, V.M., Anantha, R.W., Sokolova, E., Kanner, S., and Borowiec, J.A. (2009). Human RPA phosphorylation by ATR stimulates DNA synthesis and prevents ssDNA accumulation during DNA-replication stress. J. Cell Sci. *122*, 4070–4080.

Di Veroli, G.Y., Fornari, C., Wang, D., Mollard, S., Bramhall, J.L., Richards, F.M., and Jodrell, D.I. (2016). Combenefit: An interactive platform for the analysis and visualization of drug combinations. Bioinformatics *32*, 2866–2868.

Vietor, M., Winter, S., Groscurth, P., Naumann, U., and Weller, M. (2000). On the significance of telomerase activity in human malignant glioma cells. Eur. J. Pharmacol. *407*, 27–37.

Voon, H.P.J., Hughes, J.R., Rode, C., DeLaRosa-Velázquez, I.A., Jenuwein, T., Feil, R., Higgs, D.R., and Gibbons, R.J. (2015). ATRX Plays a Key Role in Maintaining Silencing at Interstitial Heterochromatic Loci and Imprinted Genes. Cell Rep. *11*, 405–418.

Voon, H.P.J., Collas, P., and Wong, L.H. (2016). Compromised telomeric heterochromatin promotes ALTernative lengthening of telomeres. Trends in Cancer *2*, 114–116.

Wang, Y., Yang, J., Wild, A.T., Wu, W.H., Shah, R., Danussi, C., Riggins, G.J., Kannan, K., Sulman, E.P., Chan, T.A., et al. (2019). G-quadruplex DNA drives genomic instability and represents a targetable molecular abnormality in ATRX-deficient malignant glioma. Nat.

Commun. *10*.

Wang, Y., Wild, A.T., Turcan, S., Wu, W.H., Sigel, C., Klimstra, D.S., Ma, X., Gong, Y., Holland, E.C., Huse, J.T., et al. (2020). Targeting therapeutic vulnerabilities with PARP inhibition and radiation in IDH-mutant gliomas and cholangiocarcinomas. Sci. Adv. *6*, eaaz3221.

Ward, I.M., Minn, K., van Deursen, J., and Chen, J. (2003). p53 Binding Protein 53BP1 Is Required for DNA Damage Responses and Tumor Suppression in Mice. Mol. Cell. Biol. *23*, 2556–2563.

Weldon, C., Eperon, I.C., and Dominguez, C. (2016). Do we know whether potential G-quadruplexes actually form in long functional RNA molecules? Biochem. Soc. Trans. *44*, 1761–1768.

Wong, L.H., McGhie, J.D., Sim, M., Anderson, M.A., Ahn, S., Hannan, R.D., George, A.J., Morgan, K.A., Mann, J.R., and Choo, K.H.A. (2010). ATRX interacts with H3.3 in maintaining telomere structural integrity in pluripotent embryonic stem cells. Genome Res. *20*, 351–360.

Xiong, X., Du, Z., Wang, Y., Feng, Z., Fan, P., Yan, C., Willers, H., and Zhang, J. (2015). 53BP1 promotes microhomology-mediated end-joining in G1-phase cells. Nucleic Acids Res. *43*, 1659–1670.

Xu, W., Yang, H., Liu, Y., Yang, Y., Wang, P., Kim, S.H., Ito, S., Yang, C., Wang, P., Xiao, M.T., et al. (2011). Oncometabolite 2-hydroxyglutarate is a competitive inhibitor of α-ketoglutarate-dependent dioxygenases. Cancer Cell *19*, 17–30.

Zandarashvili, L., Langelier, M.F., Velagapudi, U.K., Hancock, M.A., Steffen, J.D., Billur, R., Hannan, Z.M., Wicks, A.J., Krastev, D.B., Pettitt, S.J., et al. (2020). Structural basis for allosteric

PARP-1 retention on DNA breaks. Science (80-.). *368*.

Zimmer, J., Tacconi, E.M.C., Folio, C., Badie, S., Porru, M., Klare, K., Tumiati, M., Markkanen, E., Halder, S., Ryan, A., et al. (2016). Targeting BRCA1 and BRCA2 Deficiencies with G-Quadruplex-Interacting Compounds. Mol. Cell *61*, 449–460.